ABSTRACT

Name: James A. Maloney Department: Physics

Title: Application of Symmetry Theories to Design of Fragment Separators for Exotic Isotope Accelerators

Major: Physics Degree: Master of Science

Approved By: Date:

Thesis Director

NORTHERN ILLINOIS UNIVERSITY

ABSTRACT

Exotic isotope accelerators are posed to provide us with unique abilities to investigate and test current theories regarding nuclei structure, weak-force interaction symmetry, and cosmologic evolution. Crucial to this powerful experimental tool is the design of its fragment separator. Designs for such a fragment separator can be developed through use of symmetry theories and simulation software. The goals and requirements of such designs include mechanical specifications; minimizing the effects of beam aberrations, fringe fields and stochastic effects of the systems elements; allowing large acceptance; and providing a high intensity beam of pure ions to be transported to experiments through the accelerator.

Beam aberrations create substantial problems in any design, particularly beyond the first and second order terms. Symmetry theories help understanding the cause of these aberrations and provide clues to correct the design. This thesis explores a variety of designs have been tested and compared to develop a proposed system layout that will best meet the needs and goals of the next generation exotic isotope accelerator.

NORTHERN ILLINOIS UNIVERSITY

APPLICATION OF SYMMETRY THEORIES TO THE DESIGN OF FRAGMENT SEPARATORS FOR EXOTIC ISOTOPE ACCELERATORS

A THESIS SUBMITTED TO THE GRADUATE SCHOOL

IN PARTIAL FULFILLMENT OF THE REQUIREMENTS

FOR THE DEGREE

MASTER OF SCIENCE

DEPARTMENT OF PHYSICS

BY

JAMES A. MALONEY

DEKALB, ILLINOIS

DECEMBER 2006

Certification: In accordance with departmental and Graduate School policies, this Thesis is accepted in partial fulfillment of degree requirements.

_____

Thesis Director

_____

Date

ACKNOWLEDGEMENTS

The author would like to acknowledge and thank his advisor, Dr. Bela Erdelyi for his help and assistance in the research and preparation of this Thesis paper. Also, the author would like to acknowledge and thank Northern Illinois University students Joshua Brady and Laura Bandura who helped both directly and indirectly with the research involved in this Thesis. Lastly, the author wishes to express his gratitude to Northern Illinois University and its Physics Department who provided graduate assistantship support to the author.

TABLE OF CONTENTS

Chapter Page

Chapter Page

LIST OF TABLES

LIST OF FIGURES

LIST OF APPENDICES

I. INTRODUCTION

Prior to a discussion of how symmetry theories can be applied to the design of the fragment separator for an exotic isotope accelerator, it is helpful to discuss the nature of such an accelerator and a fragment separator. The design goals, system requirements and physical limitations of the next generation of such systems shall also be reviewed.

Exotic Isotope Accelerator

An exotic isotope accelerator provides an important experimental tool to study nuclear physics, nuclear astrophysics and the fundamental interactions of particles. The importance of an exotic isotope accelerator as a research tool was recognized by the Department of Energy when it identified the Rare Isotope Accelerator (RIA) as the highest priority machine of the nuclear physics community in the United States on its 20 year plan. [1, 2] The next generation of exotic isotope accelerators should be able to surpass results obtained by predecessors, such as the GSI facility in Germany, the RIKEN facility in Japan, and the TRIUMF facility in Canada. It should also allow the study of nuclear physics beyond the abilities of

facilities such as RHIC, which studied the nature of gluon-quark confinement, and CEBAF, which probed the gluon-quark structure in hadrons and gluons. [1] An exotic isotope accelerator can allow the study of how elements are produced in stars through the r-process, rp-process, and other methods of nucleosynthesis. Other proposed uses of exotic isotope accelerators include testing various fundamental assumptions of the Standard Model and QCD theory. [1, 2]

An example of what an exotic isotope accelerator does can be seen by review of recent proposals for the Rare Isotope Accelerator (RIA). Similar exotic beam facilities are operating or currently being designed in other countries around the world, including the United States. These include improvements to the RIKEN radioactive isotope factory in Japan, and the substantial upgrade to the GSI International Accelerator Facility for beams of ions and antiproton under development in Germany; both of which utilize in-flight separation methods. These facilities differ from RIA, which would be capable of post-separation acceleration and allow measurement of nuclear reactions at astrophysical energies. RIA would also offer greater primary beam power than either the GSI or RIKEN facilities through an acceleration scheme that in nearly 20 times more efficient. [3] RIA differs from the TRIUMF facility in Canada in that its higher primary beam power would yield a higher intensity beam with a wider variety of isotopes. [3] RIA would also allow for a more flexible combination of ion sources than the TRIUMF facility. [3]

In the proposed next generation of exotic isotope accelerators, nuclei from protons to uranium would be accelerated to energies of at least 400 MeV per nucleon before being directed at a target. [1, 2] This interaction is designed to produce a variety of statistically rare isotopes which can be selected and studied. By smashing such a high energy beam of nuclei into the target, Coulomb barrier potentials can be overcome and multi-body nuclear processes can occur that otherwise are limited to cosmic events such as the big bang, or stellar burning and stellar evolution. [1]

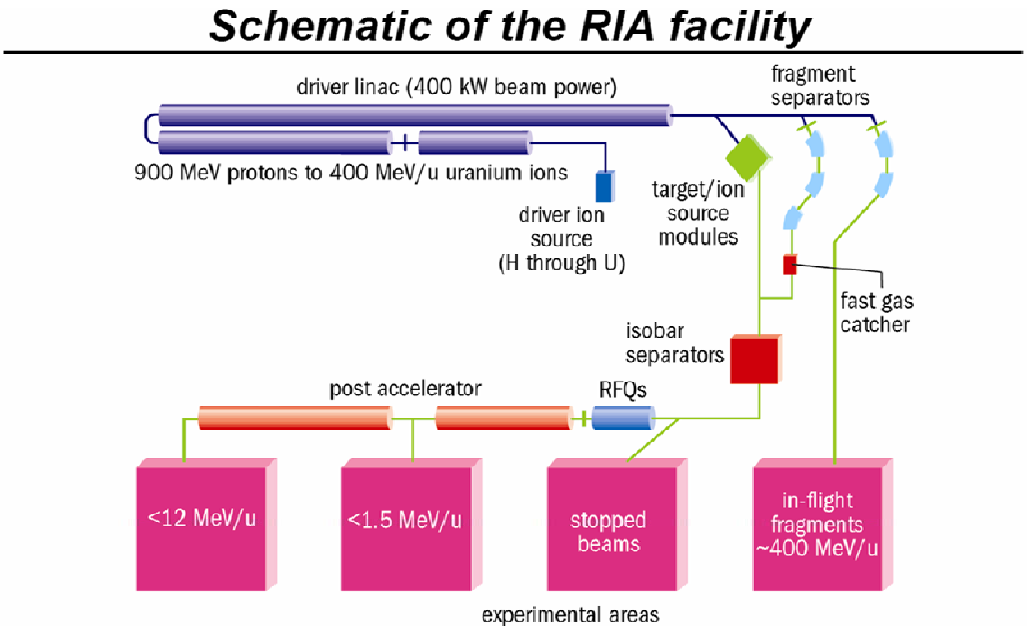

Figure 1. Simplified schematic layout of the Rare Isotope Accelerator (RIA) facility. [1, 2]

The RIA facility, depicted in Figure 1, would have allowed study of isotopes in both of the two major branch types of exotic beam facilities. First, it would have allowed study of fast beams through its in-flight high resolution fragment separator. [1, 4] Second, using a gas catcher, very rare isotopes could be accumulated and

studied at rest energies or reaccelerated to energies below or just around the Coulomb barrier. [1, 5] Both branches utilize a fragment separator to select rare isotopes from the multitude of those produced by the beam/target interaction.

Fragment Separators

The fragment separator, such as shown in Figure 2, is the work horse all designs of an exotic isotope accelerator. Its purpose is to allow experimenters to study a high intensity beam of isotopes of a selected mass and charge.

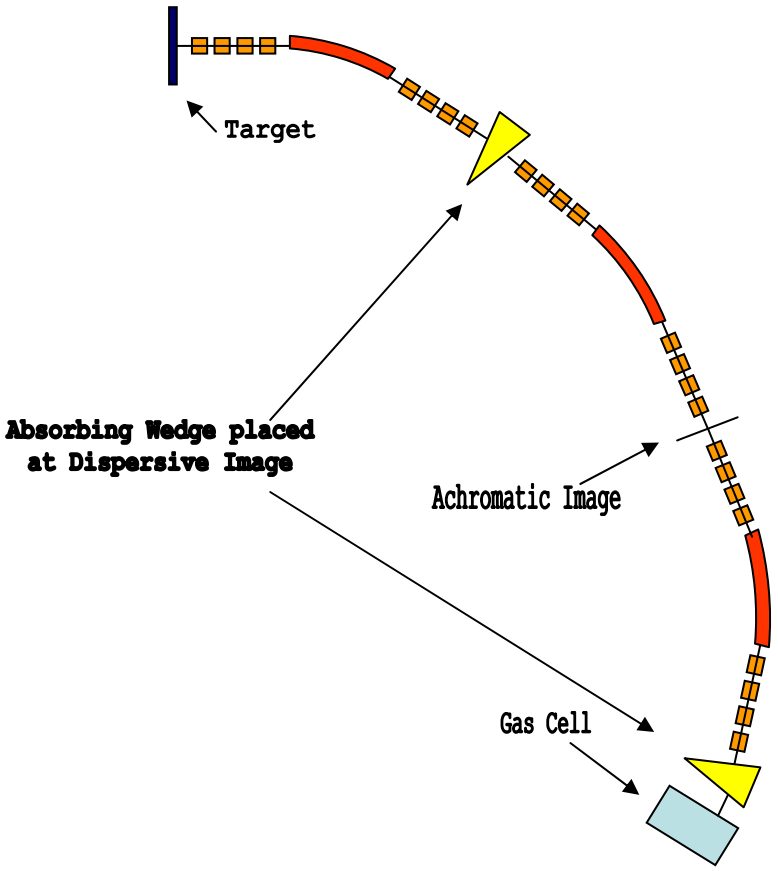

Figure 2. Schematic layout of fragment separator from target through fast gas catcher cell.

After the accelerated beam of nuclei strikes the target material, a vast array of isotopes are produced. By using magnetic multipoles the resulting beam is confined in phase-space and transported along the beam line. A magnetic dipole bending element is then used to create a dispersive array of isobars based upon their mass/charge ratio. The beam is then projected through a wedge of absorbing material (i.e., an energy degrader) that further disperses the isobar into isotopes based upon their specific mass and charge. [6, 7] The resulting beam is then focused back into an achromatic image using magnetic multipoles and a second magnetic dipole bending element. [7]

In theory, the result is a pure isotope beam that can be selected to be transported to the experimenter. Other isotopes are removed by a combination of apertures and a beam dump.

Because the dispersion of isotopes falls along a continuous spectrum, a second dipole and absorbing wedge are often used to minimize range variations in the beam leaving the fragment separator. By adjusting the types of material used in the target and the wedge, as well as the nature and energy of nuclei in the incoming accelerated beam, very rare isotopes, including isotopes that are particularly unstable and short-lived, can be produced and selected for study.

Design Goals

To achieve the maximum results in the next generation of exotic isotope accelerators certain criteria should be met to exceed the capabilities of other current and planned exotic isotope accelerators. In the proposal for RIA, for example, the initial acceleration per nuclei was targeted at greater than 900 MeV for protons to 400 MeV/u for Uranium. [1] This allowed for a minimum energy of 400 MeV/u for fragments being delivered to the in-flight experimental sections. Goals of the accelerator should also include increasing the yields of isotopes produced by several orders of magnitude. [1]

Design Limitations and Criteria

Many of the design limitations for a fragment separator will be set by the particular goals set for the exotic isotope accelerator. Some are also set by experimental factors. For example, increasing the resolution of an isotope beam will result in lower yields of rare isotopes in the transmitted beam. Costs also play a substantial role as a limiting factor in the design. In the designs discussed subsequently in this paper, critical consideration was given to the cost of the magnetic multipoles and the dipole bending elements. Consideration was also given to mechanical and engineering limitations.

From all these considerations, an extensive discussion of which would be beyond the scope of this paper, the following design limitations and goals were used:

- Horizontal (multipole) apertures and beam width less than 40 cm.
- Vertical (dipole) apertures and beam width less than 10 cm.
- Pole tip field strength for multipoles less than 3 Tesla.
- Drift lengths between element between 20 cm and 100 cm.
- Dipole radius of approximately 5 meters and angle of 35 degrees.

With respect to each of these elements, cost was a major contributing factor. Some of the limitations, such as the minimum drift length and maximum pole tip field strengths, reflect mechanical and engineering limitations. Systems that deviated substantially from these limitations would be impractical to build.

II. DESIGN TOOLS AND THEORIES

To assist in the design of a fragment separator, many tools and theories are available. Some of these fall into the category of theories that can indicate the minimally sufficient criteria that will result in a working design. Others are simulation tools to help the designer apply and test the theory and any proposed system design. Both were employed to develop the designs discussed in the following sections.

The importance of these symmetries comes from their ability to simplify otherwise complex optical systems. In the case of light optics, for example, focusing problems are simplified due to the fact that most components (lenses mirrors, and drifts) will have rotation symmetry about some optical axis. In the case of charged particle optics, however, the general lack of rotational symmetry in components makes focusing problems much more difficult to solve. In the case of a quadrupole, for example, which acts to focus a charged particle beam in much the same way as a lens focuses a beam of light, the horizontal and vertical "focal lengths" will be different. If the desired result is to achieve both point to point and parallel to parallel focusing of a beam, this means that at least 4 quadrupoles are required (two in each plane - horizontal and vertical). This contrasts with only two

lens being needed to achieve the same focusing result when rotational symmetry exists (such as in the light optics case). The trajectory of charged particles is affected by magnetic and electric fields. Rotationally symmetric devices capable of creating such field (for example, a solenoid) are generally not strong enough to be of use for beam with the energies involved in exotic isotope accelerators.

Symmetry Theories

A number of symmetry theories can be used to simplify analysis of the beam of isotopes traveling through a fragment separator. While each of these plays a different role in the system's design, they all work to reduce the criteria necessary to obtain separation of isotopes within a beam while maintaining a focused beam that can then be transported to experimenters.

Prior to any discussion of specific theories, a brief aside regarding the mathematical notation that will be used is necessary. With respect to the motion of a reference particle such as an isotope, a six-dimensional phase space vector will be used to denote to position of a particle. [7, 8, 9, 10]

$$\{r_k\} = (r_{k1} , r_{k2} , r_{k3} , r_{k4} , r_{k5} , r_{k6}) = (x_k , a_k , y_k , b_k , t_k, \delta_k) \quad (1)$$

The variables x and y reflect the horizontal and vertical positions of the particle with reference to the optic axis of the beam line. The variables a and b reflect the dimensionless horizontal (p_x/p_0) and vertical (p_y/p_0) momentum of the particle. The two remaining variables, t and δ, reflect flight time and change in total

energy ($E - E_0/E_0$) of the particle. Changes to the vector representing a particle as it moves along the beam line can be used to derive a transfer map between points in the system. This transfer map is generally a complicated, non-linear vector function.

The transfer map can, however, be thought of as a "matrix" that describes changes in the six canonical variables used to express the path of the reference particle. This is done by expanding the transfer map in a Taylor series (sometimes referred to as the Taylor map), and truncating the series to eliminate terms beyond a particular order. For example, the change in final position as a function of initial conditions of a particle might be expressed as:

$\{r_1\} = T \circ \{r_0\}$ where the r_{t1} coordinate of the vector $\{r_1\}$ can be expressed as

$$r_{t1} = \sum_{j=1}^{6} r_{j0}\{(r_t \mid r_j) + \frac{1}{2}\sum_{k=1}^{6} r_{k0}\{(r_t \mid r_j r_k) + \frac{1}{3!}\sum_{l=1}^{6} r_{l0}\{(r_t \mid r_j r_k r_l) + \ldots\}\}\} \qquad (2)$$

The resulting coordinates can also be expressed in compact notation as:

$$\begin{aligned} r_{1x} &= T_x(x_0, a_0, y_0, b_{0,} t_0, \delta_0) \\ r_{1a} &= T_a(x_0, a_0, y_0, b_{0,} t_0, \delta_0) \\ r_{1y} &= T_y(x_0, a_0, y_0, b_{0,} t_0, \delta_0) \\ r_{1b} &= T_b(x_0, a_0, y_0, b_{0,} t_0, \delta_0) \\ r_{1t} &= T_t(x_0, a_0, y_0, b_{0,} t_0, \delta_0) \\ r_{1\delta} &= T_\delta(x_0, a_0, y_0, b_{0,} t_0, \delta_0) \end{aligned} \qquad (3)$$

When the Taylor map is truncated to include only linear terms, the transfer map becomes a real matrix:

$$\begin{pmatrix} x_f \\ a_f \\ y_f \\ b_f \\ t_f \\ \delta_f \end{pmatrix} = \begin{bmatrix} (x|x) & (x|a) & (x|y) & (x|b) & (x|t) & (x|\delta) \\ (a|x) & (a|a) & (a|y) & (a|b) & (a|t) & (a|\delta) \\ (y|x) & (y|a) & (y|y) & (y|b) & (y|t) & (y|\delta) \\ (b|x) & (b|a) & (b|y) & (b|b) & (b|t) & (b|\delta) \\ (t|x) & (t|a) & (t|y) & (t|b) & (t|t) & (t|\delta) \\ (\delta|x) & (\delta|a) & (\delta|y) & (\delta|b) & (\delta|t) & (\delta|\delta) \end{bmatrix} \begin{pmatrix} x_i \\ a_i \\ y_i \\ b_i \\ t_i \\ \delta_i \end{pmatrix} \tag{4}$$

To further specify the reference particle vector and particular components of the transfer map, subscripts will be used as in the previous example. For example, the transfer map from the beginning of the system to the middle of the dipole bending element will be expressed as T_{M}. While T_{D} and T_{A} reflect the transfer maps to the dispersive and achromatic images, respectively. These same subscripts will be used to clarify when coefficients of particular transfer maps are being discussed. For example, $(x|xa)_{\mathrm{D}}$ would refer to the second order map coefficient of xa in the expansion of the canonical variable x through the dispersive image.

Time-Independence Symmetry

The first symmetry theory considered in the fragment separator design is the time-independence symmetry of the system. This symmetry arises from a design that does not utilize time-dependent elements. Fortunately, the multipoles, dipole bending elements, and absorbing wedges utilized in the designs discussed later in

this paper are all time-independent. The result of this symmetry is that the generalized coordinates x, a, y, b, and δ do not have explicit time dependence. Thus, all terms in the transfer map that involve partial derivatives of these coordinates with respect to time will vanish. This indicates that the transfer map coefficient $(t|t) = 1$. Also, all coefficients of the form $(r_{i\neq5}|t) = 0$. Put more basically, none of the transfer map coefficients can depend upon time in a time-independent system. [9, 10]

The time-independence of the magnetic elements in the system also give rise to basic energy conservation for particles transported through the fragment separator. In other words, particle transported through the fragment separator are not accelerated. Energy constancy states that the magnetic elements of the system will do no work on a particle traveling through the fragment separator. This relation requires that the transfer map coefficient $(\delta|\delta) = 1$. Also, all transfer map coefficients of the form $(\delta| r_{i\neq6}) = 0$. [8, 9, 10] From these two symmetries, our first order transfer map equation is simplified further:

$$\begin{pmatrix} x_f \\ a_f \\ y_f \\ b_f \\ t_f \\ \delta_f \end{pmatrix} = \begin{bmatrix} (x|x) & (x|a) & (x|y) & (x|b) & 0 & (x|\delta) \\ (a|x) & (a|a) & (a|y) & (a|b) & 0 & (a|\delta) \\ (y|x) & (y|a) & (y|y) & (y|b) & 0 & (y|\delta) \\ (b|x) & (b|a) & (b|y) & (b|b) & 0 & (b|\delta) \\ (t|x) & (t|a) & (t|y) & (t|b) & 1 & (t|\delta) \\ 0 & 0 & 0 & 0 & 0 & 1 \end{bmatrix} \begin{pmatrix} x_i \\ a_i \\ y_i \\ b_i \\ t_i \\ \delta_i \end{pmatrix} \tag{5}$$

Mid-Plane Symmetry

Mid-plane symmetry often arises from the symmetry along the optic axis of a system. In a system with midplane symmetry, particles that are symmetric at the beginning of the system stay symmetric throughout the system. In the case of the designs discussed in this paper, such symmetry exists around the midplane in the gap within the magnetic elements of the system (y = 0). Because of this symmetry, we see that a number of the coefficients in the transfer map will vanish.

If we let $\{r_f\} = (x_f, a_f, y_f, b_f, t_f, \delta_f) = T(x_i, a_i, y_i, b_i, t_i, \delta_i)$, then $(x_f, a_f, -y_f, -b_f, t_f, \delta_f) = T(x_i, a_i, -y_i, -b_i, t_i, \delta_i)$, as a result of the mid-plane symmetry. From this relation the following coefficients of the transfer map can be determined to be zero [7, 8, 9, 10],

$$(x \mid x^{i_x} a^{i_a} y^{i_y} b^{i_b} t^{i_t} \delta^{i_\delta}) = 0 \text{ if } i_y + i_b \text{ is odd} \quad (6)$$

$$(a \mid x^{i_x} a^{i_a} y^{i_y} b^{i_b} t^{i_t} \delta^{i_\delta}) = 0 \text{ if } i_y + i_b \text{ is odd} \quad (7)$$

$$(y \mid x^{i_x} a^{i_a} y^{i_y} b^{i_b} t^{i_t} \delta^{i_\delta}) = 0 \text{ if } i_y + i_b \text{ is even} \quad (8)$$

$$(b \mid x^{i_x} a^{i_a} y^{i_y} b^{i_b} t^{i_t} \delta^{i_\delta}) = 0 \text{ if } i_y + i_b \text{ is even} \quad (9)$$

$$(t \mid x^{i_x} a^{i_a} y^{i_y} b^{i_b} t^{i_t} \delta^{i_\delta}) = 0 \text{ if } i_y + i_b \text{ is odd} \quad (10)$$

This allows us to simplify the transfer map matrix. For example, the first-order transfer map matrix equation further reduces to:

$$\begin{pmatrix} x_f \\ a_f \\ y_f \\ b_f \\ t_f \\ \delta_f \end{pmatrix} = \begin{bmatrix} (x \mid x) & (x \mid a) & 0 & 0 & 0 & (x \mid \delta) \\ (a \mid x) & (a \mid a) & 0 & 0 & 0 & (a \mid \delta) \\ 0 & 0 & (y \mid y) & (y \mid b) & 0 & 0 \\ 0 & 0 & (b \mid y) & (b \mid b) & 0 & 0 \\ (t \mid x) & (t \mid a) & 0 & 0 & 1 & (t \mid \delta) \\ 0 & 0 & 0 & 0 & 0 & 1 \end{bmatrix} \begin{pmatrix} x_i \\ a_i \\ y_i \\ b_i \\ t_i \\ \delta_i \end{pmatrix} \tag{11}$$

Mid-plane symmetry will hold for basic system designs involving multipoles and dipole bending elements. This symmetry works, as is our example, to eliminate half of the coefficients in the transfer map matrix. Introducing the absorbing wedge, however, will break this symmetry. For the purposes of design, it is often helpful to design the system without the absorbing wedge and then insert the wedge and shape it to minimize effects caused by its introduction to the system.

Mirror Symmetry

A symmetry theory utilized in the designs discussed subsequently in this paper arises from repetitive patterns in the system's layout. As an example, consider a system where the elements through the middle of a dipole are exactly reversed in the second half of that segment of the system. Another example is the case where mirror symmetry exists for the system from the target through the dispersive image with respect to the system's configuration from the dispersive image through the final achromatic image. Both these examples are discussed in specific designs later in this paper.

In cases of mirror symmetry, certain relationships in the components of the transfer map appear which assist in the design of the system's layout. A simple example using the layout in Figure 3 illustrates the power of this symmetry in designing a Hamiltonian system.

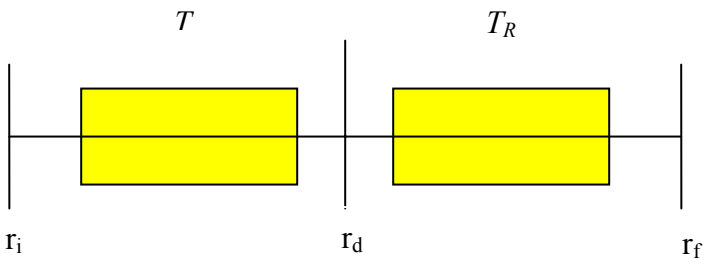

Figure 3. Layout of 2-cell system with mirror symmetry about plane designated by r_d.

In the general case pictured above, r_i, r_d and r_f represent vectors composed of 6 canonically conjugate variables. The transfer map for the left half of the system is designated by T. Thus, $\{r_d\} = T(r_i)$ specifies the motion of the reference particle through the left side of the system. If T_R represents the reversed system, we can combine this operator with the reflection operator, $R(r_k) = (x_k \; -a_k \; y_k \; -b_k \; t_k \; \delta_k)$, and note that $R(r_i) = T_R \circ R(r_d)$. But we also note that $\{r_i\} = T^{-1}(r_d)$. Combining these relationships [9, 10]:

$$T_R \circ R(r_d) = R \circ T^{-1}(r_d) \tag{12}$$

This relationship can be further generalized by noting that $\{r_d\}$ is arbitrary and $R^2 = I$,

$$T_R = R \circ T^{-1} \circ R \tag{13}$$

Now we can exploit the convenient choice of layout in our exemplar system. As we noted earlier, $T_{total} = T_R \circ T = R \circ T^{-1} \circ R \circ T$. The significance of this relationship become apparent when we apply the commutator equation for a Hamiltonian system: [A,B] = A◦B - B◦A. We see:

$$T_{\text{total}} = R \circ T^{-1} \circ \{[R, T] + T \circ R\} = R^2 + R \circ T^{-1} \circ [R, T] \quad (14)$$

Now we can clearly see that when the commutator $[R, T] \rightarrow 0$, $T_{total} \rightarrow$ I. [9, 10, 11] Thus, by designing a system where the commutator terms are zero, the transfer map becomes the identity matrix and the system focused its image point-to-point, parallel-to-parallel. This relationship can then be exploited when point-to-point, parallel-to-parallel imaging is a desired goal for our achromatic image, such as with a fragment separator.

Symplectic Symmetry

Symplectic symmetry, like mirror symmetry, provides clues to a system's layout from relationships in the transfer map elements. The importance of this symmetry arises from the fact that it can be shown that the transfer map of a Hamiltonian system will have symplectic symmetry. [9, 10] To examine how this symmetry theory works, let's again take the case of two vectors r_i and r_f composed of 6 canonically conjugate variables. Furthermore, let *A* represent the Jacobian of a

transfer map that fulfills the symplectic condition [8, 9, 10]; $(A)^T J(A) = J$. A^T represents the transpose of A, and

$$J = \begin{bmatrix} 0 & 0 & 0 & 1 & 0 & 0 \\ 0 & 0 & 0 & 0 & 1 & 0 \\ 0 & 0 & 0 & 0 & 0 & 1 \\ -1 & 0 & 0 & 0 & 0 & 0 \\ 0 & -1 & 0 & 0 & 0 & 0 \\ 0 & 0 & -1 & 0 & 0 & 0 \end{bmatrix} \tag{15}$$

$$A = \begin{bmatrix} c_{11} & c_{12} & c_{13} & c_{14} & c_{15} & c_{16} \\ c_{21} & c_{22} & \dots & \dots & \dots & \dots \\ c_{31} & \dots & c_{33} & \dots & \dots & \dots \\ c_{41} & \dots & \dots & c_{44} & \dots & \dots \\ c_{51} & \dots & \dots & \dots & c_{55} & \dots \\ c_{61} & \dots & \dots & \dots & \dots & c_{66} \end{bmatrix} \tag{16}$$

In this case, the coefficients of the matrix A represent the partial derivatives of components of the final vector with respect to the components of the initial vector:

$$c_{fi} = \frac{\partial r_f}{\partial r_i} \tag{17}$$

To calculate these coefficients, we remember that the final position vector results from operation of the transfer map matrix upon the initial position vector, $\{r_f\} = T(r_i)$. The components of this vector can be expressed as a Taylor series expansion. [8, 10]

For example we can express the terms up to second order in the two-dimensional case:

$$x_f = (x|x)x_i + (x|a)a_i + (x|xx)x_i^2 + (x|xa)x_ia_i + (a|aa)a_i^2 \quad (18)$$

$$a_f = (a|x)x_i + (a|a)a_i + (a|xx)x_i^2 + (a|xa)x_ia_i + (a|aa)a_i^2. \quad (19)$$

Then we can calculate the coefficients, through second order:

$$c_{11} = (x|x) + 2(x|xx)x_i + (x|xa)a_i \quad (20a)$$

$$c_{12} = (x|a) + (x|xa)x_i + 2(a|aa)a_i \quad (20b)$$

$$c_{21} = (a|x) + 2(a|xx)x_i + (a|xa)a_i \quad (20c)$$

$$c_{22} = (a|a) + (a|xa)x_i + 2(a|aa)a_i \quad (20d)$$

Applying the equations for the symplectic condition, $AJA^T = J$, we find:

$$\begin{pmatrix} c_{11} & c_{12} \\ c_{21} & c_{22} \end{pmatrix}\begin{pmatrix} 0 & 1 \\ -1 & 0 \end{pmatrix}\begin{pmatrix} c_{11} & c_{21} \\ c_{12} & c_{22} \end{pmatrix} = \begin{pmatrix} c_{11}c_{12} - c_{11}c_{12} & c_{11}c_{22} - c_{12}c_{21} \\ c_{12}c_{21} - c_{11}c_{22} & c_{21}c_{22} - c_{21}c_{22} \end{pmatrix} = \begin{pmatrix} 0 & 1 \\ -1 & 0 \end{pmatrix} \quad (21)$$

This equation has the solution $c_{11}c_{22} - c_{12}c_{21} = 1$. Using our expanded coefficients and grouping terms based on their dependence upon initial coordinates:

$(x|x)(a|a) - (x|a)(a|x) = 1$ from terms independent of initial coordinates

$(x|x)(a|xa) + 2(a|a)(x|xx) - 2(x|a)(a|xx) - (a|x)(x|xa) = 0$ from terms linear in x_i

$(a|a)(x|xa) + 2(x|x)(a|aa) - 2(a|x)(x|aa) - (a|xa)(x|a) = 0$ from term linear in a_i

From this symmetry, we can derive the following first order relations for the six dimension case:

$$(x|x)(a|a)-(a|x)(x|a)=1 \quad (22a)$$

$$(y|y)(b|b)-(b|y)(y|b)=1 \quad (22b)$$

$$(x|x)(a|\delta)-(a|x)(x|\delta)=(t|x) \quad (22c)$$

$$(x|a)(a|\delta)-(a|a)(x|\delta)=(t|a) \qquad (22d)$$

The first two equations represent the familiar results of Liouville's theorem of conservation of phase space volume under linear transformation. [8, 9] The last two equations detail the connection between longitudinal and dispersive effects of the system. [8, 9] If we impose our system requirements upon these relations, minimizing the terms that appear in the commutator equation [(x|a), (a|x), (y|b), (b|y) and (a|δ) at first order], we see that the symplectic symmetry leads to the following relationships [8]:

$$(x|x)(a|a) = 1 \qquad (y|y)(b|b) = 1 \qquad (23a\text{-}b)$$

$$(t|x) = 0 \qquad (a|a)(x|\delta) = (t|a) \qquad (23c\text{-}d)$$

Similar relations can be calculated at higher order and are given in Appendix A. These relations show that certain transfer map terms are proportional to other terms. From this we can see how minimizing one coefficient causes another coefficient to be minimized.

COSY Infinity as a Simulator

Difficulties arise in the study of a fragment separator from the limited software available to simulate in-flight beams. The software must be able to accurately and quickly calculate the effects of system components, including fringe

fields and higher order effects. It must also allow for separation of particles from a beam based upon charge and mass.

COSY Infinity is a differential algebra-based code that allows simulation of such a system. [12] Although the code is very powerful, it still has some limitations. In particular, the optimizers available for the system do not allow for using constrained parameters to fit solutions within a particular variable range. It was not uncommon, for example, for COSY to find a solution that focused the achromatic image of a beam by using multipoles substantially beyond the 3 Tesla design criteria limit. Another example occurred when using COSY to fit drift lengths between system elements. In some of these cases the results included non-physical negative drift lengths, effectively superimposing multipoles on top of each other.

Despite this drawback, COSY Infinity proved to be an excellent and essential tool in simulating the designs discussed later in this paper. In particular, it was used exclusively beyond the initial first order calculations.

The majority of the Figures shown in this thesis were generated using the graphing functions of COSY. To understand what is depicted in this Figures, it is important to know what they represent. All axes shown are in the scale of meters. Colors are used to distinguish between different types of magnetic elements in the system; dipoles are shown in yellow (or light gray when viewed in black and white print), quadrupoles are shown in red and other multipoles are shown in pink (or darker gray in black and white print). Rays traced by COSY represent the

maximum trajectory of isotopes at a standard energy and alternative ray traces appear in different colors to shown the effects of isotopes with differing energy. These ray traces can be compared with the apertures in the magnetic elements. These are depicted in the Figures; the quadrupoles and multipoles have a 40 cm gap both horizontal and vertical from the optical axis while the dipole gap is limited to a 10 cm vertical gap from the optical axis.

MATHEMATICA as a First Order Modeling Tool

As previously noted, COSY Infinity is a powerful simulation tool. It does, however, suffer from a major drawback of having limited built in optimizers. Another powerful computing tool was utilized to address some of the drawbacks experienced with COSY. Using Mathematica software, the beam system can be calculated to first order. The system was limited to dipole and quadrupole elements separated by drift lengths. The elements where expressed in matrix form and pole tip field strengths and drift lengths were left as variables.

To allow for quicker solution, the NMinimize optimizing function [13] was used to constrain the search for each variable within a particular range of values. The primary variables in these simulations were the drift lengths between system elements and the strengths of the quadrupole magnets. The program also allowed for variation of the lengths of the quadrupole elements, the dipole radius and angle, and conditions which needed to be met by the solution. Once a first order solution

was obtained through the Mathematica simulation, the physical layout (drift lengths, multipole lengths, dipole radius and angle) was used to set fixed parameters in further COSY simulations. The quadrupole magnet pole tip field strengths obtained from the Mathematica simulations were also used as starting values in COSY, but COSY was allow to fit the strengths independently. COSY was also used to correct for higher order effects and fringe field effects which could not be simulated in the Mathematica model.

III. FIRST ORDER DESIGN

First Order Criteria

For the first order design, the only elements we will include will be quadrupoles and dipoles. Any proposed design should address the mechanical and engineering constraints applicable to the particular project. Those constraints which were adopted in the designs considered in this paper have previously been discussed.

For all the designs considered, the system seeks to obtain point-to-point, parallel-to-parallel focusing for a segment from the target through the dispersive image. The segment was then reversed after the dispersive image to create mirror symmetry around the dispersive image. As a result of this symmetry, a design after the first segment and its inverse will focus the isotope beam point-to-point, parallel-to-parallel, to an achromatic image after the second segment. [7, 9] To maintain a high-quality beam with minimal transmission loss, the focused achromatic image should have of aberrations of less than 1 mm. [1]

From the symmetry theories previously outlined, only 5 first order terms from the transfer map matrix appear in the commutator equation. By minimizing

(x|a), (a|x), (y|b), (b|y) and (a|δ) in the transfer map through the dispersive image, the beam aberrations through the first order will also be minimized. Additionally, the first order focusing will not be affected by higher order multiples introduced later into the design. [7, 9, 10, 14]

Finally, since we are seeking to separate isotopes, we want to maximize dispersion, which we will define by the ratio (x|δ)/(x|x) of the transfer map coefficients through the dispersive image. Since the absorbing wedge will subsequently be introduced at the dispersive image to select a particular mass isobar, the resolution of the separator will link directly to the dispersion of the system segment. This qualitative factor will help in evaluating the efficiency of a proposed design.

Possible Design Layouts

Within our criteria, multiple designs for a system are possible. The next sections examine a variety of possible first order design layouts.

Non-Symmetric Model

The non-symmetric model seeks to find the simplest design that will satisfy the first order criteria. This design has no mirror symmetry within the segment from the target through the dispersive image. This design uses only 4 quadrupoles in the

segment (2 per plane) to achieve the desired point-to-point, parallel-to-parallel focusing. The result is one focusing (F) and one defocusing (D) quadrupole on each side of the dipole in the segment. For this design, four possible configurations of the order of quadrupoles are available.

For the first configuration choice, D-F-F-D, no solution was found that minimized all 5 critical transfer map terms. The horizontal and vertical projections of this layout are shown in Figures 4 and 5. The best solution, which only minimized 2 terms, also had 2 drift lengths exceeding two meters, and average dispersion (~ 1.6).

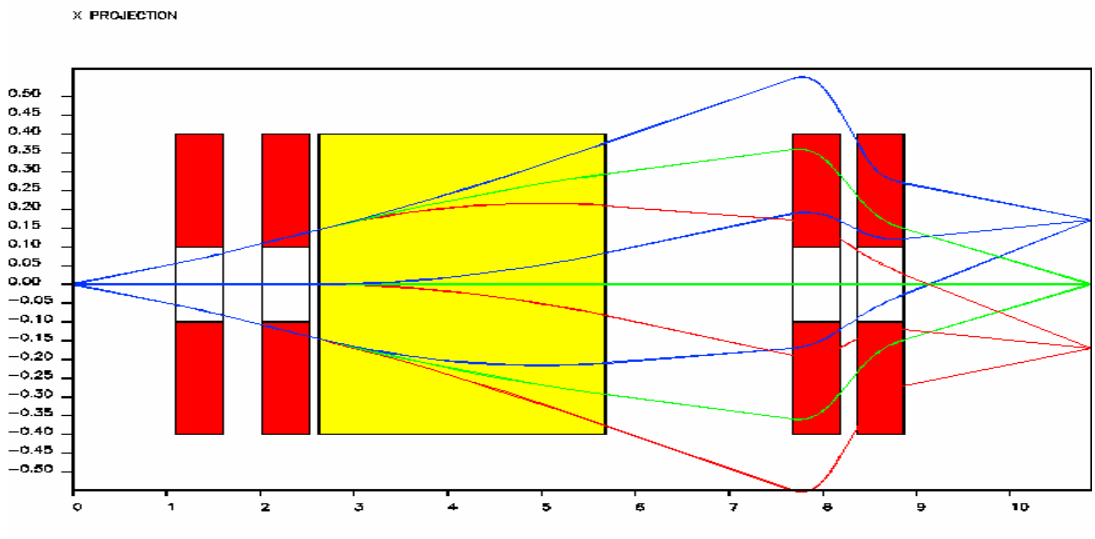

Figure 4. First order nonsymmetric (DFFD) layout – horizontal projection.

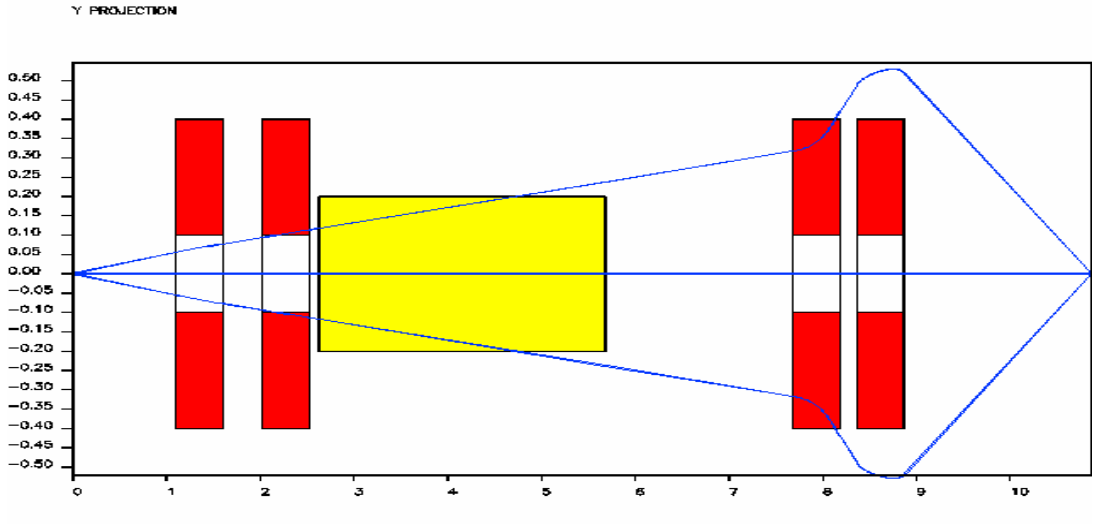

Figure 5. First order nonsymmetric (DFFD) layout – vertical projection.

The second configuration choice, D-F-D-F, did minimize all 5 critical transfer map coefficients and had very poor dispersion (~.42). The horizontal and vertical projections of this layout are shown in Figures 6 and 7. The vertical beam width, however, was nearly 50 cm. through the 10 cm. dipole gap.

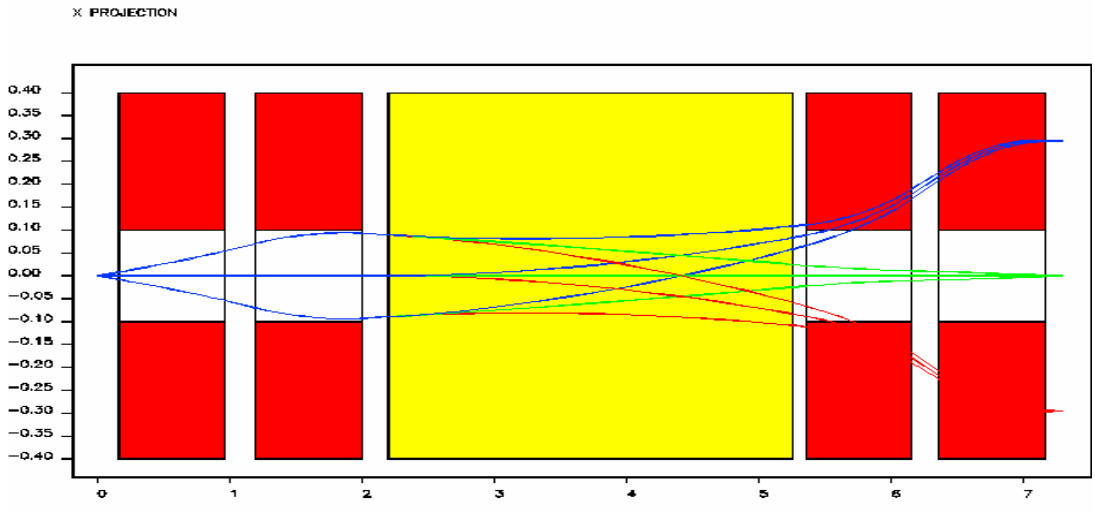

Figure 6. First Order Nonsymmetric (DFDF) Layout – Horizontal Projection.

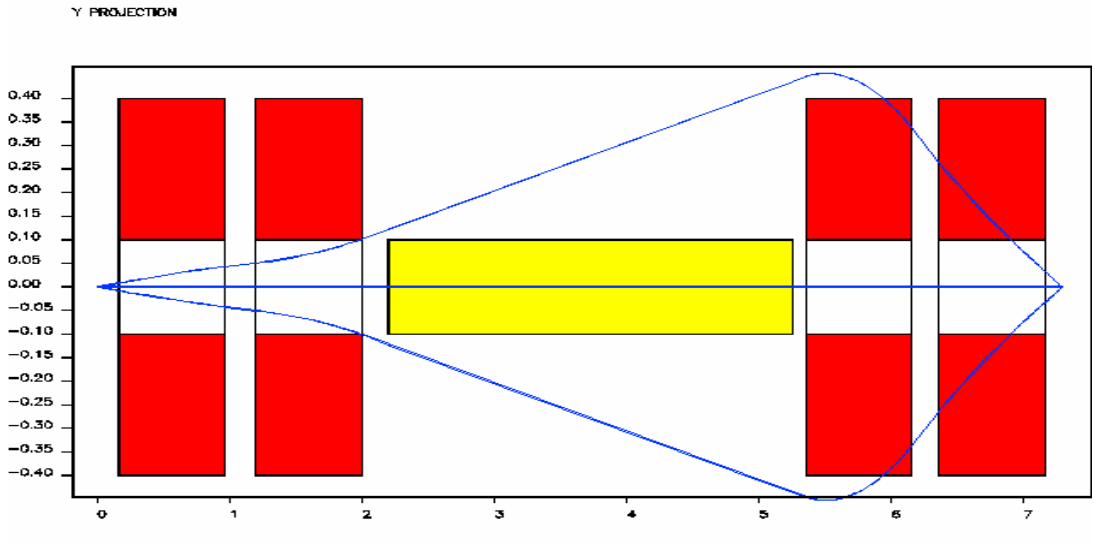

Figure 7. First order nonsymmetric (DFDF) layout – vertical projection.

The third configuration considered, F-D-D-F, also failed to minimize the 5 critical transfer map terms. The horizontal and vertical projections of this layout are shown in Figures 8 and 9. It also suffers for a vertical beam width of more than 35 cm through the dipole and two large drift lengths. It also had very poor dispersion (~.28).

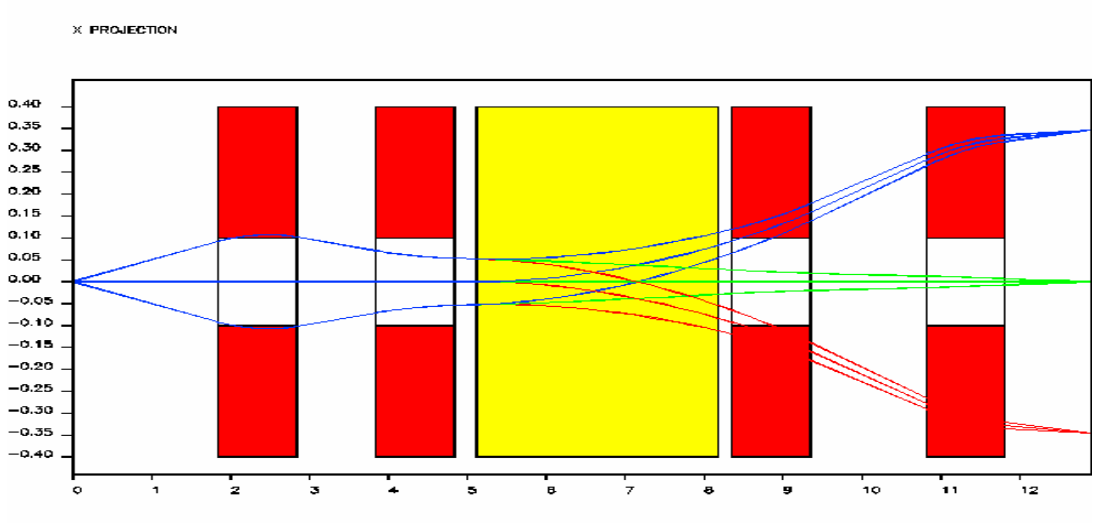

Figure 8. First order nonsymmetric (FDDF) layout – horizontal projection.

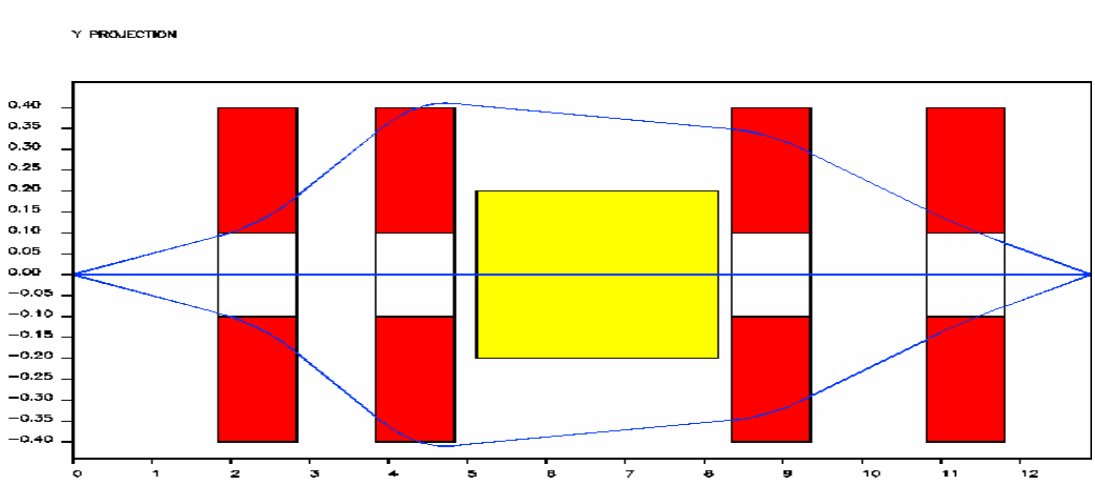

Figure 9. First order nonsymmetric (FDDF) layout – vertical projection.

The final configuration, F-D-F-D, was far superior to the other three. It minimized all 5 critical transfer map terms, and had reasonable dispersion (~1.8). The horizontal and vertical projections of this layout are shown in Figures 10 and 11. The vertical beam width was within the dipole gap, and the horizontal beam

width was only slightly above the desired limit. Also, the drift length and the quadrupole pole tip field strengths were reasonable.

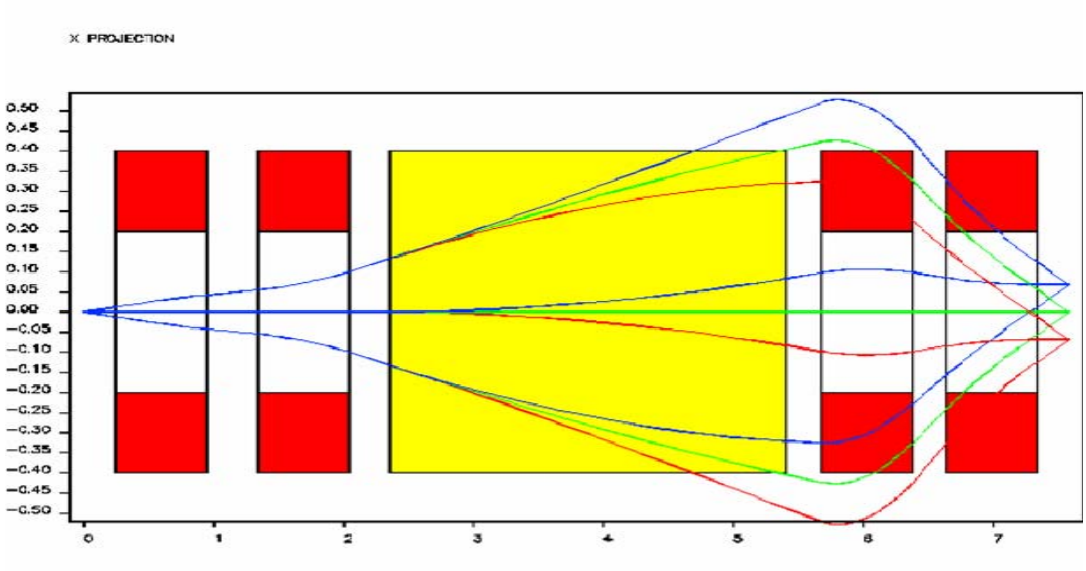

Figure 10. First order nonsymmetric (FDFD) layout – horizontal projection.

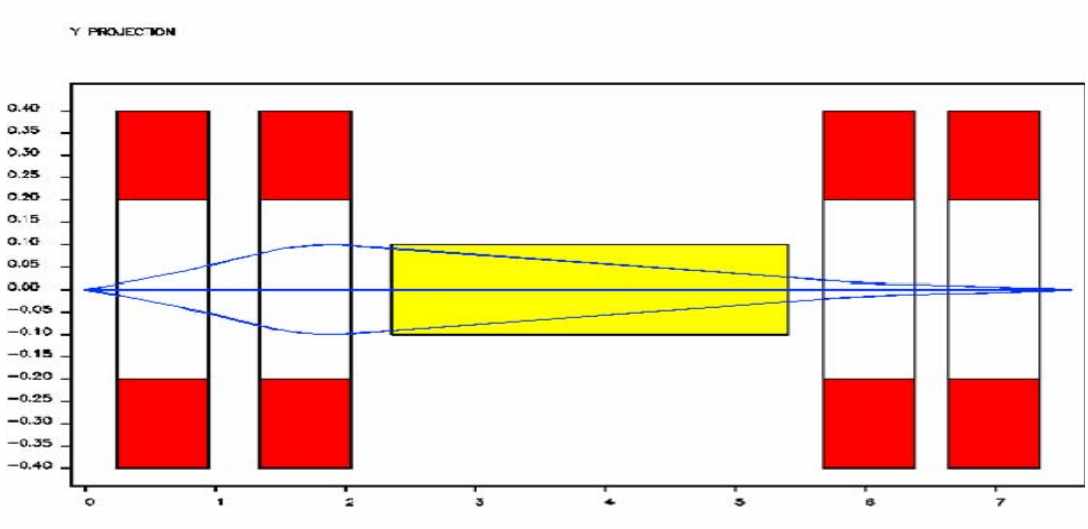

Figure 11. First order nonsymmetric (FDFD) layout – vertical projection.

First Symmetric Model

Another possible design utilizes mirror symmetry in the cell around the middle of the dipole magnet. Because of this extra symmetry within the layout of the segment, the symplectic, midplane, and mirror symmetry theories allow determination of conditions in the transfer map through the middle of the dipole that achieve point-to-point, parallel-to-parallel focusing at the dispersive image. The first set of such conditions is to require point-to-point, parallel-to-parallel focusing in the middle of the dipole. Thus, our criteria for the simulation is to minimize $(x|x)_M$ $(a|a)_M$ $(y|b)_M$ and $(b|y)_M$. [9] Then, reversing the system after the dipole will guarantee such focusing is maintained at the dispersive image. We can look back to the example of the first order transfer map, assuming energy constancy, time independence, midplane symmetry, and omitting the r_5 time-dependent terms for simplification. We will denote the transfer map through the dispersive image and the middle of the dipole by T_D and T_M, respectively.

$$T_D = T_M \circ T_{MR} = T_M \circ R \circ T_M^{-1} \circ R$$

$$T_D = \begin{bmatrix} 0 & (x|a) & 0 & 0 & (x|\delta) \\ (a|x) & 0 & 0 & 0 & (a|\delta) \\ 0 & 0 & 0 & (y|b) & 0 \\ 0 & 0 & (b|y) & 0 & 0 \\ 0 & 0 & 0 & 0 & 1 \end{bmatrix} \begin{bmatrix} 1 & 0 & 0 & 0 & 0 \\ 0 & -1 & 0 & 0 & 0 \\ 0 & 0 & 1 & 0 & 0 \\ 0 & 0 & 0 & -1 & 0 \\ 0 & 0 & 0 & 0 & 1 \end{bmatrix} \begin{bmatrix} 0 & \frac{1}{(a|x)} & 0 & 0 & -\frac{(a|\delta)}{(a|x)} \\ \frac{1}{(x|a)} & 0 & 0 & 0 & -\frac{(x|\delta)}{(x|a)} \\ 0 & 0 & 0 & \frac{1}{(b|y)} & 0 \\ 0 & 0 & \frac{1}{(y|b)} & 0 & 0 \\ 0 & 0 & 0 & 0 & 1 \end{bmatrix} \begin{bmatrix} 1 & 0 & 0 & 0 & 0 \\ 0 & -1 & 0 & 0 & 0 \\ 0 & 0 & 1 & 0 & 0 \\ 0 & 0 & 0 & -1 & 0 \\ 0 & 0 & 0 & 0 & 1 \end{bmatrix}$$

$$T_D = \begin{bmatrix} 0 & (x|a) & 0 & 0 & (x|\delta) \\ (a|x) & 0 & 0 & 0 & (a|\delta) \\ 0 & 0 & 0 & (y|b) & 0 \\ 0 & 0 & (b|y) & 0 & 0 \\ 0 & 0 & 0 & 0 & 1 \end{bmatrix} \begin{bmatrix} 0 & -\frac{1}{(a|x)} & 0 & 0 & -\frac{(a|\delta)}{(a|x)} \\ -\frac{1}{(x|a)} & 0 & 0 & 0 & -\frac{(x|\delta)}{(x|a)} \\ 0 & 0 & 0 & -\frac{1}{(b|y)} & 0 \\ 0 & 0 & -\frac{1}{(y|b)} & 0 & 0 \\ 0 & 0 & 0 & 0 & 1 \end{bmatrix} \tag{24}$$

$$T_D = \begin{bmatrix} -\frac{(x|a)}{(x|a)} & 0 & 0 & 0 & -\frac{2(a|\delta)}{(a|x)} \\ 0 & -\frac{(a|x)}{(a|x)} & 0 & 0 & 0 \\ 0 & 0 & -\frac{(y|b)}{(y|b)} & 0 & 0 \\ 0 & 0 & 0 & -\frac{(b|y)}{(b|y)} & 0 \\ 0 & 0 & 0 & 0 & 1 \end{bmatrix} = \begin{bmatrix} -1 & 0 & 0 & 0 & -\frac{2(a|\delta)}{(a|x)} \\ 0 & -1 & 0 & 0 & 0 \\ 0 & 0 & -1 & 0 & 0 \\ 0 & 0 & 0 & -1 & 0 \\ 0 & 0 & 0 & 0 & 1 \end{bmatrix}$$

To minimize $(x|x)_M$, $(a|a)_M$, $(y|y)_M$, and $(b|b)_M$, we use 4 quadrupoles (2 focusing and 2 defocusing) in front of the dipole. As was the case with the non-symmetric design, 4 configurations are possible.

The first case, D-F-F-D, minimized the 4 critical transfer map terms, but had a horizontal envelope of more than 70 cm. and the resolution was poor (~1.3). The horizontal and vertical projections of this layout are shown in Figures 12 and 13.

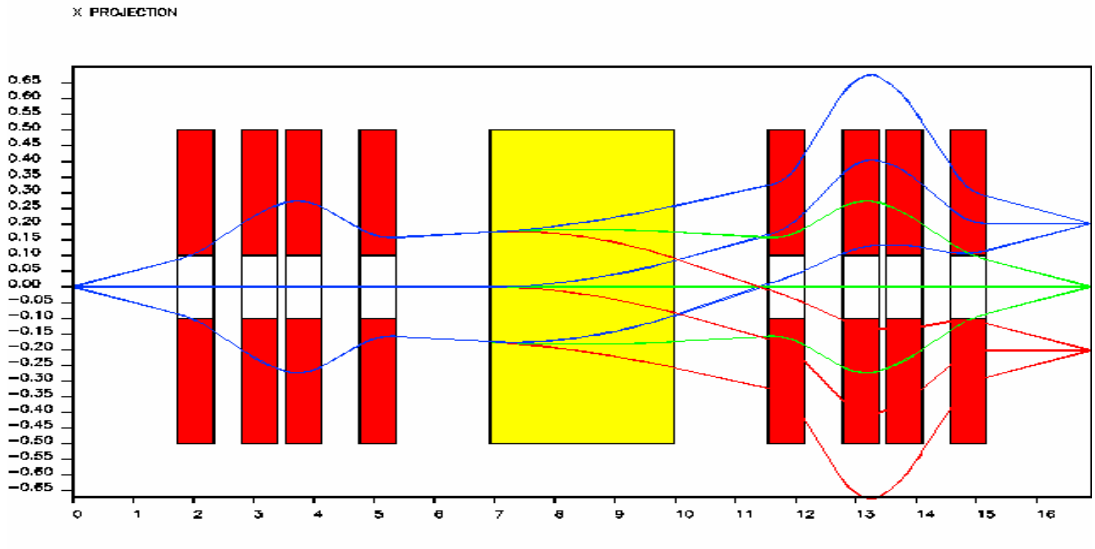

Figure 12. First order type I symmetric (DFFD) layout – horizontal projection.

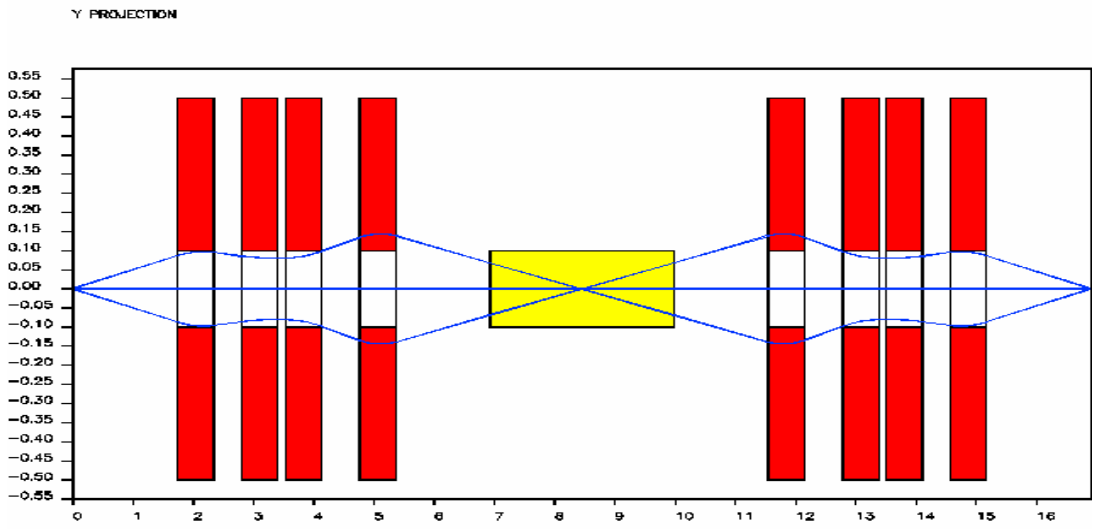

Figure 13. First order type I symmetric (DFFD) layout – vertical projection.

The second case, D-F-D-F, also minimized the 4 critical transfer map terms and had reasonable resolution (~1.6). The horizontal and vertical projections of this

layout are shown in Figures 14 and 15. This design was rejected because the horizontal beam width was nearly 65 cm.

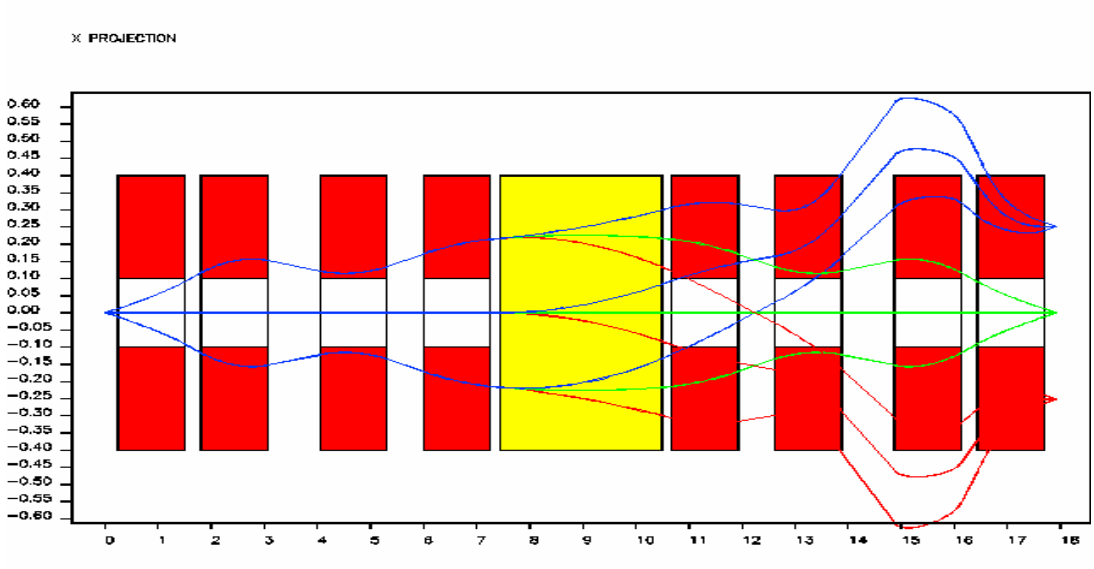

Figure 14. First order type I symmetric (DFDF) layout – horizontal projection.

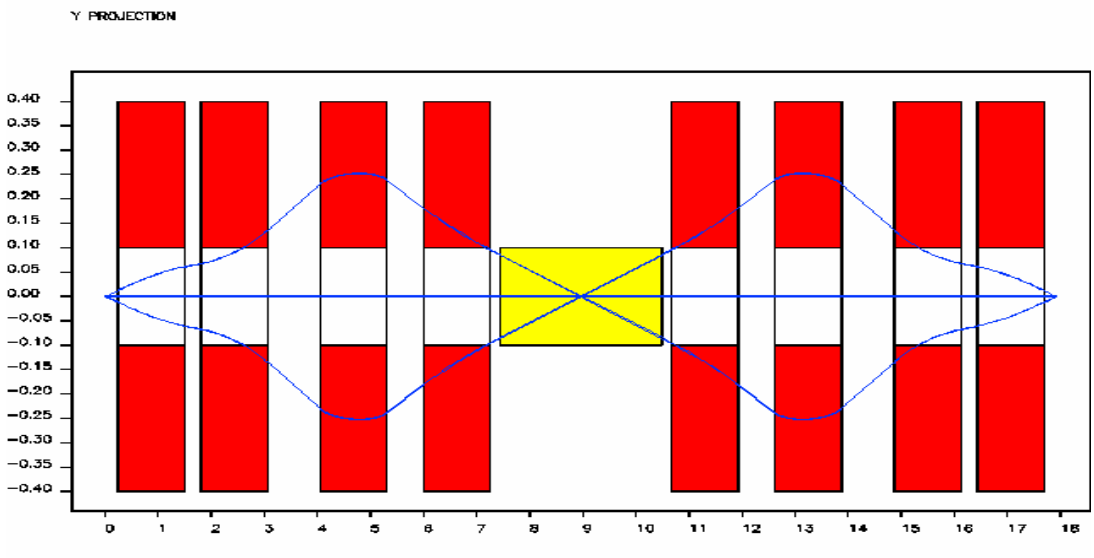

Figure 15. First order type I symmetric (DFDF) layout – vertical projection.

For the third case, F-D-D-F, no solution was found that minimized all four critical transfer map terms. The horizontal and vertical projections of this layout are shown in Figures 16 and 17. The horizontal beam width was also larger 65 cm.

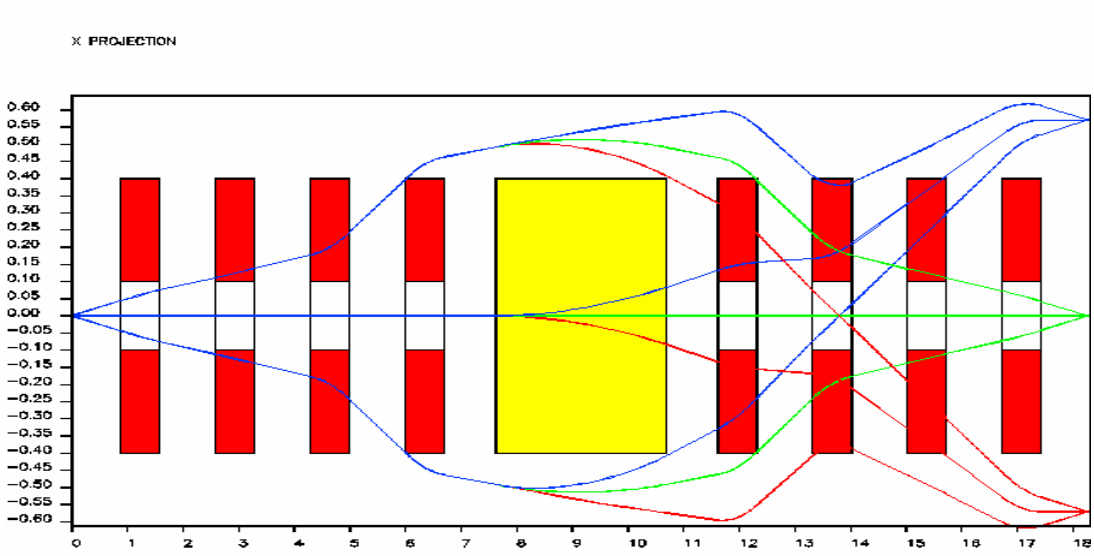

Figure 16. First order type I symmetric (FDDF) layout – horizontal projection.

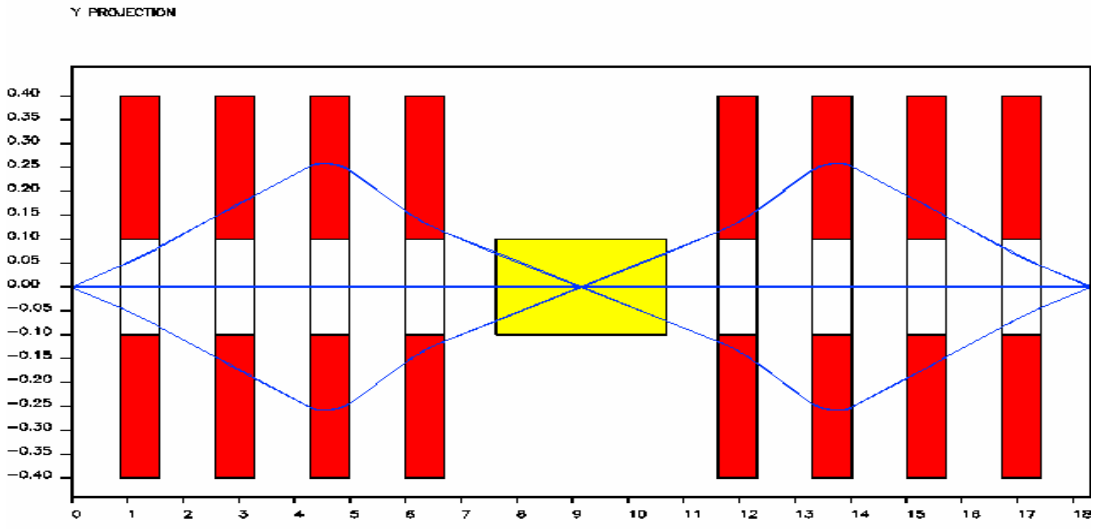

Figure 17. First order type I symmetric (FDDF) layout – vertical projection.

The final case, F-D-F-D, did minimize the 4 critical transfer map terms. The design was rejected because of its poor resolution (~1.15). The horizontal and vertical projections of this layout are shown in Figures 18 and 19.

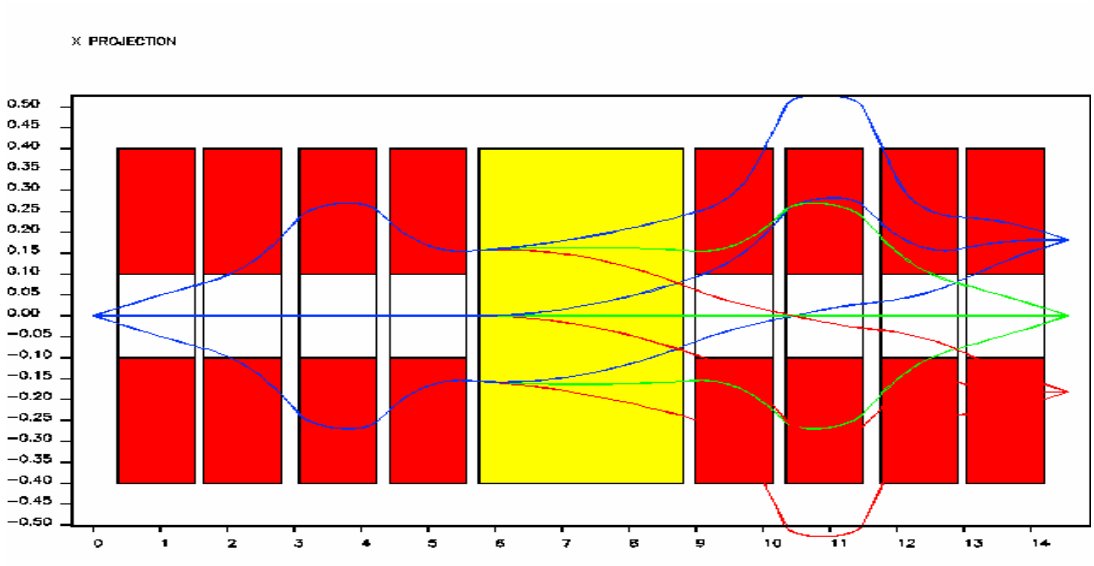

Figure 18. First order type I symmetric (FDFD) layout – horizontal projection.

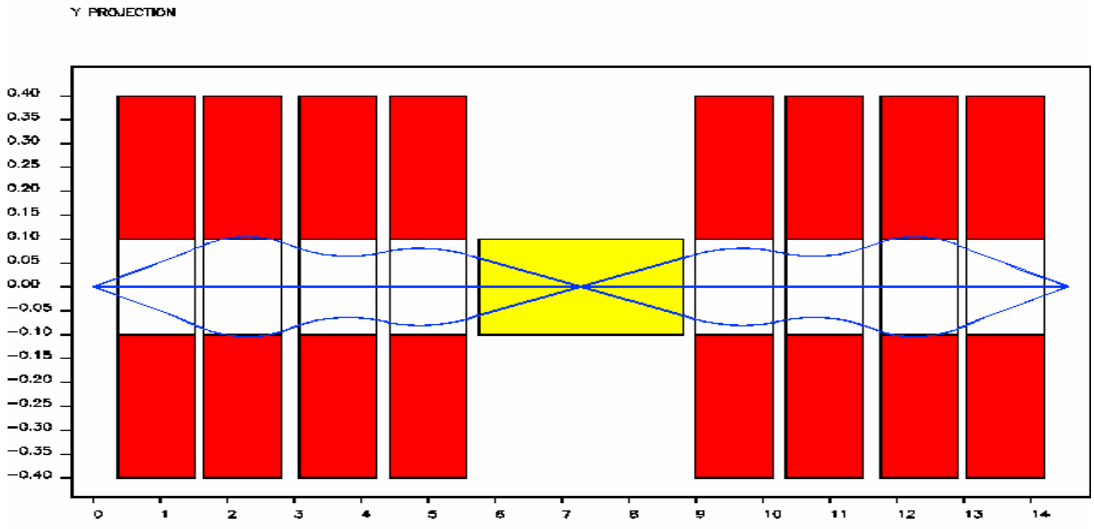

Figure 19. First order type I symmetric (FDFD) layout – vertical projection.

Second Symmetric Model

The third design considered is a variation of the previous model. The condition chosen in the middle of the dipole in the previous case was actually more restrictive than necessary. By requiring point-to-parallel, parallel-to-point imaging in the middle of the dipole, we also achieve point-to-point, parallel-to-parallel focusing at the dispersive image. Thus, our criteria is for the simulation to minimize $(x|x)_M$, $(a|a)_M$, $(y|y)_M$, and $(b|b)_M$. [9] To achieve this, 4 quadrupoles (2 focusing and 2 defocusing) are used in front of the dipole. Again, this leads to 4 possible configurations to consider.

The first case, D-F-F-D, allowed all four critical transfer map terms to be minimized. The horizontal and vertical projections of this layout are shown in Figures 20 and 21. The resolution, however, was poor (~1.2). The vertical beam width was almost 35 cm. and one of the drift lengths was only 10 cm.

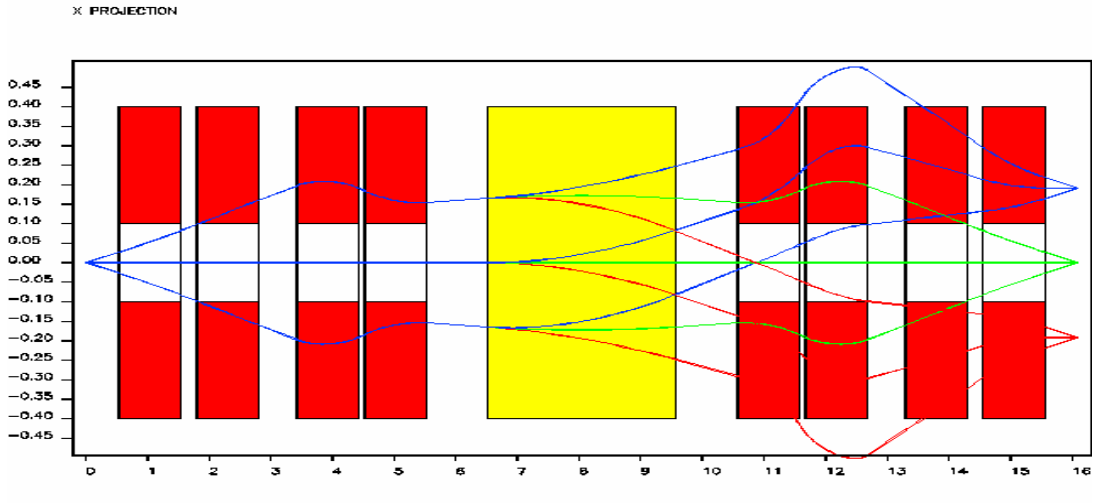

Figure 20. First order type II symmetric (DFFD) layout – Horizontal projection.

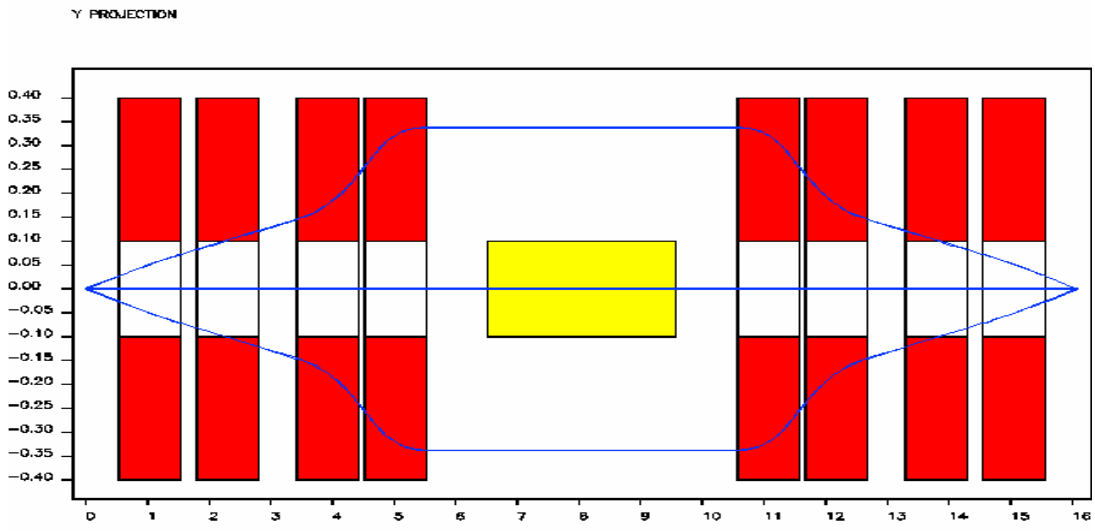

Figure 21. First order type II symmetric (DFFD) layout – vertical projection.

The second case, D-F-D-F, met all criteria except for the vertical beam width, which was 15 cm. The horizontal and vertical projections of this layout are shown in Figures 22 and 23. The resolution was good (~1.8), and magnet strengths and drift were reasonable.

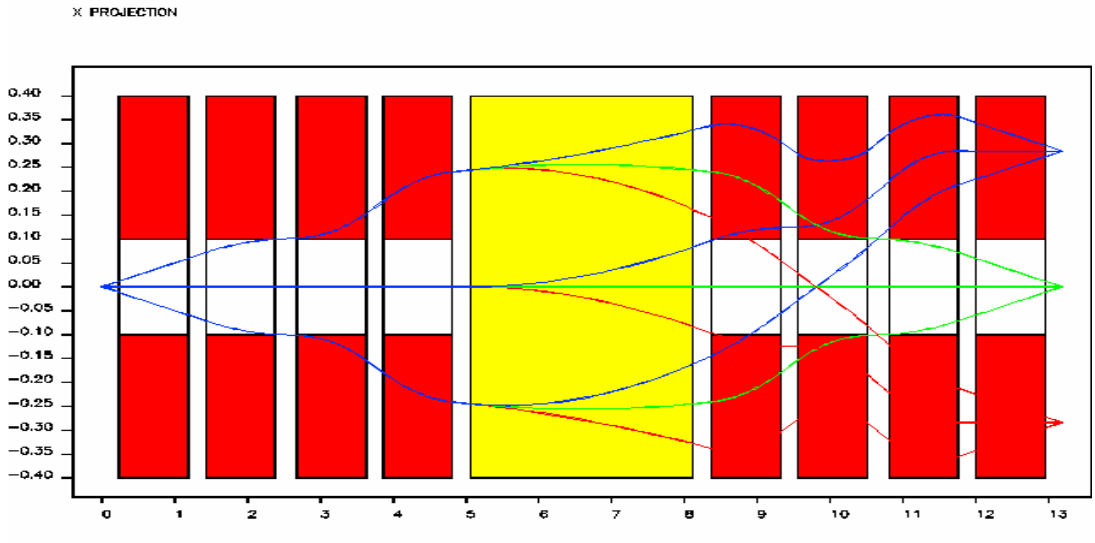

Figure 22. First order type II symmetric (DFDF) layout – horizontal projection.

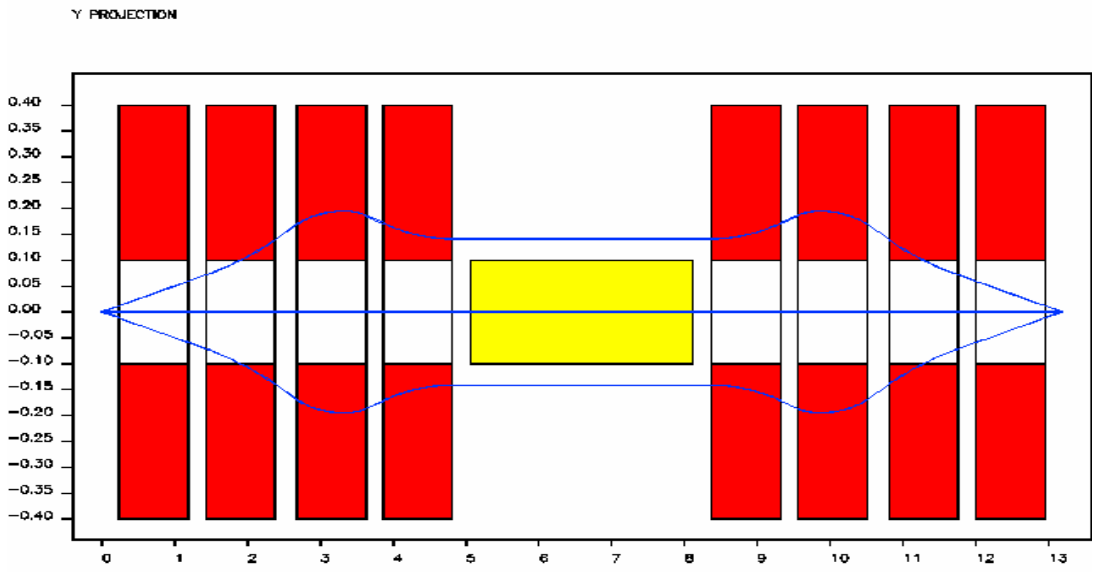

Figure 23. First order type II symmetric (DFDF) layout – vertical projection.

The third case, F-D-D-F, also met all criteria. The horizontal and vertical projections of this layout are shown in Figures 24 and 25. The resolution was very

good (~2.25), and the vertical beam width was only 12 cm. The magnet strengths and drift lengths were also reasonable.

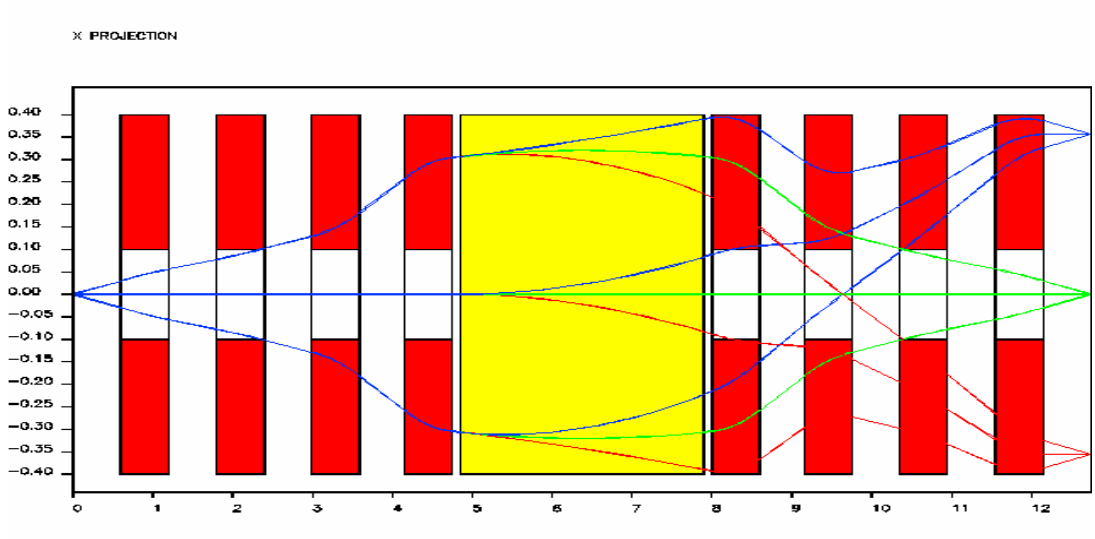

Figure 24. First order Type II symmetric (FDDF) layout – horizontal projection.

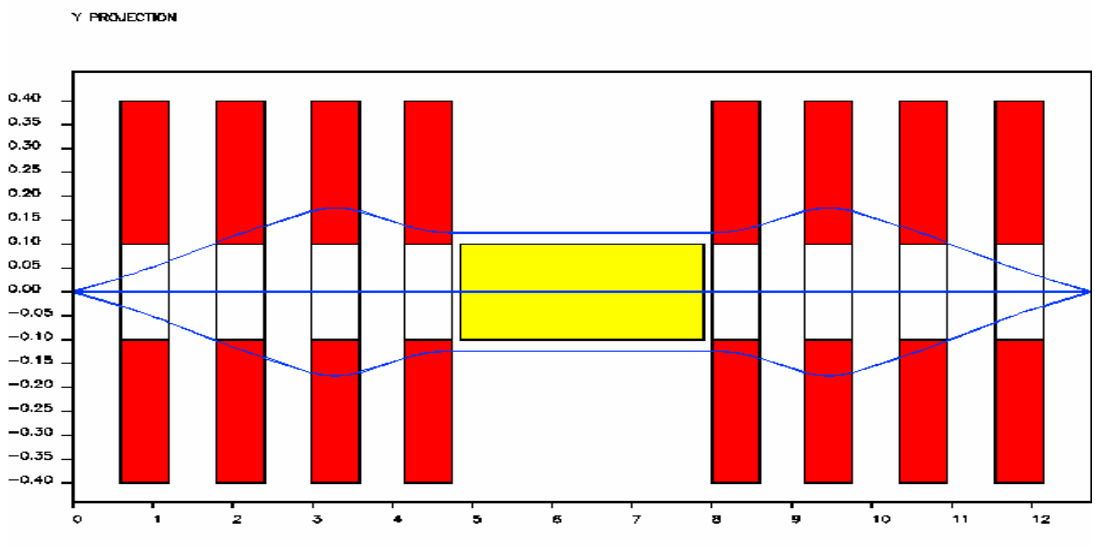

Figure 25. First order type II symmetric (FDDF) layout – vertical projection.

The final case, F-D-F-D, minimized all 4 critical transfer map terms, but had poor resolution (~1.3). The horizontal and vertical projections of this layout are shown in Figures 26 and 27. Also, the vertical beam width was 20 cm.

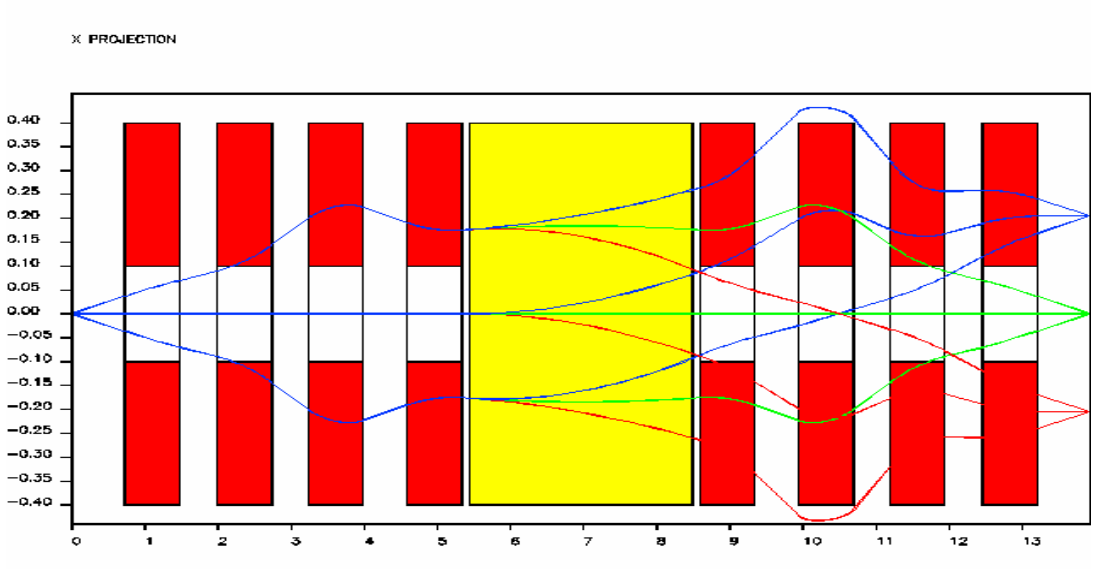

Figure 26. First order type II symmetric (FDFD) layout – horizontal projection.

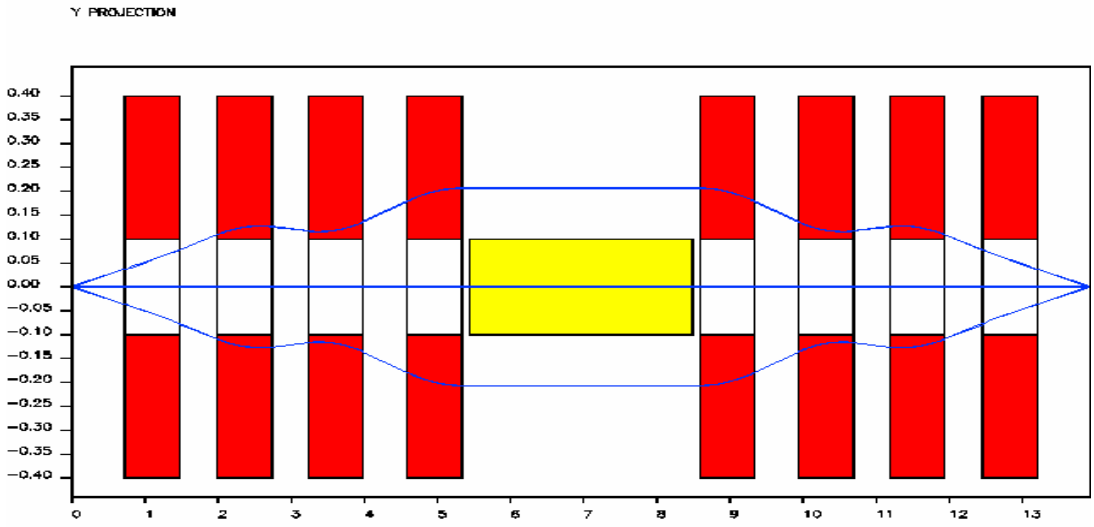

Figure 27. First order type II symmetric (FDFD) layout – vertical projection.

Triplet Model

In the triplet model, mirror symmetry is maintained around the dipole, but only three quadrupoles are used on each side of the dipole. At initial glance, this is a surprising result since the condition for a solution seeks to minimize 4 transfer map terms at the middle of the dipole. We would normally expect that 4 independent quadrupoles are required to achieve a solution except in an exotic or trivial case.

The reduction in the number of independent quadrupoles needed to achieve a solution arises from a "hidden" constraint in the system. For all of the elements in the system (i.e., quadrupoles, drifts and dipole), the map terms (x|x) = (a|a). [7, 9, 15]

The solutions for this layout also reflect a number of simulation solutions from the symmetric design where the pole tip field strength of one of the 4 quadrupoles was at least an order of magnitude less than the other three. In all these cases, the configuration was F-D-F. The best results for this layout met all criteria and had very good resolution (~2.22). The horizontal and vertical projections of this

layout are shown in Figures 28 and 29. The magnet strengths and drift lengths were reasonable. The vertical beam width was about 14 cm.

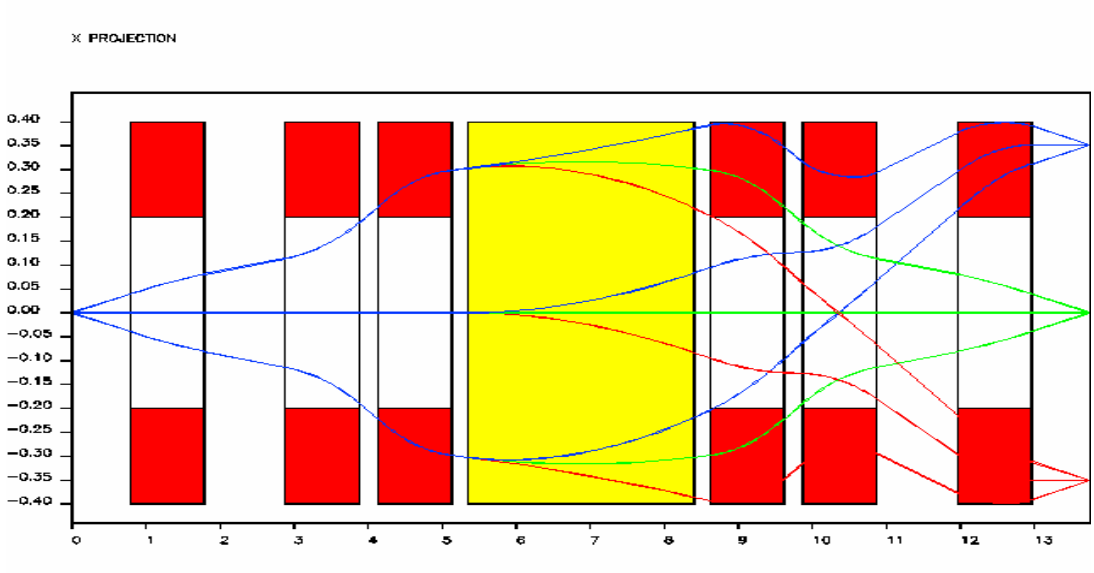

Figure 28. First order triplet (FDF) layout – horizontal projection.

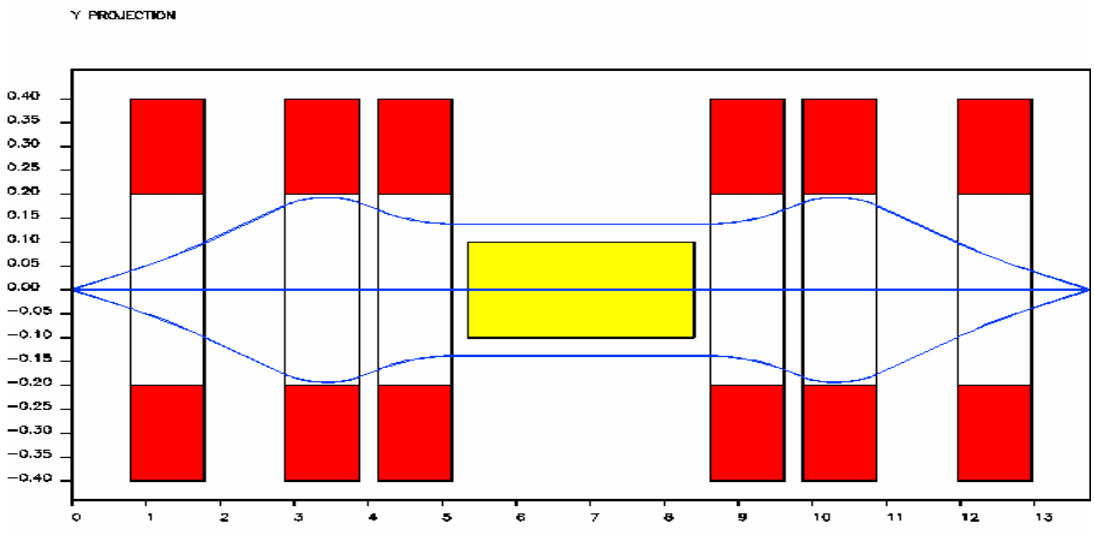

Figure 29. First order triplet (FDF) layout – vertical projection.

Other Designs Considered

In addition to the previously discussed first order layouts, other design variations were considered. These included varying the dipole radius from 25 to 40 degrees, varying the dipole radius from 4 to 6 meters, varying the lengths of the multipoles used, and using combinations of more than 2 sets of focusing-defocusing quadrupole doublets. For these configurations, as well as the layout designs discussed above, the ranges for drift lengths and multipole strengths were also varied. Also, the starting values for the variables in each type of simulation were varied.

With respect to variation in the dipole radius and angle, solutions within the ranges tested were fairly easy to obtain and consistent with those for the 35 degree angle, 5 meter radius dipole models. Changes in the dipole radius and angle did effect dispersion, but not dramatically. Ultimately, the radius and angle used in the selected layout were chosen because of the physical footprint from a possible site for the RIA facility.

For example, using a 25 degree dipole angle in the 2nd symmetric layout and the F-D-D-F configurations yielded a solution with dispersion of approximately

1.46. All other criteria of the first order design were satisfied. The horizontal and vertical projections of this layout are shown in Figures 30 and 31.

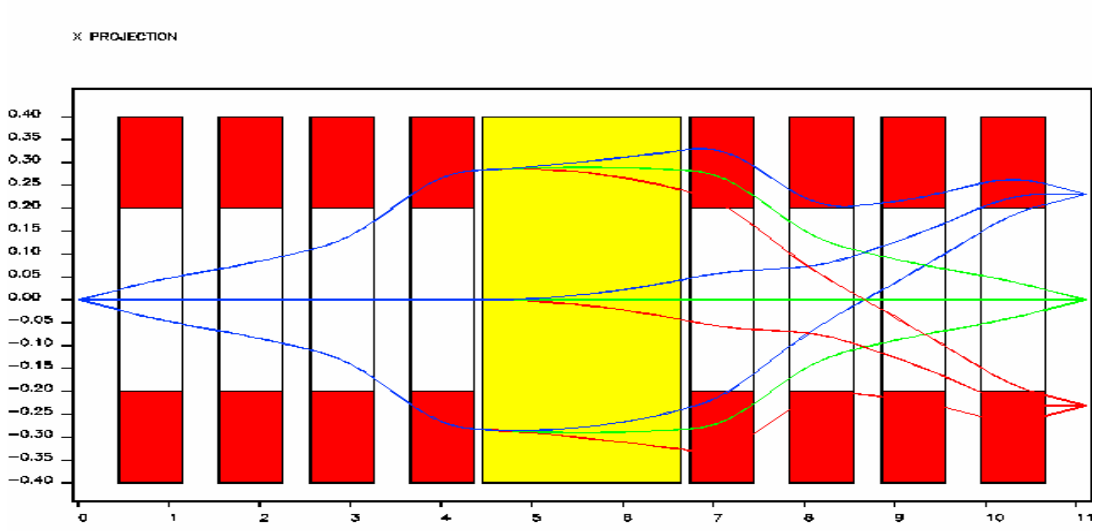

Figure 30. First order type II symmetric (FDDF) layout – 25 degree dipole – horizontal projection.

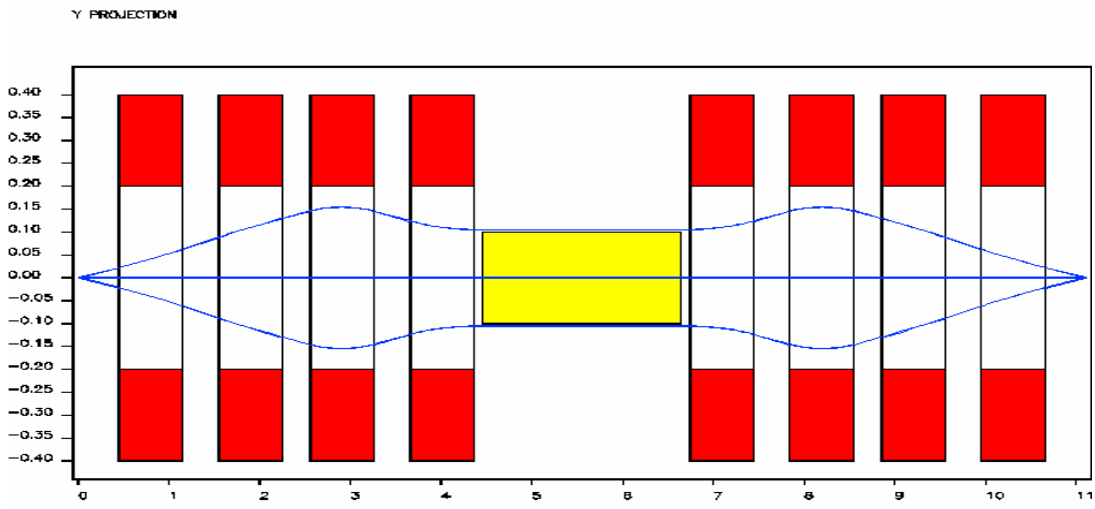

Figure 31. First order type II symmetric (FDDF) layout – 25 degree dipole – vertical projection.

When the dipole angle was increased to 45 degrees, a similar solution was found for the same layout. The horizontal and vertical projections of this layout are

shown in Figures 32 and 33. This solution, however, had dispersion of 2.27, and a wider vertical beam width. Otherwise, all first order criteria were satisfied.

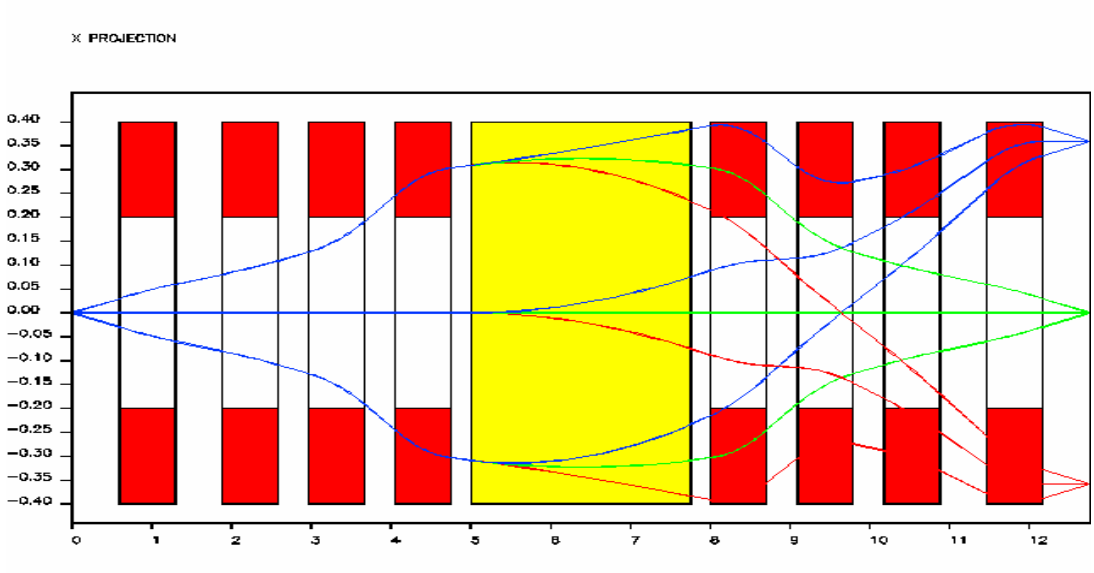

Figure 32. First order type II symmetric (FDDF) layout – 45 degree dipole – horizontal projection.

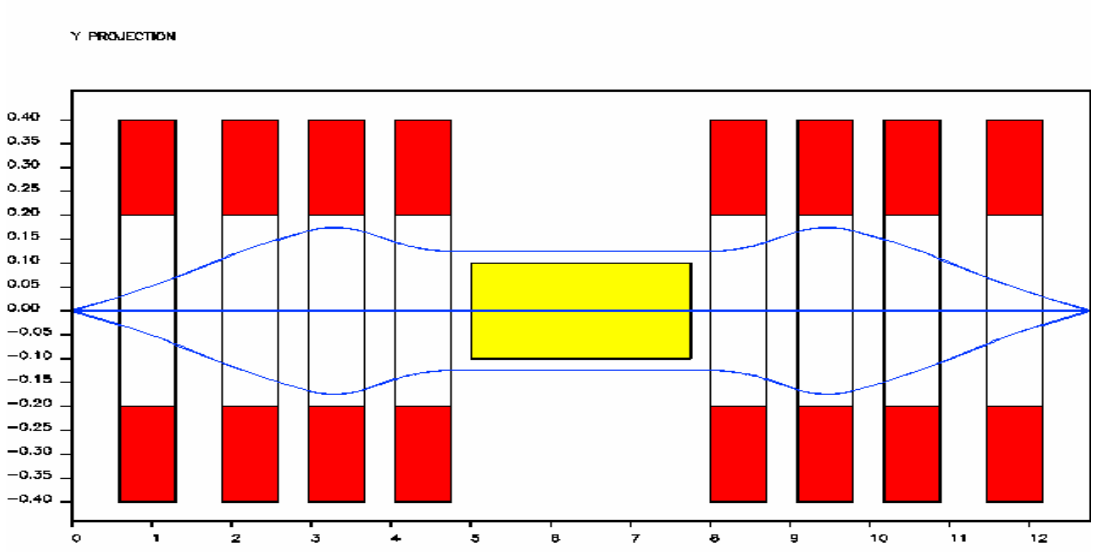

Figure 33. First order type II symmetric (FDDF) layout – 45 degree dipole – vertical projection.

In each simulation type, the length of the quadrupoles did prove to be a critical variable. Repeated testing showed that there was an optimal length for the quadrupoles, but that this optimal length varied from 60 cm. to 1.25 cm. in different layouts. As the length of the quadrupole elements was increased or decreased from its optimal value, it became more difficult to find solutions that had reasonable values for beam width, drift lengths and quadrupole strengths. The quadrupole length selected for each proposed segment design was the optimal length for that particular design as determine by repeated simulation.

Selection of First Order Design

Using the various symmetry theories, a variety of different systems of quadrupoles and dipoles were found to satisfy the first order criteria for a fragment separator design. From all the first order systems previously discussed, 3 were selected as possible design layouts: the best non-symmetric design (F-D-F-D configuration), the best symmetric design (F-D-D-F configuration of 2nd symmetric design), and the triplet design. All three of these designs minimized all 5 critical commutator terms in the transfer map through the dispersive image. All 3 had reasonable values for the drift lengths and pole tip field strengths. Also, all three had reasonable horizontal and vertical beam widths.

Table 1 gives a comparison of the three designs. The first order objective reflects the sum total of all 5 critical transfer map terms through the dispersive

image. The triplet design was very similar in terms of results to the symmetric design. It was selected for further consideration, however, because it represented a substantial number of solutions to the symmetric model simulation where the pole tip field of one of the four quadrupoles was substantially weaker than those of the other three.

Table 1

Comparison of the Components for the Three Best First Order Design Layouts.

1st Order Map Elements	**BEST SYMMETRIC**	**BEST NONSYMMETRIC**	**BEST TRIPLET**
x|a	1.433648E-11	1.704820E-11	1.221245E-15
a|x	1.746147E-09	4.429634E-11	1.276756E-15
y|b	2.795170E-11	1.749401E-11	1.554312E-15
b|y	2.078318E-08	4.528335E-11	1.433765E-04
a|δ	1.685740E-11	4.946276E-04	1.443290E-15
1^{st} order objective	2.258847E-08	4.946277E-04	1.433765E-04

max. X-projection (meters)	0.420	0.550	0.400
max. Y-projection (meters)	0.130	0.090	0.140
Xδ/xx	2.352	1.969	2.224

IV. SECOND ORDER DESIGN

Second Order Criteria

For the second order system, the layout will be modified to correct for the aberrations introduced by second order effects. This is done by superimposing sextupoles onto the quadrupole magnets. [9, 14] The quadrupole positions and strengths remain fixed.

At first order, we looked at a system which obeyed energy constancy, time-independence and mid-plane symmetry. The position of a particle traveling to the dispersive image in such a system can be expressed as follows [4, 7]:

$$x_D = (x \mid x)_D x_0 + (x \mid a)_D a_0 + (x \mid \delta)_D \delta_0 = x_0 + (x \mid \delta)\delta_0 \tag{25}$$

$$y_D = (y \mid y)_D y_0 + (y \mid b)_D b_0 \ = y_0 \tag{26}$$

The right most solution of these equations has been simplified by using the first order focusing criteria for the dispersive image: $(x|x)_D = (y|y)_D = 1$ and $(x|a)_D = (y|b)_D = 0$. At second order, the equations for the position of a particle traveling to the dispersive image are as follow [4, 7]:

$$x_D = (x|x)_D x_0 + (x|a)_D a_0 + (x|\delta)_D \delta_0 + (x|xx)_D x_0^2 + (x|xa)_D x_0 a_0 + (x|x\delta)_D x_0 \delta_0 + (x|aa)_D a_0^2 + (x|a\delta)_D a_0 \delta_0 + (x|yy)_D y_0^2 + (x|yb)_D y_0 b_0 + (x|bb)_D b_0^2 + (x|\delta\delta)_D \delta_0^2 \quad (27)$$

$$y_D = (y|y)_D y_0 + (y|b)_D b_0 + (y|yy)_D y_0^2 + (y|yb)_D y_0 b_0 + (y|bb)_D b_0^2 + (y|xx)_D x_0^2 + (y|xa)_D x_0 a_0 + (y|aa)_D a_0^2 + (y|\delta\delta)_D \delta_0^2 \quad (28)$$

The effect of the second order terms is to skew the focal plane of the system at the dispersive image. This skew can be expressed by the tilt angle θ where [4]:

$$\tan\theta = -\frac{(x \mid \delta)}{(x \mid x)(x \mid a\delta)} \quad (29)$$

This we be illustrated by examples presented later in this chapter. If we apply the symplectic and mirror symmetry relations to these equations, however, we can simplify the second order equations. Another consideration is the requirement that the beam be focused at the achromatic image. This is, in fact, the real design goal of our system. To accomplish this, we will seek to minimize all the second order coefficients from the transfer map through the dispersive image that appear in the commutator equation. As specified in Table 2, there are 15 second order terms appearing in the commutator equation:

Table 2

Second Order Terms Appearing in the Commutator Equation.

$(x|xa)_D$ $(x|a\delta)_D$ $(x|yb)_D$

$(a|xx)_D$ $(a|x\delta)_D$ $(a|aa)_D$ $(a|yy)_D$ $(a|bb)_D$ $(a|\delta\delta)_D$

$(y|xb)_D$ $(y|ay)_D$ $(y|b\delta)_D$

$(b|xy)_D$ $(b|ab)_D$ $(b|y\delta)_D$

By examining the proportionality relations from the design's symplectic symmetry, we see that five of the coefficients are simultaneously minimized along with the other 10. These relations are listed below in Table 3 [8]:

Table 3

Symplectic Relations Between Second Order Commutator Terms.

$(a\|aa)\ \alpha\ (x\|xa)$	$(x\|yb)\ \alpha\ (b\|ab)\ \alpha\ (y\|ay)$
$(a\|bb)\ \alpha\ (y\|xb)$	$(a\|yy)\ \alpha\ (b\|xy)$

The symplectic condition also yields several useful relations of proportionality between non-commutator terms. These are listed in Appendix A. This analysis leads to the primary criteria for the second order system. It should minimize the coefficients $(x|a\delta)_D$, $(a|xx)_D$, $(a|x\delta)_D$, $(a|aa)_D$, $(a|yy)_D$, $(a|bb)_D$, $(a|\delta\delta)_D$, $(y|b\delta)_D$, $(b|ab)_D$, $(b|y\delta)_D$. Satisfying this criterion will result in a system that is focused point-to-point, parallel-to-parallel at the achromatic image.

The secondary criteria would be to achieve a focused dispersive image that minimizes the skewing effect of the second order aberrations. This effect become problematic when the absorbing wedge in introduced because of stochastic effects within the wedge itself. These effects are at a minimum when the image plane is perpendicular to the beam at the dispersive image.

Theory Applied to Positioning of Sextupoles

We have already determined that sextupoles will be used to correct the second order aberrations in the optical system. Superimposing sextupoles onto the existing quadrupole in the system is a cost effective approach. Such a system would generally be easier to build than one with independent sextupoles. Will such placement allow the second order aberration to be corrected?

The method to determine optimal placement of sextupoles is discussed extensively by Brown. [14] Using this method, the coupling coefficients can be mapped as a function of the beam through the system. [2, 14] This was done by plotting independent changes throughout the system for each of variables, x, a, y, b, and δ with COSY. The transfer map and coupling coefficients can then be determined as a function of position in the system. This was done for each of the three selected first order system designs. The results are contained in the plots shown in Figures 34, 35 and 36.

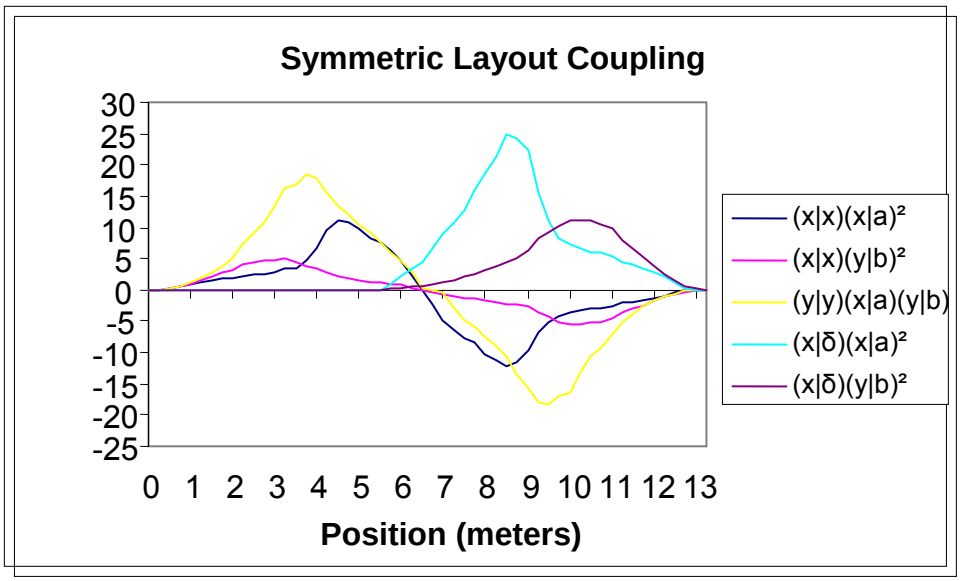

Figure 34. Plot of sextupole coupling coefficients as a function of position within the fragment separation for symmetric design layout.

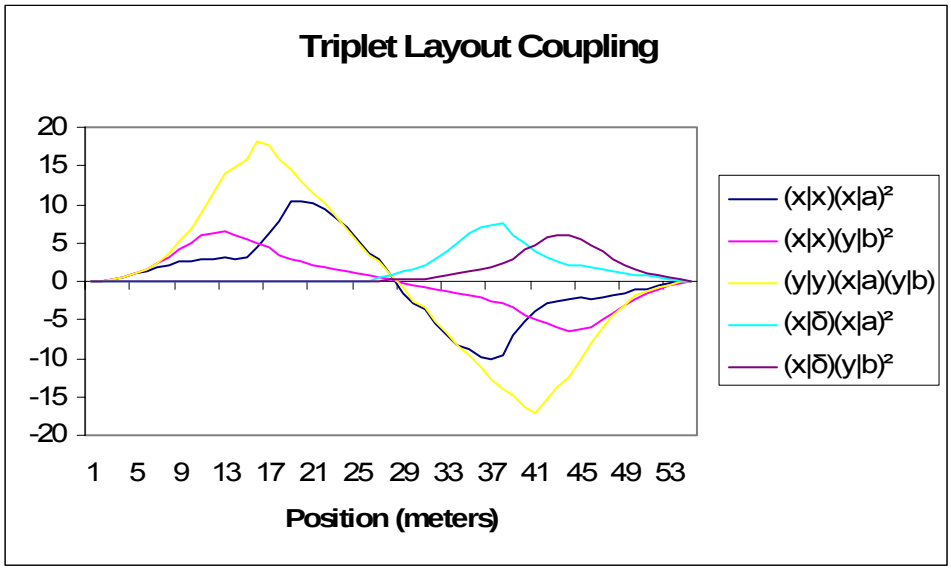

Figure 35. Plot of sextupole coupling coefficients as a function of position within the fragment separation for triplet design layout.

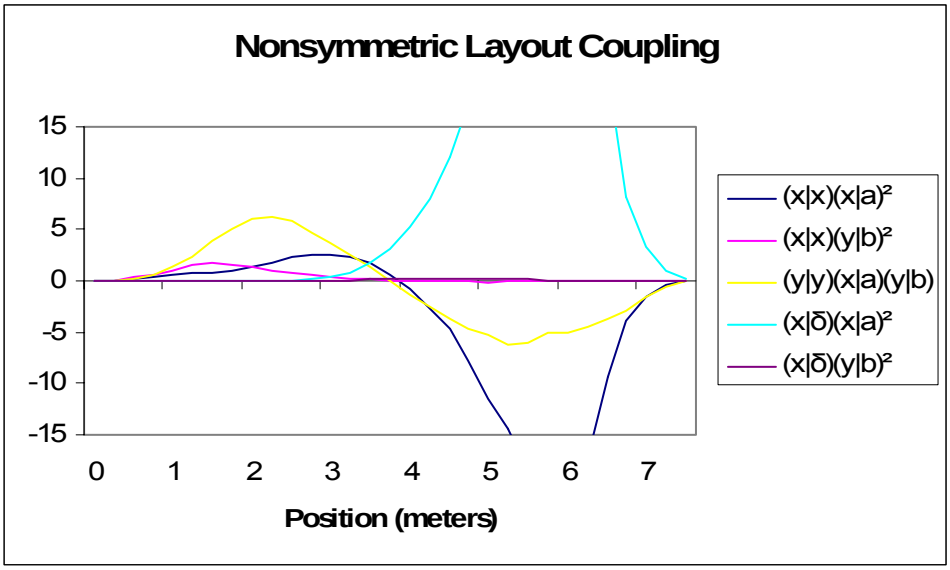

Figure 36. Plot of sextupole coupling coefficients as a function of position within fragment separator for nonsymmetric design layout.

Using these coefficients, the integrated values of the second order transfer map coefficients can be determined as a function of the strength and placement of sextupoles in the system. [14] For example, let's look at correcting aberrations by minimizing the term $(x|xx)_D$.

This second order term can be expressed as:

$$(x \mid xa) \cong -\frac{1}{2}(x \mid x)\int (a \mid x)^2 (a \mid a)(x \mid a)d\alpha \quad + \quad 2(x \mid x)\sum S(x \mid x)(a \mid x)^2 \qquad (30)$$

This equation is integrated over the bending angle of the dipole, and the variable, S, represents the sextupole strength. [4,14] The first term on the right hand side of the equation represents the aberration caused by the first order effects of the dipole. The second term on the right hand side of the equation is the dependent upon the

strength of the sextupole and a coupling coefficient. This coupling coefficient is set by the position of the sextupole and first order terms. Thus, the best place to position a sextupole to minimize the $(x|xa)_D$ aberration is at a point where the absolute value of the coupling coefficient $(x|x)(x|a)^2$ is greatest. [4, 14]

In our systems, the positions of the sextupoles are fixed by superimposing them onto the quadrupoles placed in the first order layout. This method of analysis does let us verify the efficiency of this placement. We see, for example, that the coupling coefficients for the non-symmetric layout are generally very small until after the dipole. Since we will only have 2 sextupole after the dipole, we should be concerned about whether we can achieve the second order criteria with the non-symmetric design.

Theory Applied to Number of Sextupoles

A question also arises about the number of independent sextupoles necessary to obtain a focused system. We can take advantage of the mirror symmetry about the dipole midplane in both the symmetric and triplet layouts to show the relations between the 10 critical second order commutator terms.

In both the symmetric and triplet layouts, the system maintains point-to-parallel, parallel-to-point focusing to the middle of the dipole. Thus, from mirror symmetry and the symplectic relations we know that $(x|x)_M = (a|a)_M = (y|y)_M = (b|b)_M = 0$ and $(x|a)_M(a|x)_M = (y|b)_M(b|y)_M = -1$. Using these relations, which are

calculated in detail in Appendix B, we can express the coefficients for the transfer map through the dispersive image solely in terms of the coefficients from the transfer map through the midplane of the dipole.

$$T_D = T_M \circ T_{MR} = T_M \circ R \circ T_M^{-1} \circ R \tag{31}$$

From this relationship, we see that the majority of the terms appearing in the commutator go to zero give the first order criteria. There are 5 terms, however, that can be expressed as functions of the coefficients from the transfer map through the middle of the dipole. These relations reduce to the equations contained in Table 4.

Table 4

Second Order Relations for Commutator Terms Due to Mirror Symmetry About Dipole Midplane.

$(x\|a\delta)_D = +2(a\|a\delta)_M(x\|a)_M + 2(a\|xa)_M(a\|\delta)_M(x\|a)_M^2$
$(a\|x\delta)_D = -2(x\|x\delta)_M/(x\|a)_M - 4(x\|xx)_M(a\|\delta)_M$
$(a\|\delta\delta)_D = +2(x\|x\delta)_M(a\|\delta)_M + 4(x\|xx)_M(x\|a)_M(a\|\delta)_M^2$
$(y\|b\delta)_D = +2(b\|b\delta)_M(y\|b) + 2(b\|xb)_M(a\|\delta)_M(x\|a)_M(y\|b)_M$
$(b\|y\delta)_D = -2(y\|xy)_M(x\|a)_M(a\|\delta)_M/(y\|b)_M - 2(y\|\delta\delta)_M/(y\|b)_M$

Since $(a|x)_M = -1/(x|a)_M$, the second and third equations from the preceding list are redundant. Both $(a|x\delta)_D$ and $(a|\delta\delta)_D$ are minimized if $(x|x\delta)_M=-2(x|xx)_M(x|a)_M(a|\delta)_M$. The first order criteria, requiring point-to-parallel, parallel-to-point focusing through the middle of the dipole, coupled with the mirror symmetry around the dipole

through the dispersive image, minimizes all but five of the commutator terms, only 4 of which are independent.

Each of the four independent equations provides the relation of proportionality between two second order terms from the transfer map through the middle of the dipole that we reduce a particular commutator terms to zero. If we assume that the eight dipole transfer map terms are independent, these four relations reduce the true number of independent variables from eight to four. One sextupole in front of the dipole should be sufficient to set the value of each of these four truly independent terms such that all of the commutator terms from the transfer map at the dispersive image go to zero. It is reasonable to assume, therefore, that no less than four independent sextupoles placed in front of the dipole will be necessary to minimize all second order commutator terms except in the trivial or exotic case.

From these calculations, we see the power of coupling the symplectic symmetry relationships, which reduced the number of independent commutator terms from 15 to 10, with mirror symmetry around the middle of the dipole, which further reduced the number of independent terms to 4. This theory implies that we should be able to obtain a solution for our symmetric layout which minimizes all of the commutator terms through the dispersive image, satisfying the primary second order criteria. It also suggests, however, that no such solution will exist for the triplet design.

Selection of Second Order Design

For each of the selected first order layouts, COSY was used to find the best second order layout in terms of satisfying the second order criteria previously discussed. Consideration was also given to a variety of configurations, particularly the polarity of the sextupoles. For each design simulations were run with the sextupoles that had symmetry in pole tip field strength about the dipole, and further with both identical and reversed polarity about the dipole. Simulations were also run which allowed all sextupoles in the system to be independent of each other in terms of strength and polarity through the dispersive image. Lastly, simulations were run where all sextupole through the achromatic image were allowed to be independent of each other in terms of strength and polarity.

Table 5 summarizes the second order transfer map terms of the uncorrected layouts through the dispersive image that appear in the commutator equation. The highlighted terms reflect the independent commutator terms which need to be minimized. The second order objective is the sum of these commutator terms.

Table 5

Comparison of the Second Order Commutator Terms for Three Best Design Layouts Before Aberration Correction

2nd Order Map Elements		Symmetric	Non-Symmetric	Triplet
	minimized by			
x|xa	a|aa	4.710524E-12	4.347484E-01	5.551115E-16
x|aδ		1.276111E+01	7.001756E+00	1.069018E+01
x|yb		6.125859E-09	2.608219E-01	0.000000E+00
a|xx		2.922003E-13	3.663833E-05	0.000000E+00
a|xδ		2.373888E-01	1.127275E+00	2.434154E-01
a|aa		6.882331E-11	4.496187E+00	3.053113E-16
a|yy		2.112838E-12	2.866070E-04	1.387779E-16
a|bb		0.000000E+00	7.743024E-05	1.003214E-16
a|δδ		2.791317E-01	3.556413E-01	2.706263E-01
	minimized by			
y|xb	a|bb	0.000000E+00	1.553750E-04	0.000000E+00
	minimized by			
y|ay	x|yb	6.125860E-09	5.412787E+00	6.106227E-16
y|bδ		5.869844E+00	8.108049E+00	6.855612E+00
	minimized by			
b|xy	a|yy	4.225705E-12	2.762103E-05	2.478425E-16
	minimized by			
b|ab	x|yb	6.125859E-09	2.599582E-01	3.654482E-16
b|yδ		1.078842E+00	1.180336E+00	1.075645E+00
2nd order objective		2.022632E+01	2.253047E+01	1.913548E+01

For the non-symmetric model, the uncorrected system at second order had a substantial skew. Figures 37 and 38 show the uncorrected second order plot for the non-symmetric layout.

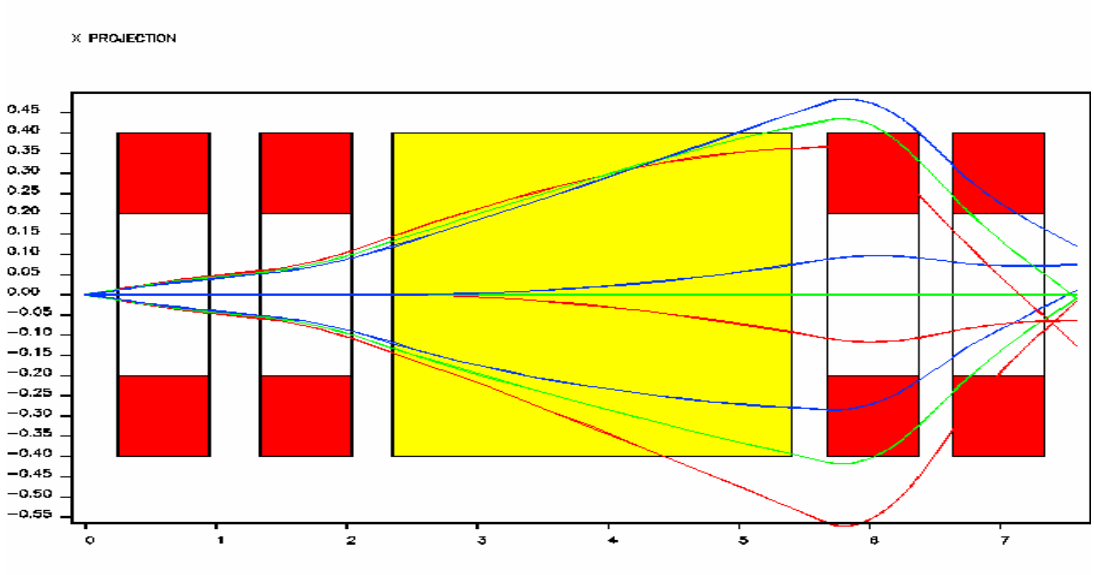

Figure 37. Uncorrected second order best nonsymmetric layout – horizontal projection.

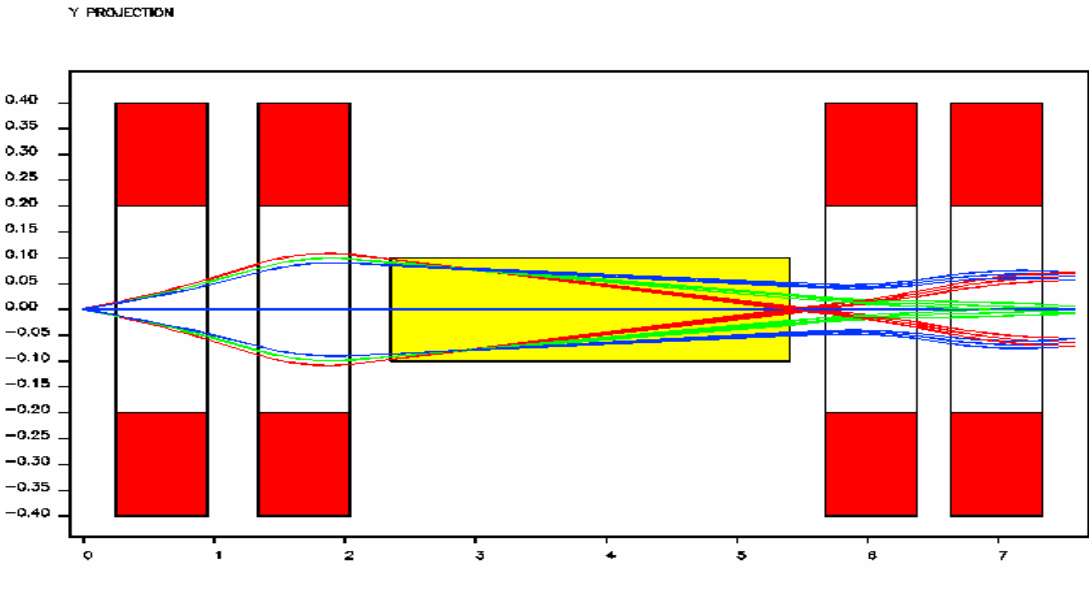

Figure 38. Uncorrected second order best nonsymmetric layout – vertical projection.

This uncorrected system had seven of the ten critical map elements which still need to be minimized even after the symplectic relationship had been considered. The mirror symmetry relationship considered for the symmetric and triplet design could not be applied here because of the lack of symmetry about the dipole.

The best second order focusing of this system required the use of 8 independent sextupoles through the achromatic image. This best fit did not minimize all independent commutator terms, nor was it able to focus at the dispersive image. The largest aberrations at the achromatic image were approximately 3 cm. in the vertical plane and 2 mm. in the horizontal plane. The horizontal and vertical projections of this layout are shown in Figures 39 and 40.

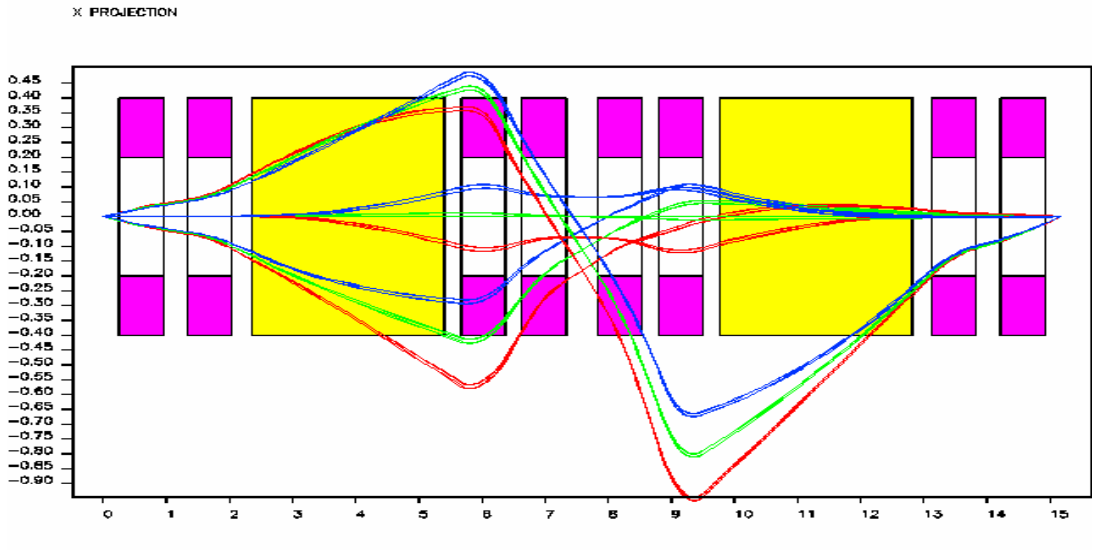

Figure 39. Best nonsymmetric layout after correction of second order aberrations – horizontal projection.

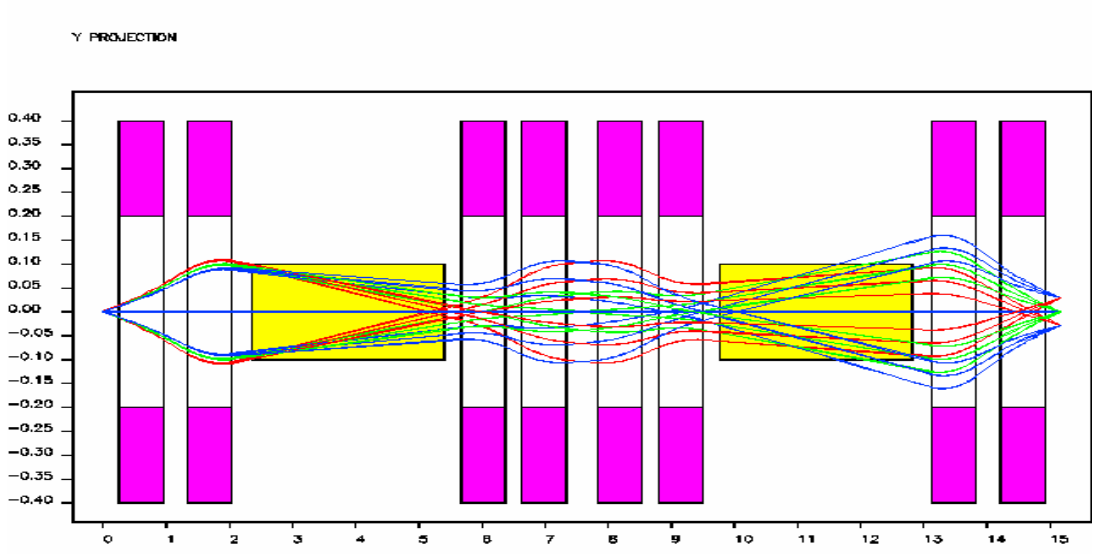

Figure 40. Best non symmetric layout after correction of second order aberrations – vertical projection.

For the triplet layout the skew, as shown in Figures 41 and 42, was more pronounced than in the non-symmetric design.

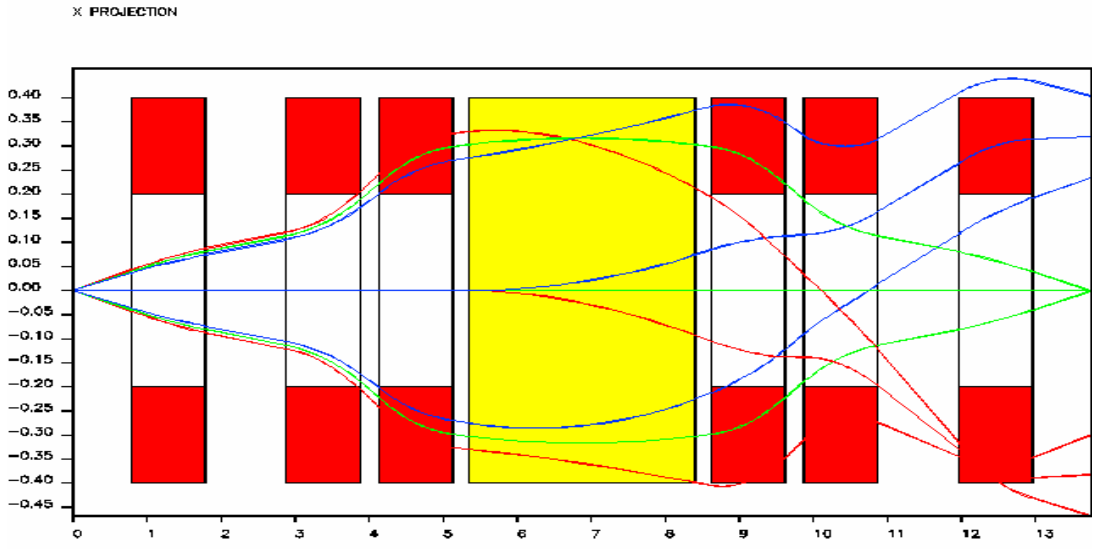

Figure 41. Uncorrected second order best triplet layout – horizontal projection.

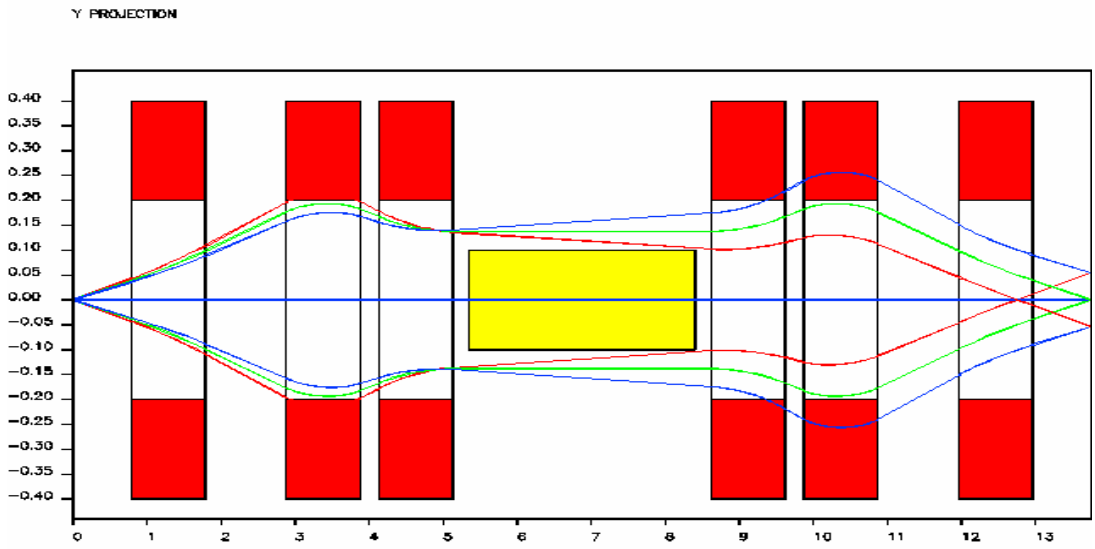

Figure 42. Uncorrected second order best triplet layout – vertical projection.

Also, only 5 of the 10 critical commutator terms were not minimized in the uncorrected system. It is worthy to note that these 5 commutator terms, $(x|a\delta)_D$,

$(a|x\delta)_D$, $(a|\delta\delta)_D$, $(y|b\delta)_D$, and $(b|y\delta)_D$, are exactly the same 5 terms we calculated would not be minimized by a system with mirror symmetry around the center of the dipole coupled with the first order criteria of point-to-parallel, parallel-to-point focusing. Using a system with 3 independent sextupole in front of the dipole, no solution was found that minimized all the commutator terms at the dispersive image. The best correction to this layout was one using three independent sextupole and reversing polarity after the dipole. The horizontal and vertical projections of this layout are shown in Figures 43 and 44. This system did maintain mirror symmetry about the dispersive image.

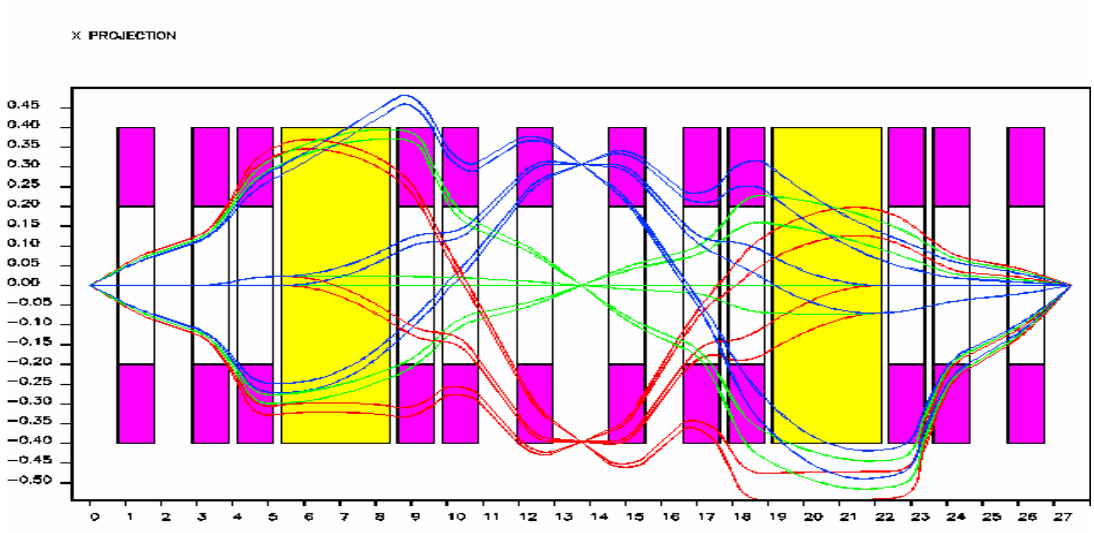

Figure 43. Best triplet layout after correction of second order aberrations – horizontal projection.

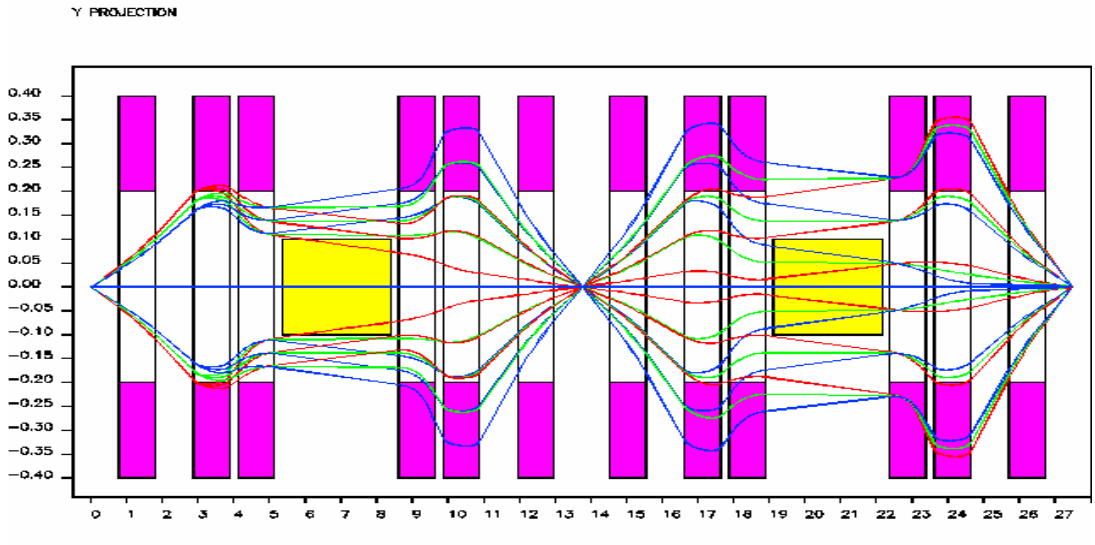

Figure 44. Best triplet layout after correction of second order aberrations – vertical projection.

The corrected second order triplet design minimized all commutator terms except $(a|aa)_D$, $(a|bb)_D$, and $(b|ab)_D$, and had an objective function of .043. This solution did focus at the achromatic image by reducing all aberrations to less than 1 mm. in both horizontal and vertical plane. The angular aberrations for (a|aa), (a|bb) and (b|ab), however, doubled from what they were at the dispersive image. Attempts to correct aberrations using 6 independent sextupole through the dispersive image did effectively reduce all but the (a|aa) angular aberrations through the achromatic image.

For the symmetric layout, the skew was very similar to the triplet layout. This is shown in Figures 45 and 46.

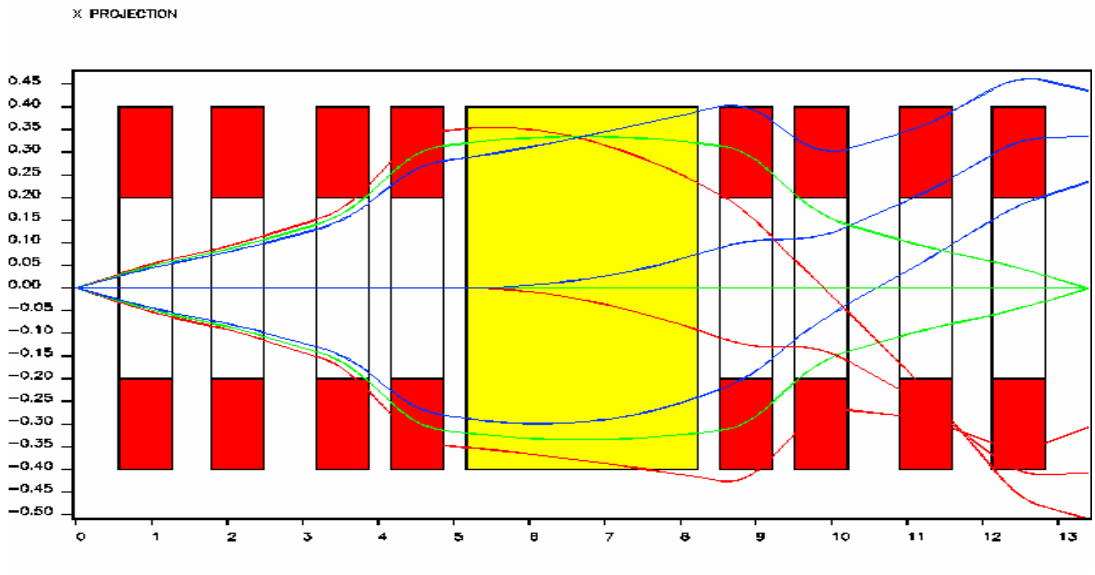

Figure 45. Uncorrected second order best symmetric layout – horizontal projection.

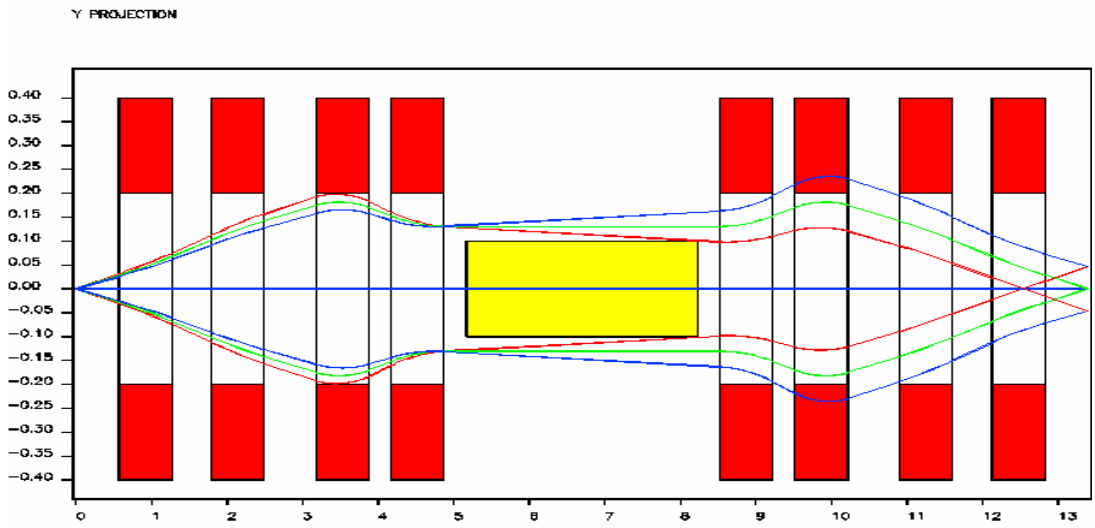

Figure 46. Uncorrected second order best symmetric layout – vertical projection.

The mirror symmetry at the middle of the dipole coupled with the first order criteria again minimized all but the same 5 commutator terms as in the triplet layout. Unlike the triplet layout, and as expected from the theory, a solution was found that

minimized all commutator elements in the transfer map through the dispersive image. This system utilized 4 independent sextupoles in front of the dipole, and maintained mirror symmetry on each side of the dipole. The horizontal and vertical projections of this layout are shown in Figures 47 and 48.

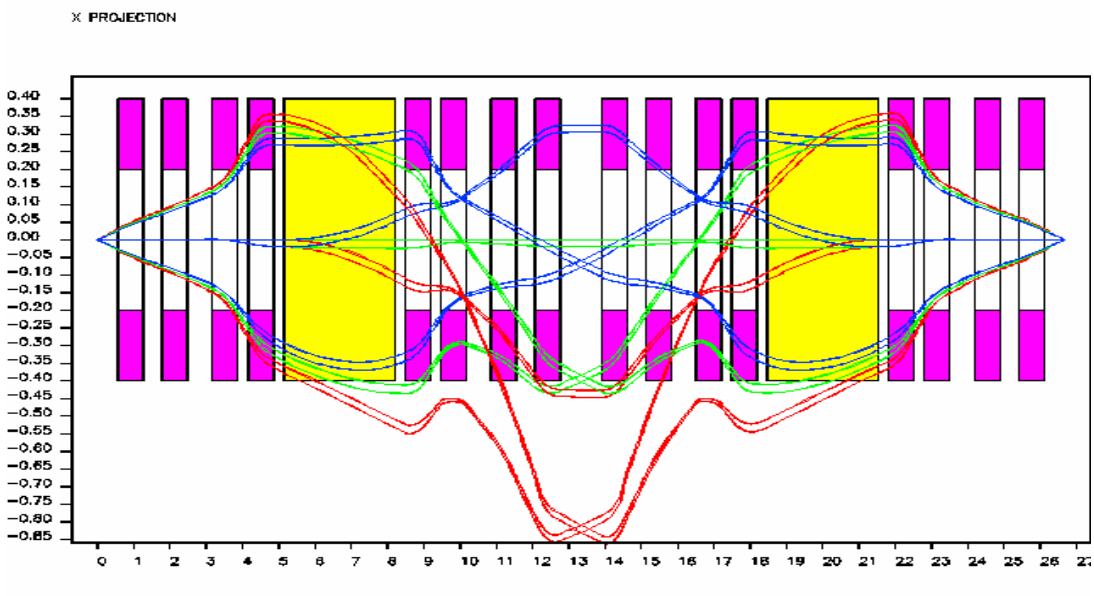

Figure 47. Best symmetric layout after correction of second order aberrations – mirror symmetry maintained about dipole midplane – horizontal projection.

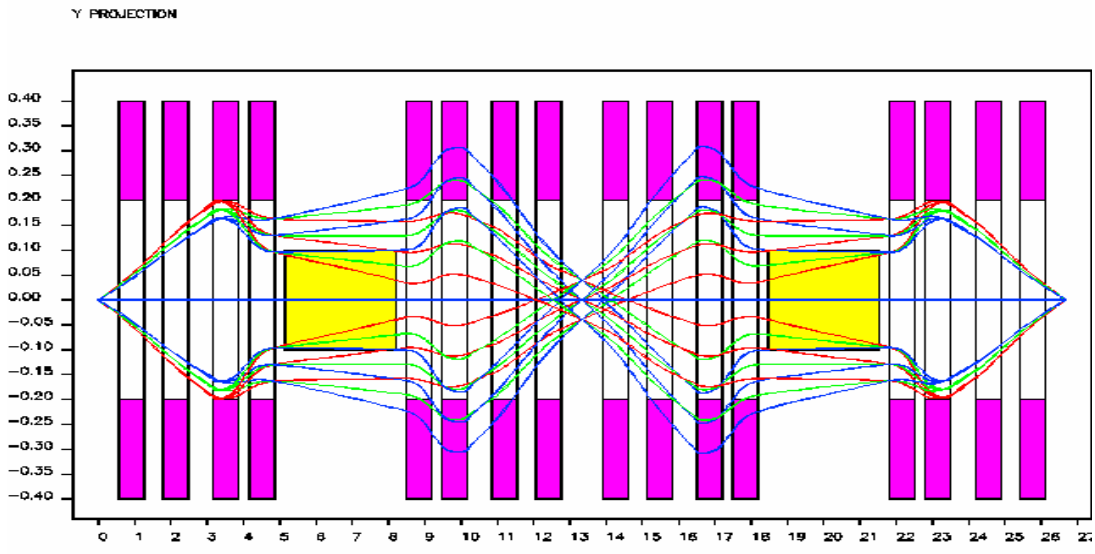

Figure 48. Best symmetric layout after correction of second order aberrations – mirror symmetry maintained about dipole midplane – vertical projection.

The major difficulty with this system is that it does not maintain focusing at the dispersive image. It did successfully minimize all commutator elements. It also minimized all aberrations to less that 1 mm. at the achromatic image. Lastly, the magnet strengths for the sextupoles remained quite reasonable. The second order transfer and aberration maps through the dispersive image for this design are given in Table 6. The coefficients in this Table are expressed in following manner: (1) the Columns correspond to x, a, y, b, and δ, and represent the first term in the coefficient; and (2) the rows correspond to the variables appearing in the second terms of the coefficient and the sixth column designates the power of each variable (x, a, y, b, t, and δ) for each particular row. Since there are no time dependent elements within the system, all rows are independent of t. For example, the

numerical value for the coefficient (x|aa) will be in the first column with the row designated by 020000.

Table 6.

Transfer Map Coefficients and Aberration at Dispersive Image for Best Symmetric Layout After Second Order Correction – Mirror Symmetry Maintained About Dipole Midplane.

```
BEAM MAP ELEMENTS – DISPERSIVE IMAGE – SYMMETRIC DESIGN
   .7164369E-13 -.1007290E-15  .0000000      .0000000      .6835275E-13 000000
  -.9999999      .5820138E-07  .0000000      .0000000      .1385417E-06 100000
  -.1056932E-11 -1.000000      .0000000      .0000000     -2.380637     010000
   .0000000      .0000000     -.9999999      .1735760E-10  .0000000     001000
   .0000000      .0000000      .1811107E-11 -1.000000      .0000000     000100
   .0000000      .0000000      .0000000      .0000000      1.000000     000010
   2.380637     -.1469933E-10  .0000000      .0000000      2.257262     000001
  -.2242649     -.7918147E-05  .8214957E-14  .7340649E-15 -.9384621E-05 200000
  -.1331026E-02  .4485299      .5544759E-13 -.6238808E-13  .5338858     110000
  -153.4473      .6744441E-03  .8013126E-12 -.5563134E-12  .8134328E-03 020000
   .6299844E-13  .1847719E-14 -2.328964     -.9033487E-04 -.5377020E-14 101000
   .1112561E-11 -.6236528E-13 -.1120900E-01  9.128255     -.1231968E-12 011000
  -4.564127     -.4490182E-04  .5994115E-13 -.3446185E-13 -.5315632E-04 002000
   .5577954E-13 -.1543478E-13  .8859451E-03  2.328965     -.7198684E-14 100100
   .1597066E-11 -.5517036E-13 -15.76992      .1120900E-01 -.2397050E-12 010100
  -.1120899E-01  2.328965      .1747891E-12 -.1183194E-12  2.771873     001100
```

```
   .5339011      .1890016E-04 -.3013210E-13 -.9843870E-14 -.1727380E-06 100001
   .1584343E-02 -.5339012      .1086476E-12  .2534200E-13  2.776615     010001
  -.2508618E-13 -.9604117E-14  2.772547      .1074773E-03  .0000000     001001
  -7.884962     -.4425137E-03  .3984935E-12 -.8717803E-13 -.5261861E-03 000200
   .1082783E-12  .2974465E-13 -.1054557E-02 -2.772547      .0000000     000101
  -2.023820     -.2246580E-04  .3586679E-13  .1171734E-13 -2.285957     000002
 --------------------------------------------------------------------------------
BEAM ABERRATIONS – DISPERSIVE IMAGE – SYMMETRIC DESIGN
   .7164369E-13 -.1007290E-15  .0000000      .0000000      .6835275E-13 000000
  -.9999999E-03  .5820138E-10  .0000000      .0000000      .1385417E-09 100000
  -.5284662E-13 -.5000001E-01  .0000000      .0000000     -.1190319     010000
   .0000000      .0000000     -.9999999E-03  .1735760E-13  .0000000     001000
   .0000000      .0000000      .9055534E-13 -.5000000E-01  .0000000     000100
   .3761407     -.2322495E-11  .0000000      .0000000      .3566474     000001
  -.2242649E-06 -.7918147E-11  .0000000      .0000000     -.9384621E-11 200000
  -.6655132E-07  .2242650E-04  .0000000      .0000000      .2669429E-04 110000
  -.3836181      .1686110E-05  .2003281E-14 -.1390784E-14  .2033582E-05 020000
   .0000000      .0000000     -.2328964E-05 -.9033487E-10  .0000000     101000
   .0000000      .0000000     -.5604498E-06  .4564127E-03  .0000000     011000
  -.4564127E-05 -.4490182E-10  .0000000      .0000000     -.5315632E-10 002000
   .0000000      .0000000      .4429725E-07  .1164482E-03  .0000000     100100
   .3992666E-14 -.1379259E-15 -.3942481E-01  .2802249E-04 -.5992624E-15 010100
  -.5604497E-06  .1164482E-03  .0000000      .0000000      .1385937E-03 001100
   .8435637E-04  .2986225E-08  .0000000      .0000000     -.2729261E-10 100001
   .1251631E-04 -.4217820E-02  .8583161E-15  .2002018E-15  .2193526E-01 010001
   .0000000      .0000000      .4380624E-03  .1698142E-07  .0000000     001001
  -.1971240E-01 -.1106284E-05  .9962338E-15 -.2179451E-15 -.1315465E-05 000200
   .8553985E-15  .2349827E-15 -.8331001E-05 -.2190312E-01  .0000000     000101
  -.5052264E-01 -.5608361E-06  .8953786E-15  .2925117E-15 -.5706663E-01 000002
 --------------------------------------------------------------------------------
```

Like the triplet design, it was possible to focus the dispersive image at the expense of minimizing the critical commutator terms. The horizontal and vertical projections of this layout are shown in Figures 49 and 50. This result maintained an image plane at the dispersive image, but did not minimize all the angular aberrations at the achromatic image.

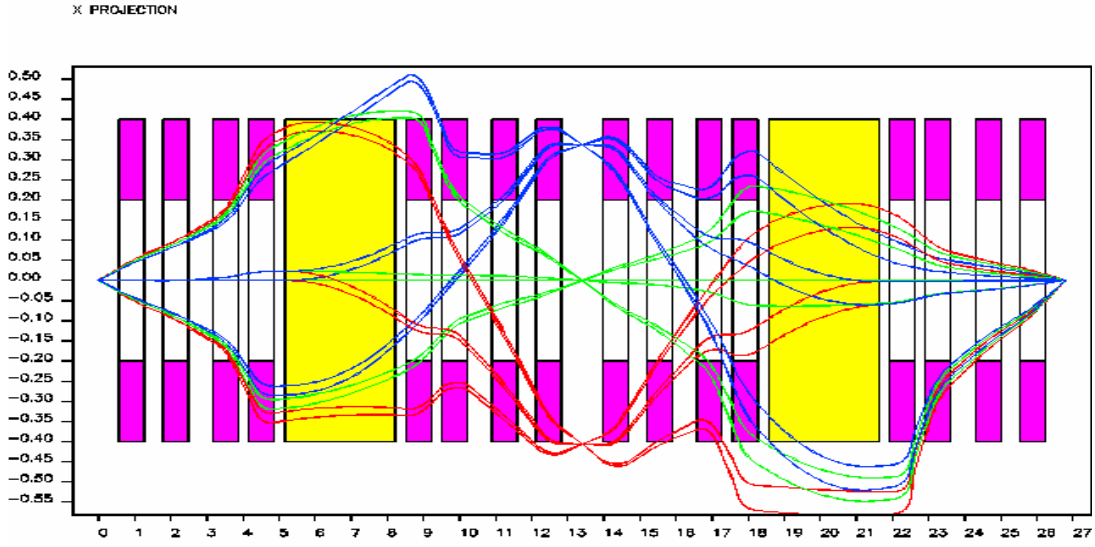

Figure 49. Alternate second order best symmetric layout – eight independent sextupoles through dispersive image – horizontal projection.

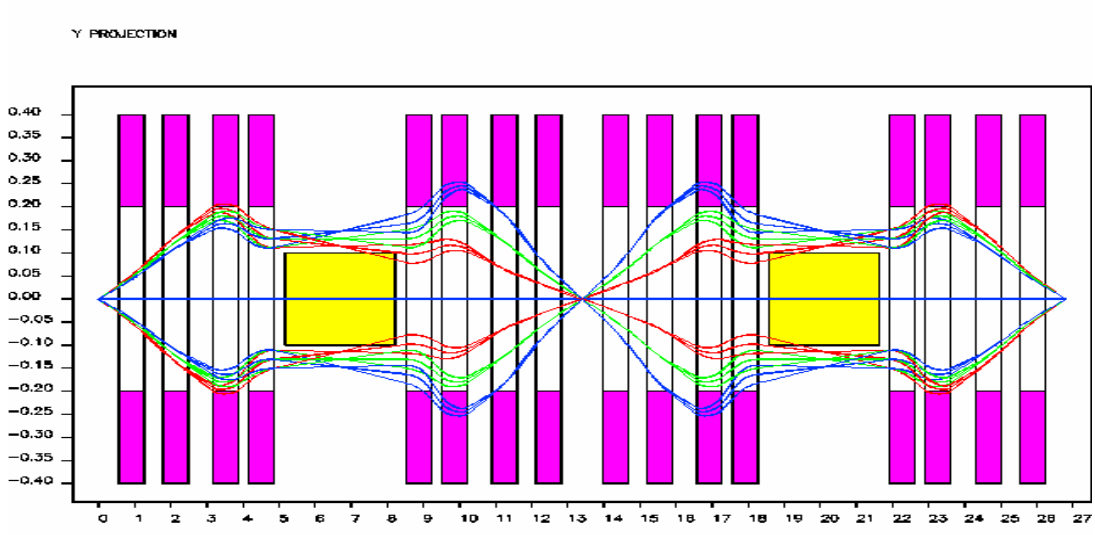

Figure 50. Alternate second order aberration for best symmetric layout –eight independent sextupoles through dispersive image – vertical projection.

In consideration of all three designs, the non-symmetric design failed to meet the criteria set at second order either by minimizing the commutator terms or by otherwise focusing at the achromatic image. The triplet design came much close, but also failed to minimize all the second order commutator terms. The triplet design was able to focus the achromatic image, but it failed to minimize all angular aberration to 10^{-3}. The symmetric design was the only one capable of satisfying the primary second order criteria of minimizing all the critical commutator terms. It also was the only system that minimized all aberrations at the achromatic image to 10^{-3}. The drawback to the design was the loss of a focused image plane at the dispersive image. This could be corrected, as in the triplet design, by sacrificing the goal of minimizing all of the critical commutator terms.

V. THIRD ORDER DESIGN

Third Order Design Criteria

At third order, the design challenges and criteria become increasingly more complicated. In terms of the commutator equations, 35 third order terms appear in this equation [8] and are listed in Table 7:

Table 7

Third Order Terms Appearing in the Commutator Equation.

$(x|xxa)_D$ $(x|xa\delta)_D$ $(x|xyb)_D$ $(x|aaa)_D$ $(x|ayy)_D$ $(x|abb)_D$ $(x|a\delta\delta)_D$ $(x|yb\delta)_D$

$(a|xxx)_D$ $(a|xx\delta)_D$ $(a|xaa)_D$ $(a|xyy)_D$ $(a|xbb)_D$ $(a|x\delta\delta)_D$ $(a|aa\delta)_D$ $(a|ayb)_D$ $(a|yy\delta)_D$ $(a|bb\delta)_D$ $(a|\delta\delta\delta)_D$

$(y|xxb)_D$ $(y|xay)_D$ $(y|xb\delta)_D$ $(y|aab)_D$ $(y|ay\delta)_D$ $(y|yyb)_D$ $(y|bbb)_D$ $(y|b\delta\delta)_D$

$(b|xxy)_D$ $(b|xab)_D$ $(b|xy\delta)_D$ $(b|aay)_D$ $(b|ab\delta)_D$ $(b|yyy)_D$ $(b|ybb)_D$ $(b|y\delta\delta)_D$

From the symplectic relations, we can reduce the number of independent commutator terms from 35 to 21. [8] These relations are listed in Table 8.

Table 8

Symplectic Relations Between Third Order Commutator Terms.

$(x\|xxa) \propto (a\|xaa)$	$(a\|aa\delta) \propto (x\|xa\delta)$
$(x\|xyb) \propto (a\|ayb) \propto (b\|xab) \propto (y\|xay)$	$(x\|ayy) \propto (b\|aay)$
$(x\|yb\delta) \propto (b\|ab\delta) \propto (y\|ay\delta)$	$(a\|xyy) \propto (b\|xxy)$
$(a\|yy\delta) \propto (b\|xy\delta)$	$(a\|xbb) \propto (y\|xxb)$
$(a\|bb\delta) \propto (y\|xb\delta)$	$(x\|abb) \propto (y\|aab)$
$(y\|yyb) \propto (b\|ybb)$	

This leaves 21 independent third order terms in the commutator equation. As it did with second order terms, the symplectic condition also gives relations of proportionality between other non-commutator terms. These are listed in Appendix A. To minimize these terms, the system design will use octupoles superimposed onto the existing multipoles. Given the limited number of multiples our system will use, it may not be possible to minimize all the third order commutator terms. Bearing this in mind, the primary goal at third order will remain to focus the achromatic image point-to-point parallel-to-parallel. Our primary criteria will seek to achieve this goal by minimizing the independent commutator terms. Attention will also be given to minimizing aberrations in the horizontal plane of the dispersive image where isobar separation occurs.

Theory Applied to the Number of Octupoles

As was done with the second order system, consideration should be given to the number of independent octupoles needed to minimize the critical third order commutator terms. Because both the symmetric and triplet designs utilize mirror symmetry about the dipole, we can examine whether this symmetry reduces the original number of 35 third order commutator terms. Just as was done at the second order, the third order commutator terms can be expressed as functions for the coefficients of the transfer map through the middle of the dipole. The first and second order criteria are then incorporated. When this is done, as detailed in Appendix B, we see that the 35 terms can be minimized by satisfying only 24 relations involving 26 third order terms from the transfer map through the middle of the dipole. These relations are listed in Table 9.

Table 9

Third Order Relations for Commutator Terms Due to Mirror Symmetry About Dipole Midplane

$(a\|xxx)_D$ and $(a\|xx\delta)_D$ minimized when $(x\|xxx)_M = -2(x\|xa)(x\|xx)/(x\|a)$
$(a\|xaa)_D$ and $(a\|aa\delta)_D$ minimized when $(x\|xaa)_M = 2(x\|aa)(x\|xa)/(x\|a) - 2(a\|aa)(x\|xx)(x\|a)$
$(a\|xyy)_D$ and $(a\|yy\delta)_D$ minimized when $(x\|xyy)_M = -2(x\|yb)(x\|yy)/(x\|a) - 2(x\|xx)(y\|ay)/(y\|b)$
$(a\|xbb)_D$ and $(a\|bb\delta)_D$ minimized when $(x\|xbb)_M = -2(a\|bb)(x\|xx)(x\|a) +4(x\|bb)(x\|yb)/(x\|a)$
$(a\|x\delta\delta)_D$ and $(a\|\delta\delta\delta)_D$ minimized when $(x\|x\delta\delta)_M + 2(x\|xx\delta)_M(a\|\delta)(x\|a) + 6(x\|xxx)_M(x\|a)^2(a\|\delta)^2 = -2\ (a\|\delta\delta)(x\|xx)(x\|a) -8(x\|xa)(x\|xx)(x\|a)(a\|\delta)^2$
$(a\|ayb)_D$ minimized when $(x\|ayb)_M = 2(x\|aa)(x\|yb)/(x\|a) - 4(a\|bb)(x\|yy)(x\|a) +4(x\|bb)(y\|ay)/(y\|b)$
$(x\|xxa)_D$ and $(x\|xa\delta)_D$ minimized when $(a\|xxa)_M = 0$
$(x\|xyb)_D$ and $(x\|yb\delta)_D$ minimized when $(a\|xyb)_M = -(x\|aa)(x\|yb)/(x\|a)$
$(x\|aaa)_D$ minimized when $(a\|aaa)_M = -(a\|aa)(x\|aa)/(x\|a)$
$(x\|ayy)_D$ minimized when $(a\|ayy)_M = (y\|ab)(y\|ay)/(x\|a)(y\|b)^2 – (x\|aa)(y\|ay)/(x\|a)^2(y\|b)$
$(x\|abb)_D$ minimized when $(a\|abb)_M = -(a\|bb)(x\|aa)/(x\|a) – (a\|bb)(y\|ab)(x\|a)^2/(y\|b)$
$(x\|a\delta\delta)_D$ minimized when $(a\|a\delta\delta)_M + (a\|xa\delta)_M(x\|a)(a\|\delta) +2(a\|xxa)_M(x\|a)^2(a\|\delta)^2 = -(x\|aa)(x\|a\delta)(a\|\delta)/(x\|a)^2 – (x\|aa)(a\|\delta)^2$
$(b\|xxy)_D$ and $(b\|xy\delta)_D$ minimized when $(y\|xxy)_M = -(x\|xa)(x\|yy)(y\|b)/(x\|a)^2 - (x\|yb)(x\|yy)(y\|b)/(x\|a)^2$
$(b\|xab)_D$ and $(b\|ab\delta)_D$ minimized when $(y\|xab)_M = -(a\|bb)(x\|yy)(y\|b) + (x\|xa)(y\|ab)/(x\|a) + (x\|yb)(y\|ab)/(x\|a)$
$(b\|aay)_D$ minimized when $(y\|aay)_M = -2(a\|aa)(x\|yy)(y\|b) + (y\|ab)(y\|ay)/(y\|b)$
$(b\|yyy)_D$ minimized when $(y\|yyy)_M = -2(xyy)(y\|ay)/(x\|a)$
$(b\|ybb)_D$ minimized when $(y\|ybb)_M = -2(a\|bb)(x\|yy)(y\|b) +2\ (x\|yb)(y\|ab)/(x\|a)$
$(b\|y\delta\delta)_D$ minimized when $2(y\|xxy)_M + (y\|xy\delta)_M/(x\|a)(a\|\delta) + (y\|y\delta\delta)_M/(x\|a)^2(a\|\delta)^2 = -(a\|\delta\delta)(x\|yy)(y\|b)/(x\|a)^2(a\|\delta)^2 - 2(x\|a\delta)(x\|yy)(y\|b)/(x\|a)^3(a\|\delta) – 2(x\|xa))(x\|yy)(y\|b)/(x\|a)^2 – (x\|yb)(x\|yy)(y\|b)/(x\|a)^2$
$(y\|xxb)_D$ and $(y\|xb\delta)_D$ minimized when $(b\|xxb)_M = -(x\|bb)(x\|xa)/(x\|a)^2(y\|b) + (x\|bb)(x\|yb)/(x\|a)^2(y\|b)$
$(y\|xay)_D$ and $(y\|ay\delta)_D$ minimized when $(b\|xay)_M = (a\|yb)(x\|xa)/(y\|b) – (a\|yb)(x\|yb)/(y\|b) + (x\|bb)(y\|ay)/(x\|a)(y\|b)^2$
$(y\|aab)_D$ minimized when $(b\|aab)_M = -(a\|bb)(a\|yb)(x\|a)^2/(y\|b) – (a\|aa)(x\|bb)/(y\|b)$

$(y\|yyb)_D$ minimized when $(b\|yyb)_M = (a\|yb)(x\|yb)/(y\|b) – (x\|bb)(y\|ay)/(x\|a)(y\|b)^2$
$(y\|bbb)_D$ minimized when $(b\|bbb)_M = - (a\|bb)(x\|bb)/(y\|b)$
$(y\|b\delta\delta)_D$ minimized when $(b\|b\delta\delta)_M + (b\|xb\delta)_M(x\|a)/(a\|\delta)(y\|b)^2 +2(b\|xxb)_M(x\|a)^2(a\|\delta)^2$ $= -(a\|\delta\delta)(x\|bb)/(y\|b) –(x\|a\delta)(x\|bb)(a\|\delta)/(x\|a)(y\|b) -2(x\|bb)(x\|yb)(a\|\delta)^2/(y\|b)$

While this seems a daunting list, we must remember that all first and second order coefficients are set to a constant value by the system's existing layout. These values are not changed when octupoles are superimposing onto the existing layout.

To determine the minimum number of octupoles that will be needed to minimized all critical third order commutator terms, we can start with an assumption that one octupole is necessary at a minimum to satisfy each of the 24 previous relations. If the symplectic relations are applied, the number of independent variables could be reduced by as many as 14. This would indicate that at least 10 octupoles in front of the dipole would be necessary to minimize all 35 third order commutator terms. Since none of our designs approaches this number of octupoles, it must be recognized that the goal of minimizing the critical third order transfer map terms will likely need to yield to the overriding goal of minimizing aberrations at the achromatic image.

To accomplish this goal, we note that if we assume a point-like beam emerging from the target, the aberrations based on angular and energy dependence will be of greatest concern. At third order, only 10 transfer map terms in the commutator equation are based only on angular and energy dependence. These are $(x|aaa)_D$, $(x|abb)_D$, $(x|a\delta\delta)_D$, $(a|aa\delta)_D$, $(a|bb\delta)_D$, $(a|\delta\delta\delta)_D$, $(y|abb)_D$, $(y|bbb)_D$, $(y|b\delta\delta)_D$, and $(b|ab\delta)_D$. The symplectic relations, however, show that two of these terms, $(x|abb)_D$ and $(y|aab)_D$, are proportional to each other and will be simultaneously

minimized. This leaves nine independent terms through the dispersive image that still need to be minimized if we assume a point-like beam at the target. Since the symmetric layout utilizes 8 multipoles (where octupole could be superimposed) ahead of the dispersive image, it should stand the best chance for a system that minimizes these 9 independent terms.

Selection of Third Order Design

Now we apply the criteria and theory to the remaining two second order layouts. With respect to the triplet design, no solution was found that minimized the commutator terms at second order, and no solution was found at third order. Even the best second order design was not able to yield a result that focused the achromatic image at third order when all the octupoles were allowed to be independent.

With respect to the symmetric model, the number of octupoles was insufficient to allow for a solution that minimized all the commutator terms. It was, however, possible to find a solution that focused the achromatic image when all eight octupoles up to the dispersive image were allowed to be independent of each other. The horizontal and vertical projections of this layout are shown in Figures 51 and 52. Mirror symmetry in this system was still maintained relative to the dispersive image.

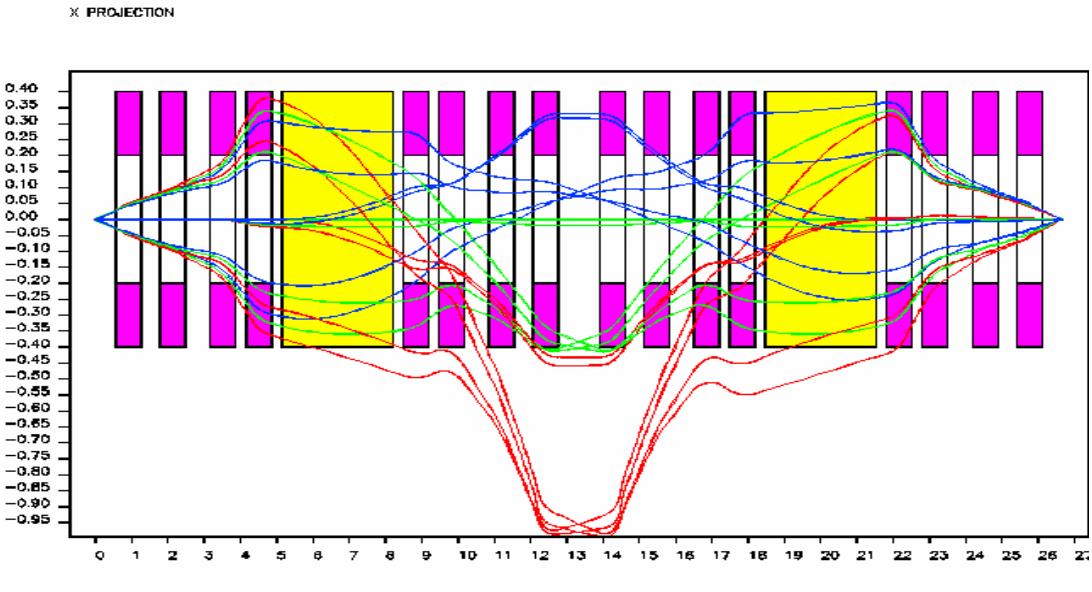

Figure 51. Best symmetric layout after correction of third order aberrations – horizontal projection.

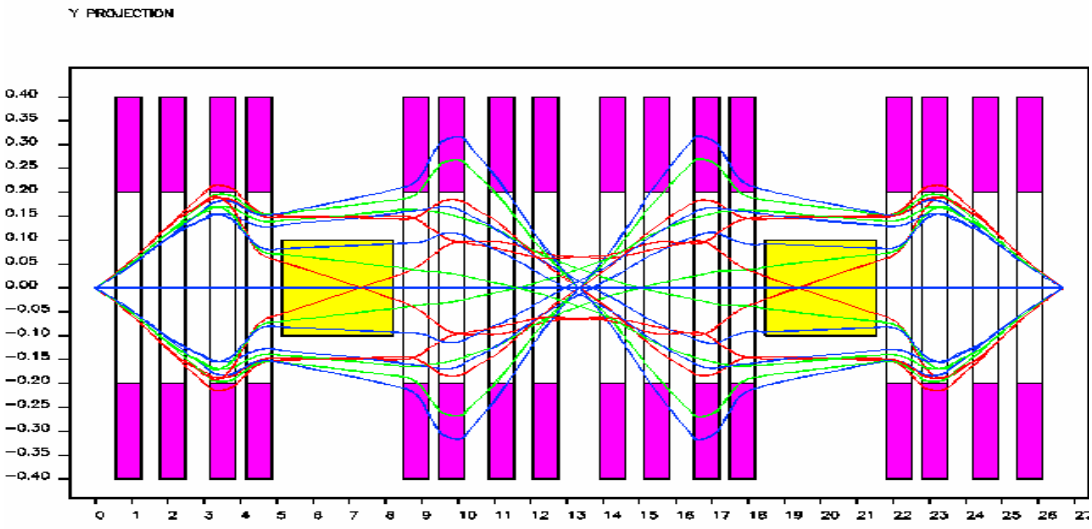

Figure 52. Best symmetric layout after correction of third order aberrations – vertical projection.

For this system, the strengths of the octupoles were reasonable, but the drawback is the same as with the second order solution. The dispersive image

remains unfocused. Still, as shown in the Table 10, the aberrations at the achromatic image were successfully reduced.

Table 10

Aberrations at Achromatic Image for Best Symmetric Design Layout After Third Order Correction.

BEAM ABERRATIONS – ACHROMATIC IMAGE – SYMMETRIC DESIGN

.2118836E-12	.0000000	.0000000	.0000000	.4014956E-12	000000
.9999998E-03	-.1164028E-09	.0000000	.0000000	-.1385564E-09	100000
.1060541E-12	.5000001E-01	.0000000	.0000000	.1315949E-07	010000
.0000000	.0000000	.9999998E-03	-.3471420E-13	.0000000	001000
.0000000	.0000000	-.1810496E-12	.5000001E-01	.0000000	000100
.4158401E-07	.2189190E-07	.0000000	.0000000	.7132948	000001
.2487550E-13	-.3915073E-13	.0000000	.0000000	.1887316E-13	200000
.8930761E-09	-.2487655E-11	.0000000	.0000000	-.7754190E-09	110000
-.1272321E-06	-.2232690E-07	.0000000	.0000000	.6612215E-12	020000
.0000000	.0000000	.2581110E-12	-.5313490E-12	.0000000	101000
.0000000	.0000000	-.4544516E-13	-.1933583E-10	.0000000	011000
.1933583E-12	-.2656745E-12	.0000000	.0000000	-.5003372E-13	002000
.0000000	.0000000	.4589526E-10	-.1290555E-10	.0000000	100100
.0000000	.0000000	-.1038767E-07	.2272213E-11	-.8703913E-15	010100
-.4544302E-13	-.1290555E-10	.0000000	.0000000	-.3372716E-07	001100
-.2450323E-08	-.5963640E-11	.0000000	.0000000	-.3353648E-12	100001
.4102102E-11	.1225162E-06	-.2751978E-14	.7705327E-15	.2881305E-06	010001
.0000000	.0000000	-.1065778E-06	.1581063E-10	.0000000	001001
-.5193832E-08	-.1147381E-08	.0000000	.0000000	.1196227E-11	000200
-.2748904E-14	-.1798597E-15	.7557628E-11	.5328893E-05	-.4249146E-15	000101
.4552461E-06	.2646751E-10	-.6515956E-15	-.4610645E-15	-.1141333	000002
-.5586939E-12	.1327918E-07	.0000000	.0000000	-.1638800E-10	300000
-.4312462E-05	.8430611E-10	.0000000	.0000000	.8460755E-11	210000
.4344054E-07	.2156232E-03	.0000000	.0000000	.6012746E-04	120000
-.5787529E-04	-.7240026E-06	.2433126E-14	.1700863E-14	.2410203E-05	030000
.0000000	.0000000	.2218913E-11	-.6755976E-07	.0000000	201000
.0000000	.0000000	.2005817E-04	.1292174E-08	.0000000	111000
-.1022781E-15	.0000000	.4807678E-06	-.8104731E-03	.0000000	021000
-.1292175E-10	-.6755977E-07	.0000000	.0000000	.3639898E-08	102000
.1620946E-04	.6442007E-09	.0000000	.0000000	.1101448E-08	012000
.0000000	.0000000	-.3379196E-11	.5396881E-07	.0000000	003000
.0000000	.0000000	.6912722E-05	-.1109459E-09	.0000000	200100
.0000000	.0000000	.3780489E-06	-.1002909E-02	.0000000	110100
.7268253E-14	.0000000	-.8376909E-04	-.2403840E-04	.1154879E-14	020100
.2005816E-04	-.2242261E-09	.0000000	.0000000	.2640737E-10	101100
.9615354E-06	-.1002909E-02	.0000000	.0000000	.1038160E-05	011100
.0000000	.0000000	-.1141123E-04	.5068800E-09	.0000000	002100
.2484775E-10	.7769571E-08	.0000000	.0000000	.2527773E-07	200001
.3800051E-03	-.2529010E-08	.0000000	.0000000	.4891422E-08	110001
.2284864E-04	-.9500131E-02	.3645404E-14	-.5856539E-15	.3927377E-03	020001
.0000000	.0000000	.9222966E-10	-.1150214E-05	.0000000	101001
.0000000	.0000000	.3281418E-05	-.3487673E-06	.0000000	011001
.3487672E-08	-.5751069E-06	.0000000	.0000000	-.7356649E-06	002001
.1890245E-06	-.3456363E-03	-.1278535E-15	.0000000	-.2041548E-04	100200
-.8376908E-04	-.9451217E-05	.1652839E-14	.2102875E-15	-.9598736E-05	010200
.0000000	.0000000	-.3498636E-06	.5705617E-03	.0000000	001200
.0000000	.0000000	-.1290252E-03	-.4611482E-08	.0000000	100101
.7300335E-14	-.5095391E-15	-.6066406E-04	-.1640710E-03	-.6907878E-15	010101
.3281418E-05	-.4611868E-08	.0000000	.0000000	.4843773E-07	001101
.7811640E-08	-.3993881E-05	.0000000	.0000000	-.1078346E-04	100002
.1241059E-02	-.3907263E-06	-.1075591E-14	-.5410862E-15	-.2002005E-05	010002
.0000000	.0000000	.7653800E-07	.1162351E-03	.0000000	001002
.5515972E-15	.2130750E-14	.4789049E-04	.5831062E-05	.0000000	000300
-.3033203E-04	.3225632E-02	.4385635E-15	-.3885806E-15	-.2112681E-03	000201
-.1081683E-14	.0000000	-.6676096E-03	-.3826333E-05	.0000000	000102

```
-.2108598E-05  .5679290E-03  .0000000      .2095413E-15  .2003393E-01 000003
```

Two other solutions were found that are worthy of discussion. Both are based upon the version of the symmetric design that focused the dispersive image at second order, but did not minimize the commutator terms. The first case, referred to as the low magnet solution, looks deceptively good through the dispersive image and in the horizontal plane. The horizontal and vertical projections of this layout are shown in figures 53 and 54. The drawback to this solution is that the aberrations in the vertical plane explode as the system's cells are repeated. The strengths of the octupoles used in this design are quite reasonable.

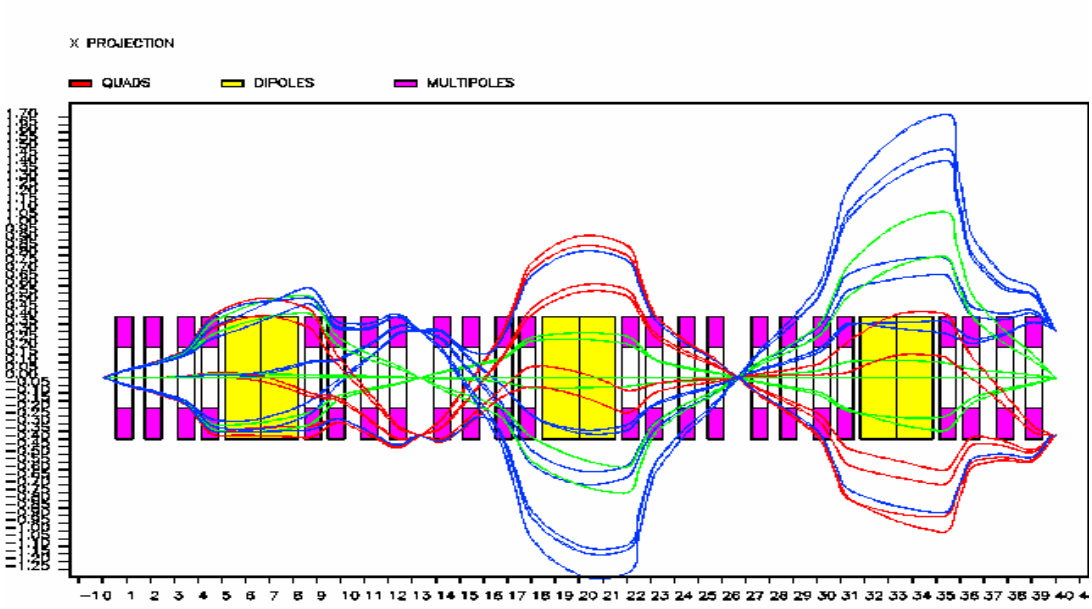

Figure 53. Low magnet strength third order aberration correction of alternative second order best symmetric design – horizontal projection.

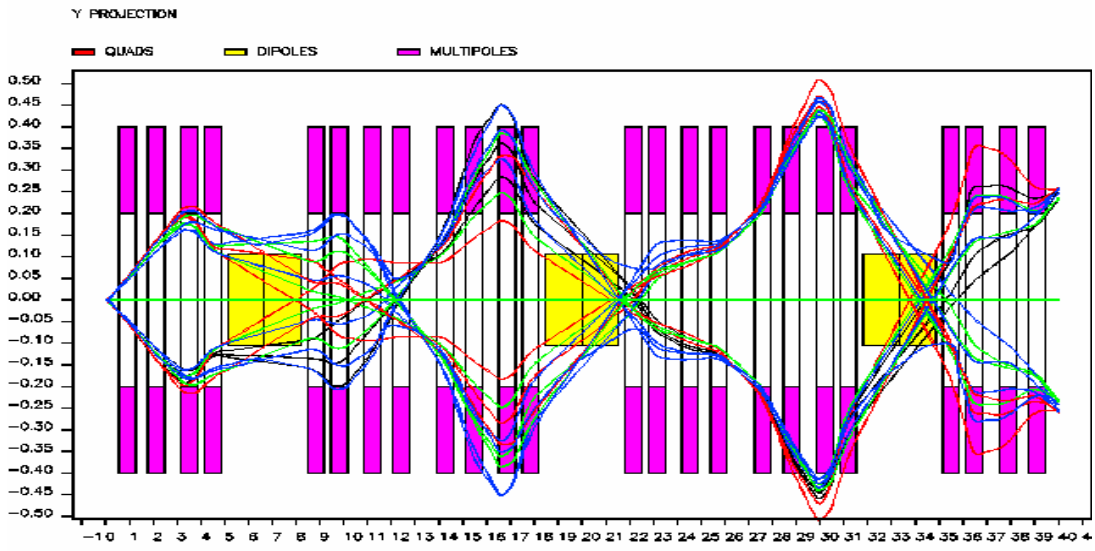

Figure 54. Low magnet strength third order aberration correction of alternative second order best symmetric design – vertical projection.

Another alternative, referred to as the high magnet solution, did focus both the dispersive and achromatic images and minimized all aberrations. The horizontal and vertical projections of this layout are shown in Figures 55 and 56. The problem with this system, however, is that one of the octupoles in each cell through the dispersive image has a pole field tip strength beyond physical limitations. This was representative of a number of solutions found by COSY during simulation. In all such cases, the pole tip field strength of one or more of the octupoles with a 40 cm aperture was in excess of 4.6 Tesla. This very large magnet also induces dramatic effects in the beam line aberrations at fifth order and beyond.

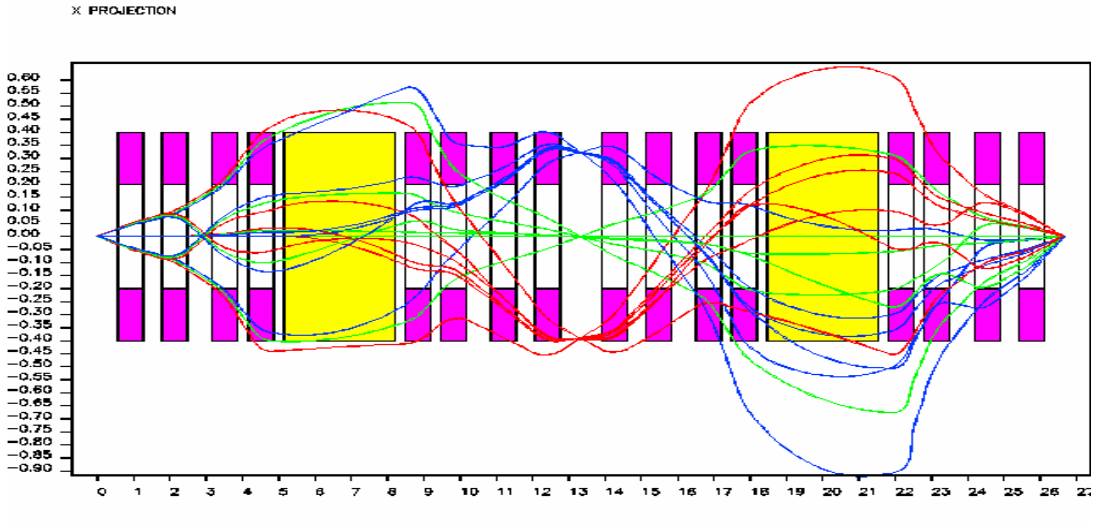

Figure 55. High magnet strength third order aberration correction of alternative second order best symmetric design – horizontal projection.

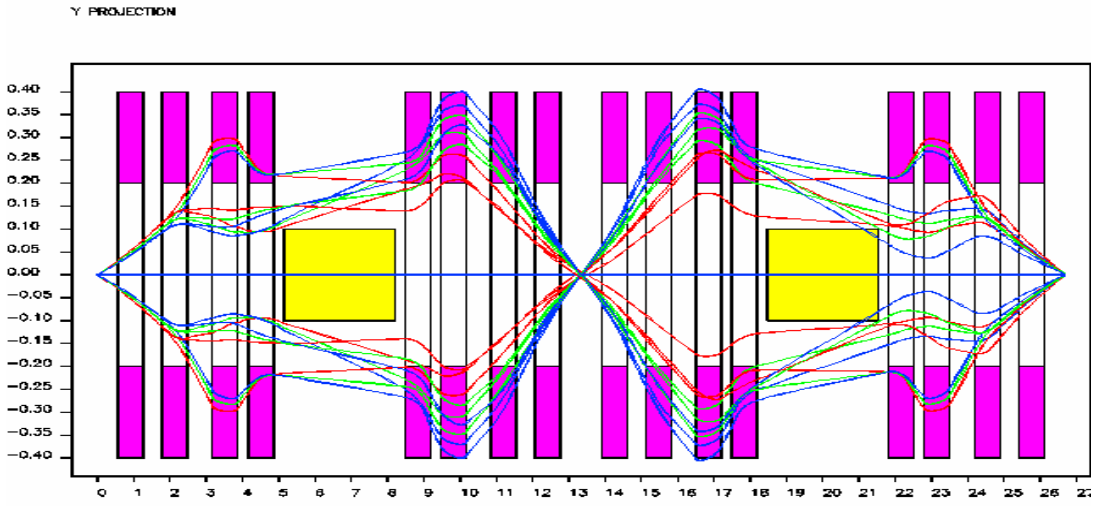

Figure 56. High magnet strength third order aberration correction of alternative second order best symmetric design – vertical projection.

After consideration of the third order results and the drawbacks of each, the first solution for the symmetric layout was selected. This solution focused at the

achromatic image and had very reasonable values (< .6 Telsa) for all octupole pole tip fields.

VI. FRINGE FIELD CORRECTIONS

All designs initially developed and simulated through third order were done without simulating the effects of fringe fields on the system. These effects obviously must be considered in any real system. While COSY is very capable of calculating these fields [12], the computing power required and time per simulation is substantial.

After determining the system through third order, it is relatively easy to correct for the effects of fringe fields. Using the values of the uncorrected system as initial values, simulations were run that incorporated the fringe field effects. This was done initially at first order. This resulted in very minor correction in the spacing and strengths of the system's quadrupoles. Further corrections were then calculated for the strengths of the sextupoles, and then the strengths of the octupoles. The data in the tables presented in the preceding sections comes from the system calculated to include the fringe field effects.

VII. EFFECTS OF HIGHER ORDER ABERRATIONS

Aberrations beyond third order will also affect the system. These effects could be corrected by using even higher order multipoles, but the practicality of such systems is very limited. With regard to all the solutions of the symmetric design, calculations through fifth order were run to determine the effect of these aberrations. This respect to both the low and high magnet solutions, the effects were substantial; both the horizontal and vertical beam widths diverge beyond several meters at fifth order. The selected symmetric layout solution, shown in Figures 57 and 58, demonstrated less extreme effects from aberrations through fifth order.

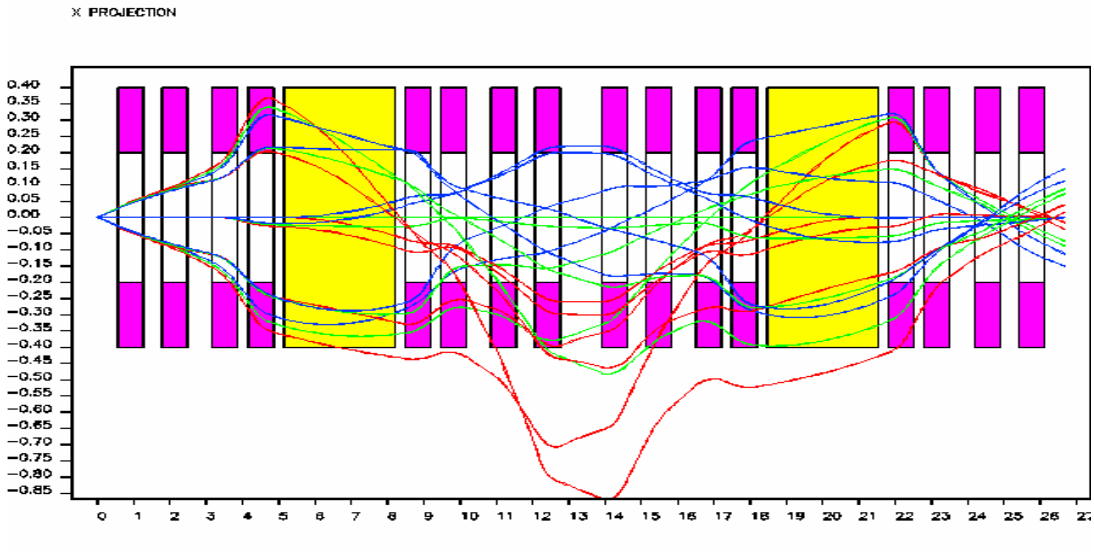

Figure 57. Best symmetric layout with aberrations through fifth order – wide angular acceptance – horizontal projection.

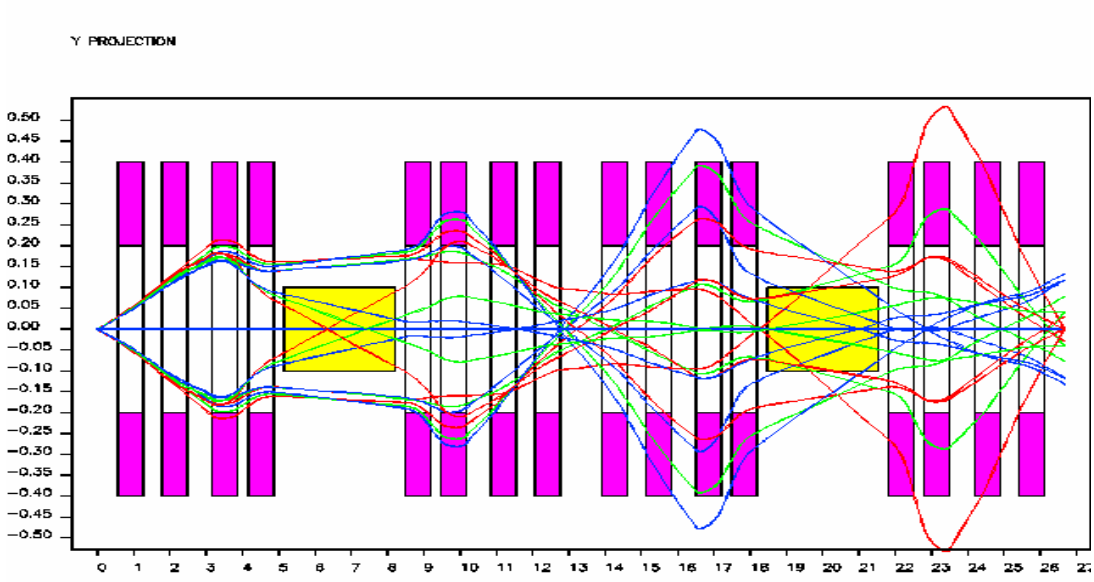

Figure 58. Best symmetric layout with aberrations through fifth order – wide angular acceptance – vertical projection.

These effects, however, primarily affect particle entering the system at a sharp angle. When the initial angular acceptance for the system is cut in half, as shown in Figures 59 and 60, the effects of the fifth order aberrations fall off dramatically.

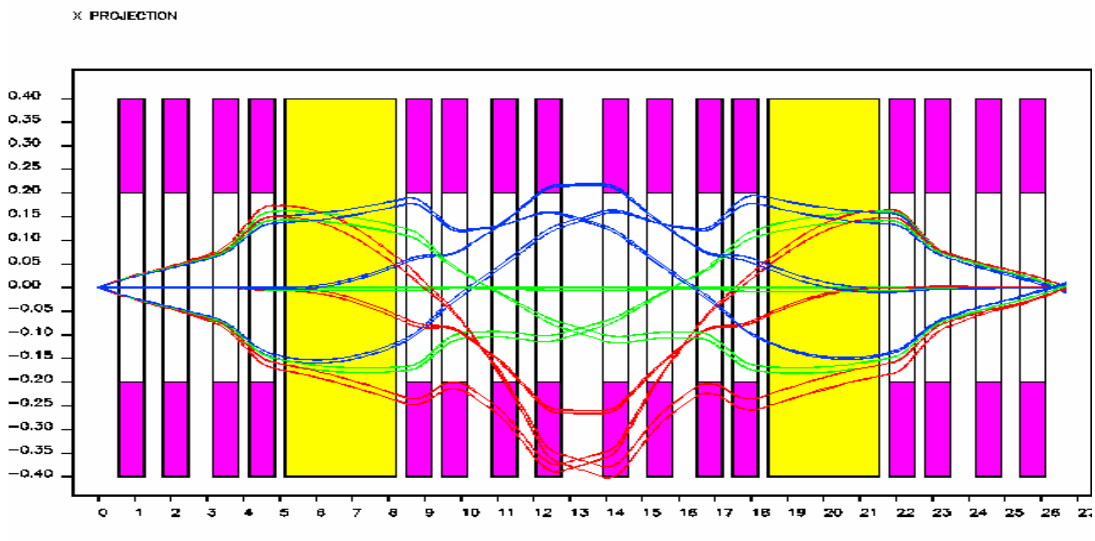

Figure 59. Best symmetric layout with aberrations through fifth order – reduced angular acceptance – horizontal projection.

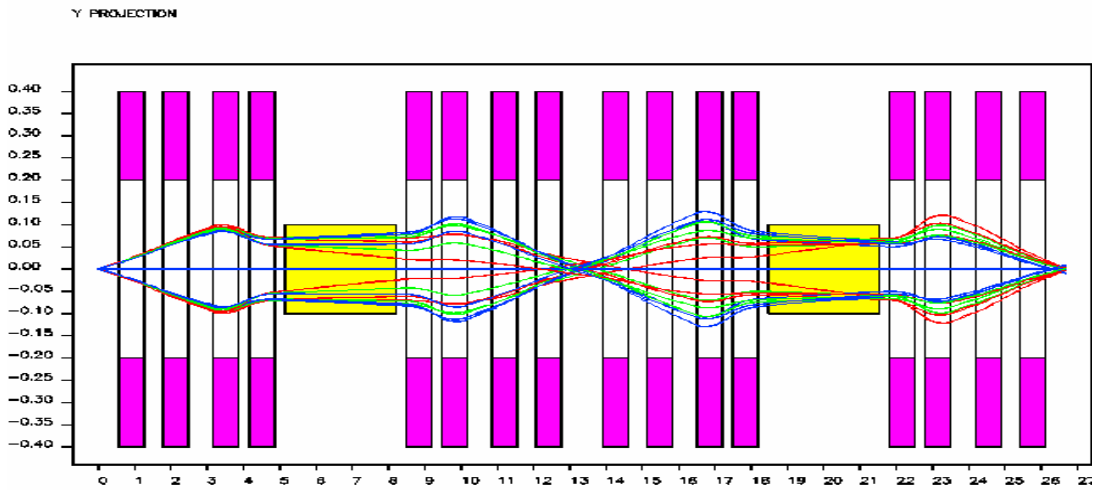

Figure 60. Best symmetric layout with aberrations through fifth order – reduced angular acceptance – vertical projection.

VIII. CONCLUSIONS

Having looked at many possible systems designs and how higher order aberrations in these systems can be corrected, the benefits of utilizing symmetry theories becomes apparent. In the area of a fragment separators, where large phase space volumes are involved, symmetry theory can play an important design role. The symmetry theories utilized in the examples previously discussed can be employed in almost any type of optical design. They demonstrate a powerful tool in finding solutions for the optical design of a fragment separator.

For the selected symmetric design, we have utilized a layout that contains 3 segments. The first spans from the target to the dispersive image where the first absorbing wedge will be placed. The second continues through the achromatic image. The third creates a second dispersive image where a second absorbing wedge can be placed before the gas catcher cell to minimize range variations.

Each of these segments maintains mirror symmetry for the first and second order elements (dipoles, quadrupoles, and sextupoles) about the dipole midplane. This mirror symmetry is with respect to both polarity and pole tip field strength of these multipoles. The result is that each segment is identical in terms of first and second order elements.

The system focuses point-to-parallel, parallel-to-point at the middle of the dipole at first order. This results in point-to-point, parallel-to-parallel focusing of both the dispersive and achromatic images. All but 5 of the critical commutator terms at second order are automatically minimized by mirror symmetry coupled with the symplectic condition.

It was also shown that our system design has only 4 truly independent second order commutator terms due to the coupled effects of the mirror and symplectic symmetries. Using the four independent sextupoles in each segment, a solution was found with the symmetric layout that met the second order criteria of minimizing all terms in the commutator equation through second order. This resulted in a system that minimized the aberrations at the achromatic image.

Theory indicates that the number of independent octupoles needed to minimize all the commutator terms at third order exceeded the number available in our system. Minimizing the third order terms in the commutator equation while maintaining mirror symmetry about the dipole midplane would require at least 10 independent octupoles ahead of the dipole in each segment. Only nine independent octupoles ahead of the dispersive image, however, are necessary to minimize all third order terms in the commutator equation with only angular and energy dependence.

A solution for the symmetry layout was found that satisfies the goal of minimizing positional aberrations at the achromatic image by breaking the mirror symmetry about the dipole midplane in the segments with regard to the third order

magnetic multipoles (octupoles). The selected design solution utilizes 8 independent octupoles in each segment, maintaining mirror symmetry with respect to the charge and polarity of these octupoles about the dispersive image plane. The result is that the order of the octupoles in adjoining segments of the separator is reversed.

The final design was corrected for the effects of fringe field and the effects of fourth and fifth order aberrations were calculated. These effects appear to have minimal effect on the system except in cases of wide angular acceptance from the initial target.

The selected symmetric design does not maintain a focused dispersive image. This will increase the stochastic effects resulting when the absorbing wedges are inserted into the system. This problem can be overcome with two alternative designs. The low magnet alternative design maintains the dispersive image, but does not minimize all aberrations at the achromatic image. It also suffers from greater higher order aberrations. The high magnet alternative design maintains focusing at both the dispersive and achromatic image, but the pole tip field strength of one of the octupole in each segment was so large that it would not be feasible to build. Also, this large octupole substantially increased the effect of fourth and fifth order aberrations in the system.

The methods employed in this paper demonstrate a repeatable and reliable method for the designing the next generation of high resolution fragment separators.

The use of symmetry theories is a powerful method which can be employed to design of such systems and correct aberrations that would affect their resolution.

REFERENCES

1) RIA physics white paper, http://www.phy.anl.gov/ria/ria-whitepaper-2000.pdf

2) J. Nolen, The U.S. Rare Isotope Acceleration Project; http://www.phy.anl.gov/ria/publications/MO302.pdf

3) Comparison of The Rare Isotope Accelerator to Other Facilities; http://www.nscl.edu/ria/idea/comparison.php

4) H. Geisel, H. Weick, M. Winkler, G. Münzenberg & M. Yavor, Ion-optical layout of a powerful next-generation pre-separator for in-flight separation of relativistic rare isotopes, *Nuclear Instruments & Methods in Physics Research*, B247 (2006) 368-376.

5) Wada, Ishida, et al., Slow & trapped RI-beams from projectile fragment separators, *Nuclear Instruments & Methods in Physics Research*, B204 (2003) 570-581.

6) T. Shimada, H. Miyatake & S. Morinobu, Design study of the secondary-beam line at RCNP, *Nuclear Instruments & Methods in Physics Research*, B70 (1992) 320-330.

7) J. Nolen & M. Portillo, Charged Particle Optics, The Optics Encyclopedia, Basic Foundations & Practical Applications, Vol. 1, ISBN 3-527-40320-5

8) H. Wollnik & M. Berz, Relations Between Elements of Transfer Matrices Due to Condition of Symplecticity, *Nuclear Instruments & Methods in Physics Research*, A238 (1985) 127-140.

9) M. Berz, Introduction to Beam Physics, Lecture Notes, MSUPA PHY 861.

10) M. Berz, Modern Map Methods in Particle Beam Physics, Academic Press (1999) ISBN 0-12-014750-5.

11) W. Wan & M. Berz, An Analytical Theory of Arbitrary Order Achromats, *Physical Review E*, Vol. 54, No. 3, (1996), 2870-83.

12) M. Berz & K. Makino, COSY Infinity Version 8.1 User's Guide & Reference Manual, (2002); http://www.bt.pa.msu.edu/index_files/cosy.htm

13) S. Wolfram, The MATHEMATICA Book, Fifth Edition,Wolfram Media (August 2003) ISBN 1579550223.

14) K. Brown & R. Servranchx, First- and Second-Order Charged Particle Optics, SLAC-PUB-3381, July 1984.

15) K. Brown, (1967) *Adv. Particle Physics* 1, 71-134.

APPENDIX A

RELATIONS IN COMMUTATOR AND NON-COMMUTATOR TERMS ARISING FROM SYMPLECTIC SYMMETRY

First, Second and Third Order Elements that appear in the commutator [*R*,*M*].

(x|a), (x|xa), (x|xδ), (x|yb), (x|xxa), (x|xaδ), (x|xyb), (x|aaa), (x|ayy), (x|abb), (x|aδδ), (x|ybδ)

(a|x), (a|δ), (a|xx), (a|xδ), (a|aa), (a|yy), (a|bb), (a|δδ), (a|xxx), (a|xxδ), (a|xaa), (a|xyy), (a|xbb), (a|xδδ), (a|aaδ), (a|ayb), (a|yyδ), (a|bbδ), (a|δδδ)

(y|b), (y|xb), (y|ay), (y|bδ), (y|xxb), (y|xay), (y|xbδ), (y|aab), (y|ayδ), (y|yyb), (y|bbb), (y|bδδ)

(b|y), (b|xy), (b|ab), (b|yδ), (b|xxy), (b|xab), (b|xyδ), (b|aay), (b|abδ), (b|yyy), (b|ybb), (b|yδδ)

(t|a), (t|xa), (t|aδ), (t|yb), (t|xxa), (t|xaδ), (t|xyb), (t|aaa), (t|ayy), (t|abb), (t|aδδ), (t|ybδ)

Relations of Interest Second Order Elements.

These elements appear in the commutator:

$(a|aa) \propto (x|xa)$

$(x|yb) \propto (b|ab) \propto (y|ay)$

$(a|bb) \propto (y|xb)$

$(a|yy) \propto (b|xy)$

This allows for 9 commutator elements to be minimized by only minimizing 4.

These elements do not appear in the commutator:

$(a|xa) \propto (x|xx)$

$(a|a\delta) \propto (x|x\delta)$

$(x|bb) \propto (y|ab)$

$(x|yy) \propto (b|ay)$

$(b|b\delta) \propto (y|y\delta)$

$(a|yb) \propto (b|xb) \propto (y|xy)$

Although these coefficients do not appear in the commutator, these relations are helpful for minimizing coefficients that do not appear in the commutator.

Relations of Interest Involving Third Order Elements.

$(x|xxa) \propto (a|xaa)$

$(a|aa\delta) \propto (x|xa\delta)$

$(x|xyb) \propto (a|ayb) \propto (b|xab) \propto (y|xay)$

$(x|ayy) \propto (b|aay)$

$(x|yb\delta) \propto (b|ab\delta) \propto (y|ay\delta)$

$(a|xyy) \propto (b|xxy)$

$(a|yy\delta) \propto (b|xy\delta)$

$(a|xbb) \propto (y|xxb)$

$(a|bb\delta) \propto (y|xb\delta)$

$(x|abb) \propto (y|aab)$

$(y|yyb) \propto (b|ybb)$

First, Second and Third Order Relations as derived by the method described in Wollnick & Berz [8].

-2(a|xx)(x|xa)+2(a|xa)(x|xx)+(a|xxa)(x|x)-(a|x)(x|xxa)-(a|xxx)(x|a)+(a|a)(x|xxx)=0

-2(a|xx)(x|aa)+2(a|aa)(x|xx)+(a|xaa)(x|x)-(a|x)(x|xaa)-(a|xxa)(x|a)+(a|a)(x|xxa)=0

2(a|δa)(x|xx)-2(a|xx)(x|δa)+(a|xδa)(x|x)-(a|x)(x|xδa)-(a|xxδ)(x|a)+(a|a)(x|xxδ)=0

-((a|x)(x|axa))+(a|axa)(x|x)-(a|xax)(x|a)+(a|a)(x|xax)=0

-2(a|xa)(x|aa)+2(a|aa)(x|xa)-((a|x)(x|aaa))+(a|aaa)(x|x)-(a|xaa)(x|a)+(a|a)(x|xaa)=0

2(a|δa)(x|xa)-2(a|xa)(x|δa)-((a|x)(x|aδa))+(a|aδa)(x|x)-(a|xaδ)(x|a)+(a|a)(x|xaδ)=0

-2(a|xδ)(x|xa)+2(a|xa)(x|xδ)+(a|δxa)(x|x)-(a|x)(x|δxa)-(a|xδx)(x|a)+(a|a)(x|xδx)=0

-2(a|xδ)(x|aa)+2(a|aa)(x|xδ)+(a|δaa)(x|x)-(a|x)(x|δaa)-(a|xδa)(x|a)+(a|a)(x|xδa)=0

2(a|δa)(x|xδ)-2(a|xδ)(x|δa)+(a|$\delta\delta$a)(x|x)-(a|x)(x|$\delta\delta$a)-(a|x$\delta\delta$)(x|a)+(a|a)(x|x$\delta\delta$)=0

2(b|ya)(y|xy)-2(b|xy)(y|ya)+(a|yya)(x|x)-(a|x)(x|yya)-(a|xyy)(x|a)+(a|a)(x|xyy)=0

-2(b|xy)(y|ba)+2(b|ba)(y|xy)+(a|yba)(x|x)-(a|x)(x|yba)-(a|xyb)(x|a)+(a|a)(x|xyb)=0

2(b|ya)(y|xb)-2(b|xb)(y|ya)-((a|x)(x|bya))+(a|bya)(x|x)-(a|xby)(x|a)+(a|a)(x|xby)=0

-2(b|xb)(y|ba)+2(b|ba)(y|xb)-((a|x)(x|bba))+(a|bba)(x|x)-(a|xbb)(x|a)+(a|a)(x|xbb)=0

-2(b|yx)(y|ya)+2(b|ya)(y|yx)-((b|y)(y|xya))+(b|xya)(y|y)-(a|yxy)(x|a)+(a|a)(x|yxy)=0

-2(b|yx)(y|ba)+2(b|ba)(y|yx)-((b|y)(y|xba))+(b|xba)(y|y)-(a|yxb)(x|a)+(a|a)(x|yxb)=0

-((b|y)(y|aya))+(b|aya)(y|y)-(a|yay)(x|a)+(a|a)(x|yay)=0

-2(b|ya)(y|ba)+2(b|ba)(y|ya)-((b|y)(y|aba))+(b|aba)(y|y)-(a|yab)(x|a)+(a|a)(x|yab)=0

-2(b|yδ)(y|ya)+2(b|ya)(y|yδ)+(b|δya)(y|y)-(b|y)(y|δya)-(a|yδy)(x|a)+(a|a)(x|yδy)=0

-2(b|yδ)(y|ba)+2(b|ba)(y|yδ)+(b|δba)(y|y)-(b|y)(y|δba)-(a|yδb)(x|a)+(a|a)(x|yδb)=0

-2(a|yy)(x|xa)+2(a|xa)(x|yy)+(b|yxa)(y|y)-(b|y)(y|yxa)-(a|yyx)(x|a)+(a|a)(x|yyx)=0

-2(a|yy)(x|aa)+2(a|aa)(x|yy)+(b|yaa)(y|y)-(b|y)(y|yaa)-(a|yya)(x|a)+(a|a)(x|yya)=0

2(a|δa)(x|yy)-2(a|yy)(x|δa)+(b|yδa)(y|y)-(b|y)(y|yδa)-(a|yyδ)(x|a)+(a|a)(x|yyδ)=0

-2(a|yb)(x|xa)+2(a|xa)(x|yb)-((b|y)(y|bxa))+(b|bxa)(y|y)-(a|ybx)(x|a)+(a|a)(x|ybx)=0

-2(a|yb)(x|aa)+2(a|aa)(x|yb)-((b|y)(y|baa))+(b|baa)(y|y)-(a|yba)(x|a)+(a|a)(x|yba)=0

2(a|δa)(x|yb)-2(a|yb)(x|δa)-((b|y)(y|bδa))+(b|bδa)(y|y)-(a|ybδ)(x|a)+(a|a)(x|ybδ)=0

2(a|yy)(x|xx)-2(a|xx)(x|yy)+(a|xyy)(x|x)-(a|x)(x|xyy)+(b|y)(y|xxy)-(b|xxy)(y|y)=0

-2(a|xx)(x|by)+2(a|by)(x|xx)+(a|xby)(x|x)-(a|x)(x|xby)+(b|y)(y|xxb)-(b|xxb)(y|y)=0

2(a|yy)(x|xa)-2(a|xa)(x|yy)-((a|x)(x|ayy))+(a|ayy)(x|x)+(b|y)(y|xay)-(b|xay)(y|y)=0

-2(a|xa)(x|by)+2(a|by)(x|xa)-((a|x)(x|aby))+(a|aby)(x|x)+(b|y)(y|xab)-(b|xab)(y|y)=0

2(a|yy)(x|xδ)-2(a|xδ)(x|yy)+(a|δyy)(x|x)-(a|x)(x|δyy)+(b|y)(y|xδy)-(b|xδy)(y|y)=0

-2(a|xδ)(x|by)+2(a|by)(x|xδ)+(a|$\delta$by)(x|x)-(a|x)(x|$\delta$by)+(b|y)(y|xδb)-(b|xδb)(y|y)=0

2(a|yb)(x|xx)-2(a|xx)(x|yb)+(a|xyb)(x|x)-(a|x)(x|xyb)-(b|xxy)(y|b)+(b|b)(y|xxy)=0

-2(a|xx)(x|bb)+2(a|bb)(x|xx)+(a|xbb)(x|x)-(a|x)(x|xbb)-(b|xxb)(y|b)+(b|b)(y|xxb)=0

2(a|yb)(x|xa)-2(a|xa)(x|yb)-((a|x)(x|ayb))+(a|ayb)(x|x)-(b|xay)(y|b)+(b|b)(y|xay)=0

-2(a|xa)(x|bb)+2(a|bb)(x|xa)-((a|x)(x|abb))+(a|abb)(x|x)-(b|xab)(y|b)+(b|b)(y|xab)=0

2(a|yb)(x|xδ)-2(a|xδ)(x|yb)+(a|δyb)(x|x)-(a|x)(x|δyb)-(b|xδy)(y|b)+(b|b)(y|xδy)=0

-2(a|xδ)(x|bb)+2(a|bb)(x|xδ)+(a|δbb)(x|x)-(a|x)(x|δbb)-(b|xδb)(y|b)+(b|b)(y|xδb)=0

2(a|yb)(x|ax)-2(a|ax)(x|yb)+(a|xyb)(x|a)-(a|a)(x|xyb)+(b|b)(y|axy)-(b|axy)(y|b)=0

2(a|bb)(x|ax)-2(a|ax)(x|bb)+(a|xbb)(x|a)-(a|a)(x|xbb)+(b|b)(y|axb)-(b|axb)(y|b)=0

2(a|yb)(x|aa)-2(a|aa)(x|yb)+(a|ayb)(x|a)-(a|a)(x|ayb)+(b|b)(y|aay)-(b|aay)(y|b)=0

2(a|bb)(x|aa)-2(a|aa)(x|bb)+(a|abb)(x|a)-(a|a)(x|abb)+(b|b)(y|aab)-(b|aab)(y|b)=0

2(a|yb)(x|aδ)-2(a|aδ)(x|yb)+(a|δyb)(x|a)-(a|a)(x|δyb)+(b|b)(y|aδy)-(b|aδy)(y|b)=0

2(a|bb)(x|aδ)-2(a|aδ)(x|bb)+(a|δbb)(x|a)-(a|a)(x|δbb)+(b|b)(y|aδb)-(b|aδb)(y|b)=0

(a|yxy)(x|x)-(a|x)(x|yxy)+(b|y)(y|xyx)-(b|xyx)(y|y)=0

-2(b|xy)(y|ay)+2(b|ay)(y|xy)+(a|yay)(x|x)-(a|x)(x|yay)+(b|y)(y|xya)-(b|xya)(y|y)=0

2(b|δy)(y|xy)-2(b|xy)(y|δy)+(a|yδy)(x|x)-(a|x)(x|yδy)+(b|y)(y|xyδ)-(b|xyδ)(y|y)=0

2(b|xy)(y|xb)-2(b|xb)(y|xy)+-((a|x)(x|bxy))+(a|bxy)(x|x)+(b|y)(y|xbx)-(b|xbx)(y|y)=0

-2(b|xb)(y|ay)+2(b|ay)(y|xb)-((a|x)(x|bay))+(a|bay)(x|x)+(b|y)(y|xba)-(b|xba)(y|y)=0

2(b|δy)(y|xb)-2(b|xb)(y|δy)-((a|x)(x|bδy))+(a|bδy)(x|x)+(b|y)(y|xbδ)-(b|xbδ)(y|y)=0

-2(b|xy)(y|xb)+2(b|xb)(y|xy)+(a|yxb)(x|x)-(a|x)(x|yxb)-(b|xyx)(y|b)+(b|b)(y|xyx)=0

-2(b|xy)(y|ab)+2(b|ab)(y|xy)+(a|yab)(x|x)-(a|x)(x|yab)-(b|xya)(y|b)+(b|b)(y|xya)=0

2(b|δb)(y|xy)-2(b|xy)(y|δb)+(a|yδb)(x|x)-(a|x)(x|yδb)-(b|xyδ)(y|b)+(b|b)(y|xyδ)=0

-((a|x)(x|bxb))+(a|bxb)(x|x)-(b|xbx)(y|b)+(b|b)(y|xbx)=0

-2(b|xb)(y|ab)+2(b|ab)(y|xb)-((a|x)(x|bab))+(a|bab)(x|x)-(b|xba)(y|b)+(b|b)(y|xba)=0

2(b|δb)(y|xb)-2(b|xb)(y|δb)-((a|x)(x|bδb))+(a|bδb)(x|x)-(b|xbδ)(y|b)+(b|b)(y|xbδ)=0

2(b|xb)(y|ay)-2(b|ay)(y|xb)+(a|yxb)(x|a)-(a|a)(x|yxb)+(b|b)(y|ayx)-(b|ayx)(y|b)=0

-2(b|ay)(y|ab)+2(b|ab)(y|ay)+(a|yab)(x|a)-(a|a)(x|yab)+(b|b)(y|aya)-(b|aya)(y|b)=0

2(b|δb)(y|ay)-2(b|ay)(y|δb)+(a|yδb)(x|a)-(a|a)(x|yδb)+(b|b)(y|ayδ)-(b|ayδ)(y|b)=0

2(b|xb)(y|ab)-2(b|ab)(y|xb)+(a|bxb)(x|a)-(a|a)(x|bxb)+(b|b)(y|abx)-(b|abx)(y|b)=0

(a|bab)(x|a)-(a|a)(x|bab)+(b|b)(y|aba)-(b|aba)(y|b)=0

2(b|δb)(y|ab)-2(b|ab)(y|δb)+(a|bδb)(x|a)-(a|a)(x|bδb)+(b|b)(y|abδ)-(b|abδ)(y|b)=0

-2(b|yx)(y|xb)+2(b|xb)(y|yx)-((b|y)(y|xxb))+(b|xxb)(y|y)-(b|yxx)(y|b)+(b|b)(y|yxx)=0

-2(b|yx)(y|ab)+2(b|ab)(y|yx)-((b|y)(y|xab))+(b|xab)(y|y)-(b|yxa)(y|b)+(b|b)(y|yxa)=0

2(b|δb)(y|yx)-2(b|yx)(y|δb)-((b|y)(y|xδb))+(b|xδb)(y|y)-(b|yxδ)(y|b)+(b|b)(y|yxδ)=0

-2(b|ya)(y|xb)+2(b|xb)(y|ya)-((b|y)(y|axb))+(b|axb)(y|y)-(b|yax)(y|b)+(b|b)(y|yax)=0

-2(b|ya)(y|ab)+2(b|ab)(y|ya)-((b|y)(y|aab))+(b|aab)(y|y)-(b|yaa)(y|b)+(b|b)(y|yaa)=0

2(b|δb)(y|ya)-2(b|ya)(y|δb)-((b|y)(y|aδb))+(b|aδb)(y|y)-(b|yaδ)(y|b)+(b|b)(y|yaδ)=0

-2(b|yδ)(y|xb)+2(b|xb)(y|yδ)+(b|δxb)(y|y)-(b|y)(y|δxb)-(b|yδx)(y|b)+(b|b)(y|yδx)=0

-2(b|yδ)(y|ab)+2(b|ab)(y|yδ)+(b|δab)(y|y)-(b|y)(y|δab)-(b|yδa)(y|b)+(b|b)(y|yδa)=0

2(b|δb)(y|yδ)-2(b|yδ)(y|δb)+(b|$\delta\delta$b)(y|y)-(b|y)(y|$\delta\delta$b)-(b|y$\delta\delta$)(y|b)+(b|b)(y|y$\delta\delta$)=0

-2(a|yy)(x|yb)+2(a|yb)(x|yy)+(b|yyb)(y|y)-(b|y)(y|yyb)-(b|yyy)(y|b)+(b|b)(y|yyy)=0

-2(a|yy)(x|bb)+2(a|bb)(x|yy)+(b|ybb)(y|y)-(b|y)(y|ybb)-(b|yyb)(y|b)+(b|b)(y|yyb)=0

-((b|y)(y|byb))+(b|byb)(y|y)-(b|yby)(y|b)+(b|b)(y|yby)=0

-2(a|yb)(x|bb)+2(a|bb)(x|yb)-((b|y)(y|bbb))+(b|bbb)(y|y)-(b|ybb)(y|b)+(b|b)(y|ybb)=0

2(a|xδ)(x|xx)-2(a|xx)(x|xδ)+(a|xxδ)(x|x)-(a|x)(x|xxδ)+(a|δ)(x|xxx)-(a|xxx)(x|δ)=-
(t|xxx)

-2(a|xx)(x|aδ)+2(a|aδ)(x|xx)+(a|xaδ)(x|x)-(a|x)(x|xaδ)+(a|δ)(x|xxa)-(a|xxa)(x|δ)=-
(t|xxa)

2(a|$\delta\delta$)(x|xx)-2(a|xx)(x|$\delta\delta$)+(a|x$\delta\delta$)(x|x)-(a|x)(x|x$\delta\delta$)+(a|δ)(x|xxδ)-(a|xxδ)(x|δ)=-
(t|xxδ)

2(a|xδ)(x|xa)-2(a|xa)(x|xδ)-((a|x)(x|axδ))+(a|axδ)(x|x)+(a|δ)(x|xax)-(a|xax)(x|δ)=-
(t|xxa)

-2(a|xa)(x|aδ)+2(a|aδ)(x|xa)-((a|x)(x|aaδ))+(a|aaδ)(x|x)+(a|δ)(x|xaa)-(a|xaa)(x|δ)=-
(t|xaa)

2(a|$\delta\delta$)(x|xa)-2(a|xa)(x|$\delta\delta$)-((a|x)(x|a$\delta\delta$))+(a|a$\delta\delta$)(x|x)+(a|δ)(x|xaδ)-(a|xaδ)(x|δ)=-
(t|xaδ)

(a|δxδ)(x|x)-(a|x)(x|δxδ)+(a|δ)(x|xδx)-(a|xδx)(x|δ)=-(t|xxδ)

-2(a|xδ)(x|aδ)+2(a|aδ)(x|xδ)+(a|δaδ)(x|x)-(a|x)(x|δaδ)+(a|δ)(x|xδa)-(a|xδa)(x|δ)-

(t|xaδ)

2(a|δδ)(x|xδ)-2(a|xδ)(x|δδ)+(a|δδδ)(x|x)-(a|x)(x|δδδ)+(a|δ)(x|xδδ)-(a|xδδ)(x|δ)=-

(t|xδδ)

2(a|xδ)(x|ax)-2(a|ax)(x|xδ)+(a|xxδ)(x|a)-(a|a)(x|xxδ)+(a|δ)(x|axx)-(a|axx)(x|δ)=-

(t|xxa)

2(a|aδ)(x|ax)-2(a|ax)(x|aδ)+(a|xaδ)(x|a)-(a|a)(x|xaδ)+(a|δ)(x|axa)-(a|axa)(x|δ)=-

(t|xaa)

2(a|δδ)(x|ax)-2(a|ax)(x|δδ)+(a|xδδ)(x|a)-(a|a)(x|xδδ)+(a|δ)(x|axδ)-(a|axδ)(x|δ)=-

(t|xaδ)

2(a|xδ)(x|aa)-2(a|aa)(x|xδ)+(a|axδ)(x|a)-(a|a)(x|axδ)+(a|δ)(x|aax)-(a|aax)(x|δ)=-

(t|xaa)

2(a|aδ)(x|aa)-2(a|aa)(x|aδ)+(a|aaδ)(x|a)-(a|a)(x|aaδ)+(a|δ)(x|aaa)-(a|aaa)(x|δ)=-

(t|aaa)

2(a|δδ)(x|aa)-2(a|aa)(x|δδ)+(a|aδδ)(x|a)-(a|a)(x|aδδ)+(a|δ)(x|aaδ)-(a|aaδ)(x|δ)=-

(t|aaδ)

2(a|xδ)(x|aδ)-2(a|aδ)(x|xδ)+(a|δxδ)(x|a)-(a|a)(x|δxδ)+(a|δ)(x|aδx)-(a|aδx)(x|δ)=-

(t|xaδ)

(a|δaδ)(x|a)-(a|a)(x|δaδ)+(a|δ)(x|aδa)-(a|aδa)(x|δ)=-(t|aaδ)

2(a|δδ)(x|aδ)-2(a|aδ)(x|δδ)+(a|δδδ)(x|a)-(a|a)(x|δδδ)+(a|δ)(x|aδδ)-(a|aδδ)(x|δ)=-

(t|aδδ)

$2(b|y\delta)(y|xy)-2(b|xy)(y|y\delta)+(a|yy\delta)(x|x)-(a|x)(x|yy\delta)+(a|\delta)(x|xyy)-(a|xyy)(x|\delta)=-$

$(t|xyy)$

$-2(b|xy)(y|b\delta)+2(b|b\delta)(y|xy)+(a|yb\delta)(x|x)-(a|x)(x|yb\delta)+(a|\delta)(x|xyb)-(a|xyb)(x|\delta)=-$

$(t|xyb)$

$2(b|y\delta)(y|xb)-2(b|xb)(y|y\delta)-((a|x)(x|by\delta))+(a|by\delta)(x|x)+(a|\delta)(x|xby)-(a|xby)(x|\delta)=-$

$(t|xyb)$

$-2(b|xb)(y|b\delta)+2(b|b\delta)(y|xb)-((a|x)(x|bb\delta))+(a|bb\delta)(x|x)+(a|\delta)(x|xbb)-$

$(a|xbb)(x|\delta)=-(t|xbb)$

$2(b|y\delta)(y|ay)-2(b|ay)(y|y\delta)+(a|yy\delta)(x|a)-(a|a)(x|yy\delta)+(a|\delta)(x|ayy)-(a|ayy)(x|\delta)=-$

$(t|ayy)$

$2(b|b\delta)(y|ay)-2(b|ay)(y|b\delta)+(a|yb\delta)(x|a)-(a|a)(x|yb\delta)+(a|\delta)(x|ayb)-(a|ayb)(x|\delta)=-$

$(t|ayb)$

$2(b|y\delta)(y|ab)-2(b|ab)(y|y\delta)+(a|by\delta)(x|a)-(a|a)(x|by\delta)+(a|\delta)(x|aby)-(a|aby)(x|\delta)=-$

$(t|ayb)$

$2(b|b\delta)(y|ab)-2(b|ab)(y|b\delta)+(a|bb\delta)(x|a)-(a|a)(x|bb\delta)+(a|\delta)(x|abb)-(a|abb)(x|\delta)=-$

$(t|abb)$

$2(b|y\delta)(y|yx)-2(b|yx)(y|y\delta)+-((b|y)(y|xy\delta))+(b|xy\delta)(y|y)+(a|\delta)(x|yxy)-$

$(a|yxy)(x|\delta)=-(t|yxy)$

$-2(b|yx)(y|b\delta)+2(b|b\delta)(y|yx)-((b|y)(y|xb\delta))+(b|xb\delta)(y|y)+(a|\delta)(x|yxb)-$

$(a|yxb)(x|\delta)=-(t|yxb)$

$2(b|y\delta)(y|ya)-2(b|ya)(y|y\delta)-((b|y)(y|ay\delta))+(b|ay\delta)(y|y)+(a|\delta)(x|yay)-(a|yay)(x|\delta)=-$

$(t|yay)$

-2(b|ya)(y|bδ)+2(b|bδ)(y|ya)-((b|y)(y|abδ))+(b|abδ)(y|y)+(a|δ)(x|yab)-(a|yab)(x|δ)=-(t|yab)

(b|δyδ)(y|y)-(b|y)(y|δyδ)+(a|δ)(x|yδy)-(a|yδy)(x|δ)=-(t|yδy)

-2(b|yδ)(y|bδ)+2(b|bδ)(y|yδ)+(b|δbδ)(y|y)-(b|y)(y|δbδ)+(a|δ)(x|yδb)-(a|yδb)(x|δ)=-(t|ybδ)

2(b|yδ)(y|bx)-2(b|bx)(y|yδ)+(b|xyδ)(y|b)-(b|b)(y|xyδ)+(a|δ)(x|bxy)-(a|bxy)(x|δ)=-(t|yxb)

2(b|bδ)(y|bx)-2(b|bx)(y|bδ)+(b|xbδ)(y|b)-(b|b)(y|xbδ)+(a|δ)(x|bxb)-(a|bxb)(x|δ)=-(t|bxb)

2(b|yδ)(y|ba)-2(b|ba)(y|yδ)-((b|b)(y|ayδ))+(b|ayδ)(y|b)+(a|δ)(x|bay)-(a|bay)(x|δ)=-(t|yab)

2(b|bδ)(y|ba)-2(b|ba)(y|bδ)-((b|b)(y|abδ))+(b|abδ)(y|b)+(a|δ)(x|bab)-(a|bab)(x|δ)=-(t|bab)

2(b|yδ)(y|bδ)-2(b|bδ)(y|yδ)+(b|δyδ)(y|b)-(b|b)(y|δyδ)+(a|δ)(x|bδy)-(a|bδy)(x|δ)=-(t|bδy)

(b|δbδ)(y|b)-(b|b)(y|δbδ)+(a|δ)(x|bδb)-(a|bδb)(x|δ)=-(t|bbδ)

-2(a|yy)(x|xδ)+2(a|xδ)(x|yy)+(b|yxδ)(y|y)-(b|y)(y|yxδ)+(a|δ)(x|yyx)-(a|yyx)(x|δ)=-(t|yyx)

-2(a|yy)(x|aδ)+2(a|aδ)(x|yy)+(b|yaδ)(y|y)-(b|y)(y|yaδ)+(a|δ)(x|yya)-(a|yya)(x|δ)=-(t|yya)

2(a|$\delta\delta$)(x|yy)-2(a|yy)(x|$\delta\delta$)+(b|y$\delta\delta$)(y|y)-(b|y)(y|y$\delta\delta$)+(a|δ)(x|yyδ)-(a|yyδ)(x|δ)=-(t|yyδ)

-2(a|yb)(x|xδ)+2(a|xδ)(x|yb)-((b|y)(y|bxδ))+(b|bxδ)(y|y)+(a|δ)(x|ybx)-(a|ybx)(x|δ)=-(t|ybx)

-2(a|yb)(x|aδ)+2(a|aδ)(x|yb)-((b|y)(y|baδ))+(b|baδ)(y|y)+(a|δ)(x|yba)-(a|yba)(x|δ)=-(t|yab)

2(a|$\delta\delta$)(x|yb)-2(a|yb)(x|$\delta\delta$)-((b|y)(y|b$\delta\delta$))+(b|b$\delta\delta$)(y|y)+(a|δ)(x|ybδ)-(a|ybδ)(x|δ)=-(t|ybδ)

2(a|xδ)(x|by)-2(a|by)(x|xδ)+(b|yxδ)(y|b)-(b|b)(y|yxδ)+(a|δ)(x|byx)-(a|byx)(x|δ)=-(t|byx)

-2(a|by)(x|aδ)+2(a|aδ)(x|by)+(b|yaδ)(y|b)-(b|b)(y|yaδ)+(a|δ)(x|bya)-(a|bya)(x|δ)=-(t|bya)

2(a|$\delta\delta$)(x|by)-2(a|by)(x|$\delta\delta$)+(b|y$\delta\delta$)(y|b)-(b|b)(y|y$\delta\delta$)+(a|δ)(x|byδ)-(a|byδ)(x|δ)=-(t|byδ)

2(a|xδ)(x|bb)-2(a|bb)(x|xδ)+(b|bxδ)(y|b)-(b|b)(y|bxδ)+(a|δ)(x|bbx)-(a|bbx)(x|δ)=-(t|bbx)

-2(a|bb)(x|aδ)+2(a|aδ)(x|bb)+(b|baδ)(y|b)-(b|b)(y|baδ)+(a|δ)(x|bba)-(a|bba)(x|δ)=-(t|bba)

2(a|$\delta\delta$)(x|bb)-2(a|bb)(x|$\delta\delta$)+(b|b$\delta\delta$)(y|b)-(b|b)(y|b$\delta\delta$)+(a|δ)(x|bbδ)-(a|bbδ)(x|δ)= -(t|bbδ)

APPENDIX B

RELATIONS FROM THE EFFECTS OF COUPLING MIRROR SYMMETRY AND SYMPLECTIC SYMMETRY IN BEAM OPTIC IMAGING

Mirror symmetry about the dipole midplane can be used to find criteria for minimizing commutator terms from the transfer map through the dispersive image. These relations coupled with sympletic symmetry relations can provide a method to reduce aberrations in an optical beam system at the achromatic image. Initially we want a system that focuses an image point-to-point, parallel-to-parallel at both the dispersive and achromatic image. We can achieve this by focusing point-to-parallel, parallel-to-point through the middle of the dipole and maintaining mirror symmetry about the dipole midplane.

First Order Criteria at Dipole Mid-Plane (point-to-parallel, parallel-to-point):

$(x|x)_M = (a|a)_M = (y|y)_M = (b|b)_M = 0$
$(x|a)_M(a|x)_M = (y|b)_M(b|y)_M = -1$

Non-zero second order dispersive image commutator terms as function of dipole midplane coefficients then reduced by first order criteria at the dipole midplane.

$(x|ad)_D = +2(a|ad)_M(x|a)_M + 2(a|xa)_M(a|d)_M(x|a)_M^2$
$(a|xd)_D = -2(x|xd)_M/(x|a)_M - 4(x|xx)_M(a|d)_M$
$(a|dd)_D = +2(x|xd)_M(a|d)_M + 4(x|xx)_M(x|a)_M(a|d)_M^2$
$(y|bd)_D = +2(b|bd)_M(y|b)_M + 2(b|xb)_M(a|d)_M(x|a)_M(y|b)_M$
$(b|yd)_D = -2(y|xy)_M(x|a)_M(a|d)_M/(y|b)_M - 2(y|dd)_M/(y|b)_M$

Assuming $(x|x)_M = (a|a)_M = (y|y)_M = (b|b)_M = 0$; then $(x|a)_M = -1/(a|x)_M$; and $(y|b)_M = -1/(b|y)_M$, the second order symplectic relations given in Wollnik/Berz p. 133-34 reduce to:

$-(a\|x)_M(x\|xa)_M - (a\|xx)_M(x\|a)_M = 0$	$(x\|xa)_M = (a\|xx)_M/(a\|x)_M^2 = (a\|xx)_M(x\|a)_M^2$
$-(a\|x)_M(x\|aa)_M - (a\|xa)_M(x\|a)_M = 0$	$(x\|aa)_M = (a\|xa)_M/(a\|x)_M^2 = (a\|xa)_M(x\|a)_M^2$
$-(a\|x)_M(x\|\delta a)_M - (a\|x\delta)_M(x\|a)_M = 0$	$(x\|\delta a)_M = (a\|x\delta)_M/(a\|x)_M^2 = (a\|x\delta)_M(x\|a)_M^2$
$+(x\|a)_M(a\|yy)_M + (y\|ay)_M(b\|y)_M = 0$	$(a\|yy)_M = (y\|ay)_M(b\|y)_M(a\|x)_M = (y\|ay)_M/(y\|b)_M(x\|a)_M$
$+(x\|a)_M(a\|by)_M + (y\|ab)_M(b\|y)_M = 0$	$(a\|by)_M = (y\|ab)_M(b\|y)_M(a\|x)_M = (y\|ab)_M/(y\|b)_M(x\|a)_M$
$-(a\|x)_M(x\|yy)_M + (y\|xy)_M(b\|y)_M = 0$	$(x\|yy)_M = (y\|xy)_M(b\|y)_M/(a\|x)_M = (y\|xy)_M(x\|a)_M/(y\|b)_M$
$-(a\|x)_M(x\|by)_M + (y\|xb)_M(b\|y)_M = 0$	$(x\|by)_M = (y\|xb)_M(b\|y)_M/(a\|x)_M = (y\|xb)_M(x\|a)_M/(y\|b)_M$
$-(a\|x)_M(x\|yb)_M - (b\|xy)_M(y\|b)_M = 0$	$(x\|yb)_M = (b\|xy)_M/(b\|y)_M(a\|x)_M = (b\|xy)_M(y\|b)_M(x\|a)_M$
$-(a\|x)_M(x\|bb)_M - (b\|xb)_M(y\|b)_M = 0$	$(x\|bb)_M = (b\|xb)_M/(b\|y)_M(a\|x)_M = (b\|xb)_M(y\|b)_M(x\|a)_M$
$+(x\|a)_M(a\|yb)_M - (b\|ay)_M(y\|b)_M = 0$	$(a\|yb)_M = (b\|ay)_M(a\|x)_M/(b\|y)_M = (b\|ay)_M(y\|b)_M/(x\|a)_M$
$+(x\|a)_M(a\|bb)_M - (b\|ab)_M(y\|b)_M = 0$	$(a\|bb)_M = (b\|ab)_M(a\|x)_M/(b\|y)_M = (b\|ab)_M(y\|b)_M/(x\|a)_M$
$-(b\|y)_M(y\|xb)_M - (b\|yx)_M(y\|b)_M = 0$	$(y\|xb)_M = (b\|yx)_M/(b\|y)_M^2 = (b\|yx)_M(y\|b)_M^2$
$-(b\|y)_M(y\|ab)_M - (b\|ya)_M(y\|b)_M = 0$	$(y\|ab)_M = (b\|ya)_M/(b\|y)_M^2 = (b\|ya)_M(y\|b)_M^2$
$-(b\|y)_M(y\|\delta b)_M - (b\|y\delta)_M(y\|b)_M = 0$	$(y\|\delta b)_M = (b\|y\delta)_M/(b\|y)_M^2 = (b\|y\delta)_M(y\|b)_M^2$

Third order dispersive image commutator terms as function of dipole midplane coefficients then reduced by substituting symplectic relations and then by

substituting second order relations at dipole midplane which minimize second Order dispersive image commutator terms. Calculation of the third order terms of form (x|__) are shown for illustration.

$(x|xxa)_D = +2(a|xxa)_M(x|a)_M + 2(a|xa)_M(a|xx)_M(x|a)_M^2 - 2(a|xa)_M(x|xa)_M$
$= +2(a|xxa)_M(x|a)_M$

$(x|xa\delta)_D = -4(a|xxa)_M(x|a)_M^2(a|\delta)_M - 4(a|a\delta)_M(a|xx)_M(x|a)_M^2 -$
$8(a|xa)_M(a|xx)_M(x|a)_M^3(a|\delta)_M + 2(a|a\delta)_M(x|xa)_M + 6(a|xa)_M(x|xa)_M(x|a)_M(a|\delta)_M$
$+ 4(a|aa)_M(x|xd)_M + 8(a|aa)_M(x|xx)_M(x|a)_M(a|\delta)_M$
$= -4(a|xxa)_M(x|a)_M^2(a|\delta)_M - 2(a|a\delta)_M(a|xx)_M(x|a)_M^2 -$
$2(a|xa)_M(a|xx)_M(x|a)_M^3(a|\delta)_M + 4(a|aa)_M(x|xd)_M + 8(a|aa)_M(x|xx)_M(x|a)_M(a|\delta)_M$
$= -4(a|xxa)_M(x|a)_M^2(a|\delta)_M$

$(x|xyb)_D = +2(a|xyb)_M(x|a)_M - 2(a|xa)_M(x|yb)_M + 2(a|yb)_M(b|xy)_M(x|a)_M(y|b)_M -$
$2(a|yb)_M(y|xb)_M(x|a)_M/(y|b)_M$
$= +2(a|xyb)(x|a) -2 (a|xa)(x|yb)$

$(x|aaa)_D = +2(a|aaa)_M(x|a)_M + 2(a|aa)_M(a|xa)_M(x|a)_M^2$

$(x|ayy)_D = +2(a|ayy)_M(x|a)_M + 2(a|xa)_M(a|yy)_M(x|a)_M^2 - 2(a|yb)_M(y|ay)_M(x|a)_M/(y|b)_M$
$= +2(a|ayy)_M(x|a)_M + 2(a|xa)_M(a|yy)_M(x|a)_M^2 - 2(a|yb)_M(a|yy)_M(x|a)_M^2$

$(x|abb)_D = +2(a|abb)_M(x|a)_M + 2(a|bb)_M(a|xa)_M(x|a)_M^2 + 2(a|yb)_M(b|ab)_M(x|a)_M(y|b)_M$
$= +2(a|abb)_M(x|a)_M + 2(a|xa)_M(a|bb)_M(x|a)_M^2 + 2(a|yb)_M(a|bb)_M(x|a)_M^2$

$(x|a\delta\delta)_D = +2(a|a\delta\delta)_M(x|a)_M + 2(a|xad)_M(x|a)_M^2(a|\delta)_M + 4(a|xxa)_M(x|a)_M^3(a|\delta)_M^2 +$
$2(a|\delta\delta)_M(a|xa)_M(x|a)_M^2 + 2(a|a\delta)_M(a|x\delta)_M(x|a)_M^2 +$
$4(a|xa)_M(a|x\delta)_M(x|a)_M^3(a|\delta)_M + 8(a|a\delta)_M(a|xx)_M(x|a)_M^3(a|\delta)_M +$
$12(a|xa)_M(a|xx)_M(x|a)_M^4(a|\delta)_M^2 - 2(a|a\delta)_M(x|xa)_M(x|a)_M(a|\delta)_M^2 -$
$4(a|xa)_M(x|xa)_M(x|a)_M^2(a|\delta)_M^2 - 4(a|aa)_M(x|x\delta)_M(x|a)_M(a|\delta)_M -$
$8(a|aa)_M(x|xx)_M(x|a)_M^2(a|\delta)_M^2$
$= +2(a|a\delta\delta)_M(x|a)_M + 2(a|xad)_M(x|a)_M^2(a|\delta)_M + 4(a|xxa)_M(x|a)_M^3(a|\delta)_M^2 +$
$2(a|\delta\delta)_M(a|xa)_M(x|a)_M^2 + 2(a|a\delta)_M(a|x\delta)_M(x|a)_M^2 - 4(a|aa)_M(x|x\delta)_M(x|a)_M(a|\delta)_M$
$+ 4(a|xa)_M(a|x\delta)_M(x|a)_M^3(a|\delta)_M + 6(a|a\delta)_M(a|xx)_M(x|a)_M^3(a|\delta)_M +$
$8(a|xa)_M(a|xx)_M(x|a)_M^4(a|\delta)_M^2 - 8(a|aa)_M(x|xx)_M(x|a)_M^2(a|\delta)_M^2$
$= 2(a|a\delta\delta)_M(x|a)_M + 2(a|xad)_M(x|a)_M^2(a|\delta)_M + 4(a|xxa)_M(x|a)_M^3(a|\delta)_M^2 +$
$2(a|\delta\delta)_M(a|xa)_M(x|a)_M^2 + (a|xa)_M(a|x\delta)_M(x|a)_M^3(a|\delta)_M +$
$(a|xa)_M(a|xx)_M(x|a)_M^4(a|\delta)_M$

$(x|yb\delta)_D = -2(a|xyb)_M(x|a)_M^2(a|\delta)_M + 2(a|a\delta)_M(x|yb)_M + 4(a|xa)_M(x|yb)_M(x|a)_M(a|\delta)_M -$
$4(a|yy)_M(b|b\delta)_M(x|a)_M(y|b)_M - 4(a|yy)_M(b|xb)_M(x|a)_M^2(y|b)_M(a|\delta)_M -$

$2(a|yb)_M(b|xy)_M(x|a)_M^2(y|b)_M(a|\delta)_M + 2(a|yb)_M(y|xb)_M(x|a)_M^2(a|\delta)_M/(y|b)_M +$
$4(a|bb)_M(y|xy)_M(x|a)_M^2(a|\delta)_M/(y|b)_M + 4(a|bb)_M(y|y\delta)_M(x|a)_M/(y|b)_M$
$= -2(a|xyb)_M(x|a)_M^2(a|\delta)_M + 2(a|xa)_M(y|xb)_M(x|a)_M^2(a|\delta)_M/(y|b)_M$

Of these eight equations, only 6 are truly independent. Equations 1 and 2 merely state the same relationship. Equations 3 and 8 also state the same relationship.

These six equations contain 7 independent third order dipole midplane transfer map coefficients.

When this process is repeated for all of the commutator terms, we are left with only 24 independent relationships from the transfer map to dipole midplane that minimize the third order commutator terms. These are as follows, group in terms of the third order term(s) since the second order terms will be fixed values at third order:

$(a|xxx)_D$ and $(a|xx\delta)_D$ minimized when $(x|xxx)_M = -2(x|xa)_M(x|xx)_M/(x|a)_M$

$(a|xaa)_D$ and $(a|aa\delta)_D$ minimized when $(x|xaa)_M = 2(x|aa)_M(x|xa)_M/(x|a)_M -$
$2(a|aa)_M(x|xx)_M(x|a)_M$

$(a|xyy)_D$ and $(a|yy\delta)_D$ minimized when $(x|xyy)_M = -2(x|yb)_M(x|yy)_M/(x|a)_M -$
$2(x|xx)_M(y|ay)_M/(y|b)_M$

$(a|xbb)_D$ and $(a|bb\delta)_D$ minimized when $(x|xbb)_M = -2(a|bb)_M(x|xx)_M(x|a)_M +$
$4(x|bb)_M(x|yb)_M/(x|a)_M$

$(a|x\delta\delta)_D$ and $(a|\delta\delta\delta)_D$ minimized when $(x|x\delta\delta)_M + 2(x|xx\delta)_M(a|\delta)_M(x|a)_M +$
$6(x|xxx)_M(x|a)_M^2(a|\delta)_M^2 = -2(a|\delta\delta)_M(x|xx)_M(x|a)_M -$
$8(x|xa)_M(x|xx)_M(x|a)_M(a|\delta)_M^2$

$(a|ayb)_D$ minimized when $(x|ayb)_M = 2(x|aa)_M(x|yb)_M/(x|a)_M - 4(a|bb)_M(x|yy)_M(x|a)_M$
$+ 4(x|bb)_M(y|ay)_M/(y|b)_M$

$(x|xxa)_D$ and $(x|xa\delta)_D$ minimized when $(a|xxa)_M = 0$

$(x|xyb)_D$ and $(x|yb\delta)_D$ minimized when $(a|xyb)_M = -(x|aa)_M(x|yb)_M/(x|a)_M$

$(x|aaa)_D$ minimized when $(a|aaa)_M = -(a|aa)_M(x|aa)_M/(x|a)_M$

$(x|ayy)_D$ minimized when $(a|ayy)_M = (y|ab)_M(y|ay)_M/(x|a)_M(y|b)_M^2 –$
$(x|aa)_M(y|ay)_M/(x|a)_M^2(y|b)_M$

$(x|abb)_D$ minimized when $(a|abb)_M = -(a|bb)_M(x|aa)_M/(x|a)_M - (a|bb)_M(y|ab)_M(x|a)_M^2/(y|b)_M$

$(x|a\delta\delta)_D$ minimized when $(a|a\delta\delta)_M + (a|xa\delta)_M(x|a)_M(a|\delta)_M + 2(a|xxa)_M(x|a)_M^2(a|\delta)_M^2 = -(x|aa)_M(x|a\delta)_M(a|\delta)_M/(x|a)_M^2 - (x|aa)_M(a|\delta)_M^2$

$(b|xxy)_D$ and $(b|xy\delta)_D$ minimized when $(y|xxy)_M = -(x|xa)_M(x|yy)_M(y|b)_M/(x|a)_M^2 - (x|yb)_M(x|yy)_M(y|b)_M/(x|a)_M^2$

$(b|xab)_D$ and $(b|ab\delta)_D$ minimized when $(y|xab)_M = -(a|bb)_M(x|yy)_M(y|b)_M + (x|xa)_M(y|ab)_M/(x|a)_M + (x|yb)_M(y|ab)_M/(x|a)_M$

$(b|aay)_D$ minimized when $(y|aay)_M = -2(a|aa)_M(x|yy)_M(y|b)_M + (y|ab)_M(y|ay)_M/(y|b)_M$

$(b|yyy)_D$ minimized when $(y|yyy)_M = -2(xyy)_M(y|ay)_M/(x|a)_M$

$(b|ybb)_D$ minimized when $(y|ybb)_M = -2(a|bb)_M(x|yy)_M(y|b)_M + 2(x|yb)_M(y|ab)_M/(x|a)_M$

$(b|y\delta\delta)_D$ minimized when $2(y|xxy)_M + (y|xy\delta)_M/(x|a)_M(a|\delta)_M + (y|y\delta\delta)_M/(x|a)_M^2(a|\delta)_M^2 = -(a|\delta\delta)_M(x|yy)_M(y|b)_M/(x|a)_M^2(a|\delta)_M^2 - 2(x|a\delta)_M(x|yy)_M(y|b)_M/(x|a)_M^3(a|\delta)_M - 2(x|xa)_M(x|yy)_M(y|b)_M/(x|a)_M^2 - (x|yb)_M(x|yy)_M(y|b)_M/(x|a)_M^2$

$(y|xxb)_D$ and $(y|xb\delta)_D$ minimized when $(b|xxb)_M = -(x|bb)_M(x|xa)_M/(x|a)_M^2(y|b)_M + (x|bb)_M(x|yb)_M/(x|a)_M^2(y|b)_M$

$(y|xay)_D$ and $(y|ay\delta)_D$ minimized when $(b|xay)_M = (a|yb)_M(x|xa)_M/(y|b)_M - (a|yb)_M(x|yb)_M/(y|b)_M + (x|bb)_M(y|ay)_M/(x|a)_M(y|b)_M^2$

$(y|aab)_D$ minimized when $(b|aab)_M = -(a|bb)_M(a|yb)_M(x|a)_M^2/(y|b)_M - (a|aa)_M(x|bb)_M/(y|b)_M$

$(y|yyb)_D$ minimized when $(b|yyb)_M = (a|yb)_M(x|yb)_M/(y|b)_M - (x|bb)_M(y|ay)_M/(x|a)_M(y|b)_M^2$

$(y|bbb)_D$ minimized when $(b|bbb)_M = -(a|bb)_M(x|bb)_M/(y|b)_M$

$(y|b\delta\delta)_D$ minimized when $(b|b\delta\delta)_M + (b|xb\delta)_M(x|a)_M/(a|\delta)_M(y|b)_M^2 + 2(b|xxb)_M(x|a)_M^2(a|\delta)_M^2 = -(a|\delta\delta)_M(x|bb)_M/(y|b)_M - (x|a\delta)_M(x|bb)_M(a|\delta)_M/(x|a)_M(y|b)_M - 2(x|bb)_M(x|yb)_M(a|\delta)_M^2/(y|b)_M$

APPENDIX C

COSY SIMULATION FOR BEST SYMMETRIC DESIGN AFTER CORRECTION FOR THIRD ORDER ABERRATIONS – SYMMETRY MAINTAINED ABOUT DIPOLE MIDPLANE

```
INCLUDE 'COSY';
PROCEDURE RUN;
VARIABLE Q1 1; VARIABLE Q2 1; VARIABLE Q3 1; VARIABLE Q4 1;
VARIABLE L1 1; VARIABLE L2 1; VARIABLE L3 1; VARIABLE L4 1;
VARIABLE L5 1; VARIABLE AP 1; VARIABLE OBJ 1; VARIABLE QL 1;
VARIABLE S1 1; VARIABLE S2 1; VARIABLE S3 1; VARIABLE S4 1;
VARIABLE D1 1; VARIABLE D2 1; VARIABLE D3 1; VARIABLE D4 1;
VARIABLE D5 1; VARIABLE D6 1; VARIABLE D7 1; VARIABLE D8 1;
PROCEDURE WRITEMAP FILENAME; OPENF 8 FILENAME 'UNKNOWN';
WRITE 8 'QL Q1 Q2 Q3 Q4' QL Q1 Q2 Q3 Q4;
WRITE 8 'S1 S2 S3 S4' S1 S2 S3 S4;
WRITE 8 'D1 D2 D3 D4 D5 D6 D7 D8' D1 D2 D3 D4 D5 D6 D7 D8;
WRITE 8 'L1 L2 L3 L4 L5 OBJ' L1 L2 L3 L4 L5 OBJ;
WRITE 8 'BEAM MATRIX'; PM 8; WRITE 8 'BEAM ABERRATIONS'; PA 8;
CLOSEF 8; ENDPROCEDURE;
PROCEDURE BEAMLINE;
DL L1; M5 QL Q1 S1 D1 0 0 AP; DL L2; M5 QL Q2 S2 D2 0 0 AP;
DL L3; M5 QL Q3 S3 D3 0 0 AP; DL L4; M5 QL Q4 S4 D4 0 0 AP;
DL L5; DI 5 35 .1 0 0 0 0; DL L5;
M5 QL Q4 S4 D5 0 0 AP; DL L4; M5 QL Q3 S3 D6 0 0 AP; DL L3;
M5 QL Q2 S2 D7 0 0 AP; DL L2; M5 QL Q1 S1 D8 0 0 AP; DL L1;
DL L1; M5 QL Q1 S1 D8 0 0 AP; DL L2; M5 QL Q2 S2 D7 0 0 AP;
DL L3; M5 QL Q3 S3 D6 0 0 AP; DL L4; M5 QL Q4 S4 D5 0 0 AP;
DL L5; DI 5 35 .1 0 0 0 0; DL L5;
M5 QL Q4 S4 D4 0 0 AP; DL L4; M5 QL Q3 S3 D3 0 0 AP; DL L3;
M5 QL Q2 S2 D2 0 0 AP; DL L2; M5 QL Q1 S1 D1 0 0 AP; DL L1;
ENDPROCEDURE;
OV 5 3 0; DR2 := .4;
LAX := 0;
LCE := 0;
FR 2;
RPM 2398*50 132 50;
SB .001 .05 0 .001 .05 0 0 .10 0 0 0;
AP := .2;
QL :=  .7;
Q1 :=  .7359080669258169;
Q2 := -.2752689607259485;
Q3 := -1.517467263959876;
Q4 :=  1.098340326114576;
S1 := .02361502431797905;
S2 := .02995126241888397;
S3 := -.2895539864520602;
S4 := .2343973615723920;
```

```
D1 := -.6031246413700748;
D2 := -.5936465751515769;
D3 := -.03469126560807764;
D4 := .08061321164000852;
D5 := -.05741064577545293;
D6 := .097094320718321163;
D7 := -.009875128290919846;
D8 := -.001201562227302961;
L1 := .57;
L2 := .51;
L3 := .69;
L4 := .29;
L5 := .28;
UM; CR; ER 1 3 1 3 1 3 1 1; BP; LDREL :=1;
BEAMLINE;
EP;
PP -10 0 0; PP -10 0 90; UM;
BEAMLINE TBPG -101 'X PROJECTION'
    -102 'Y PROJECTION'
    -103 'XY PROJECTION' .05 1;
WRITEMAP 'MATRIX.TXT';
ENDPROCEDURE; RUN; END;
```